Oligonucleotide Analogues with Integrated Bases and Backbone

Part 17[1])

Conformational Analysis and Association of Ethylene-, Oxymethylene-, and Thiomethylene-Linked Self-Complementary Adenosine and Uridine Dimers

by **Anne Ritter**, **Daniel Egli**, **Bruno Bernet**, and **Andrea Vasella***

Laboratorium für Organische Chemie, ETH Zürich, CH-8093 Zürich
e-mail: vasella@org.chem.ethz.ch

The formation of cyclic duplexes (pairing) of known oxymethylene-linked self-complementary U*[o]A(*) dinucleosides contrasts with the absence of pairing of the ethylene-linked U*[c_a]A(*) analogues. The origin of this difference, and the expected association of U*[x]A(*) and A*[x]U(*) dinucleosides with x = CH_2, O, or S was analysed. According to this analysis, pairing occurs *via* constitutionally isomeric *Watson–Crick*, reverse *Watson–Crick*, *Hoogsteen*, or reverse *Hoogsteen* H-bonded linear duplexes. Each one of them may give rise to three diastereoisomeric cyclic duplexes, and each one of them can adopt three main conformations. The relative stability of all conformers with x = CH_2, O, or S were analysed. U*[x]A(*) dinucleosides with x = CH_2 do not form stable cyclic duplexes, dinucleosides with x = O may form cyclic duplexes with a *gg*-conformation about the C(4′)–C(5′) bond, and dinucleosides with x = S may form cyclic duplexes with a *gt*-conformation about this bond.

The temperature dependence of the chemical shift of H–N(3) of the self-complementary, oxymethylene-linked U*[o]A(*) dinucleosides **1**–**6** in $CDCl_3$ in the concentration range of 0.4–50 mM evidences equilibria between the monoplex, mainly linear duplexes, and higher associates for **3**, between the monoplex and cyclic duplexes for **6**, and between the monoplex, linear, and cyclic duplexes as well as higher associates for **1**, **2**, **4**, and **5**.

The self-complementary, thiomethylene-linked U*[s]A(*) dinucleosides **27**–**32** and the sequence isomeric A*[s]U(*) analogues **33**–**38** were prepared by *S*-alkylation of the 6-(mesyloxymethyl)uridine **12** and the 8-(bromomethyl)adenosine **22**. The required thiolates were prepared *in situ* from the *C(5′)*-acetylthio derivatives **9**, **15**, **19**, and **25**. The association in $CHCl_3$ of the thiomethylene-linked dinucleoside analogues was studied by ^{1}H-NMR and CD spectroscopy, and by vapour-pressure osmometric determination of the apparent molecular mass. The U*[s]A(*) alcohols **28**, **30**, and **31** form cyclic duplexes connected by *Watson–Crick* H-bonds, while the fully protected dimers **27** and **29** form mainly linear duplexes and higher associates. The diol **32** forms mainly cyclic duplexes in solution and corrugated ribbons in the solid state. The nucleobases of crystalline **32** form reverse *Hoogsteen* H-bonds, and the resulting ribbons are cross-linked by H-bonds between $HOCH_2$–C(8/I) and N(3/I). Among the A*[s]U(*) dimers, only the *C(8/I)*-hydroxymethylated **37** forms (mainly) a cyclic duplex, characterized by reverse *Hoogsteen* base pairing. The dimers **34**–**36** form mainly linear duplexes and higher associates. Dimers **34** and particularly **38** gelate $CHCl_3$. Temperature-dependent CD spectra of **28**, **30**, **31**, and **37** evidence π-stacking in the cyclic duplexes. Base stacking in the particularly strongly associating diol **32** in $CHCl_3$ solution is evidenced by a melting temperature of *ca.* 2°.

Introduction. – We have shown that the differentiation between backbone and nucleobases of oligonucleotide analogues is not an absolute requirement for pairing *via*

[1]) Part 16: [1].

H-bonding and base stacking [2]. This conclusion is based on the association, in $CHCl_3$ solution, of partially protected, self-complementary dimeric and tetrameric oligonucleotide analogues integrating backbone and bases (ONIBs), characterized by uridine (U) and adenosine (A) units connected by ethynylene [3][4], (*Z*)- and (*E*)-ethenylene [5], ethylene [1], or oxymethylene [6][7] linkers[2]). Ethynylene-linked, self-complementary dimers pair, *i.e.*, they form cyclic duplexes, with the nucleobase in a *syn* conformation (favoured by substitution at C(6) of U and at C(8) of A) and a *gg*-type orientation of the ethynyl substituent at C(5′/I) [3]. U*[c_y]A* dimers[3]) possessing a propargylic HO–(C5′/I) group do not form cyclic duplexes, the persistent H-bond of HO–(C5′/I) to N(3/I) preventing a *gg*-orientation of the ethynylene linker. A weaker tendency to form cyclic duplexes was observed for (*Z*)-ethenylene-linked dimers [5]. Neither (*E*)-ethenylene-linked A*[c_e]U$^{(*)}$ dimers, nor any dimers possessing the fully saturated ethylene linker form cyclic duplexes [1][5]. These observations evidence that pairing depends mainly on the conformation of the linker and the orientation of the nucleobase of unit I (*Fig. 1*,*a*). The rotational freedom of the linker in the cyclic duplex is restricted, and pairing is favoured by a small energy difference between the conformation of the monoplex and of the cyclic duplex ('preorganisation'), as it appears to be the case in the ethynylene series devoid of a propargylic hydroxy group.

Oxymethylene-linked dimers were designed to simplify the synthesis of ONIBs [7], taking into account that pairing requires a *syn*-conformation of the nucleobase of unit I. In contradistinction to ethylene-linked U*[c_a]A$^{(*)}$ and A*[c_a]U$^{(*)}$ dimers, oxymethylene-linked U*[o]A$^{(*)}$ analogues form cyclic duplexes in $CHCl_3$ [7]. Unfortunately, the projected synthesis of the A*[o]U$^{(*)}$ sequence-isomers failed, presumably due to a facile solvolysis of adenosine derivatives possessing a leaving group at CH_2C(8), and an ineffective reaction of the resulting stabilised immonium cation with HO–C(5′) of a partially protected uridine. This interpretation suggested to replace the OH at C(5′) with an SH group, and to synthesise thiomethylene analogues. However, as the origin of the different behaviour of dimers linked by either a propane-1,3-diyl or a 2-oxapropane-1,3-diyl unit between C(4′) and C(6) of U or C(8) of A had not been analysed, we considered it necessary to understand the origin of this difference, resulting from formal replacement of a CH_2 group by an O-atom, and to predict the pairing potential of thiomethylene-linked analogues.

In the following, we discuss the association of the propane-, 2-oxapropane-, and 2-thiapropane-1,3-diyl-linked U*[x]A$^{(*)}$ and A*[x]U$^{(*)}$ dinucleosides (x = CH_2, O, or S) to form linear duplexes, the transformation of the linear to cyclic duplexes, and the conformations of the cyclic duplexes. We also describe the synthesis and association of thiomethylene-linked U*[s]A$^{(*)}$ and A*[s]U$^{(*)}$ analogues.

---

[2]) For the duplex formation of a self-complementary AU dimer connected by an anthracene-1,8-diethynyl linker, see [8]. This linker does not allow the preparation of oligomers.

[3]) *Conventions for abbreviated notation:* The substitution at C(6) of pyrimidines and C(8) of purines is denoted by an asterisk (*); for example, U* and A* for hydroxymethylated uridine and adenosine derivatives, respectively. U$^{(*)}$ and A$^{(*)}$ represent both unsubstituted and hydroxymethylated nucleobases. The moiety linking C(6)–CH_2 or C(8)–CH_2 of unit II and C(5′) of unit I is indicated in square brackets, *i.e.,* [c] for a C-, [o] for an O-, and [s] for a S-atom. The indices y, e, and a indicate a triple, double, or single bond, respectively.

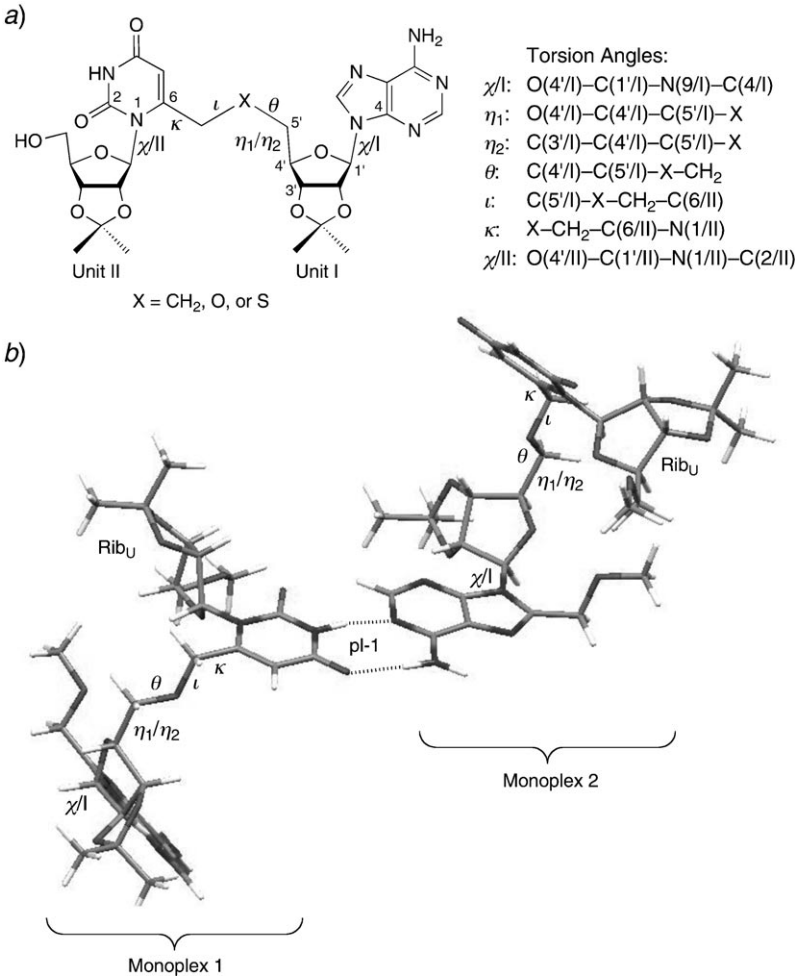

Fig. 1. a) *U*[x]A(*) Dimers: definition of the torsion angles relevant for duplex formation.* Analogous definitions are valid for the A*[x]U(*) sequence isomers. b) *A* WC *base-paired linear duplex of a U*[o]A* dimer.*

Results and Discussion. – 1. *Evaluation of the Pairing Propensity of Self-Complementary Ethylene-, Oxymethylene-, and Thiomethylene-Linked Uridine- and Adenosine-Derived Dimers.* The propensity of forming cyclic duplexes of U*[x]A(*) and of A*[x]U(*) dimers was evaluated by comparing the conformations of the monoplexes and the corresponding cyclic duplexes. As mentioned in the *Introduction*, analysis of the duplex formation of ethynylene-linked dimers showed the critical role of the torsion angles χ and η_1/η_2 (*cf. Fig. 1,a*, for the definition of the torsion angles). Analysis of the pairing of dinucleosides with $X = CH_2$, O, and S requires the analysis also of the torsion angles θ, ι, and κ, and of the effect of the nature of X, *i.e.*, of the centre unit of the linker between C(4′) and C(6 or 8).

We assume that the formation of cyclic duplexes, possessing two H-bonded base pairs, is preceded by the formation of linear duplexes, characterized by a single base pair. Constitutional isomers of linear duplexes result from the different possible pairing modes (*Watson–Crick* (*WC*), reverse *Watson–Crick* (r*WC*), *Hoogsteen* (*H*), and reverse *Hoogsteen* (r*H*)). Each one of the constitutionally isomeric linear duplexes may form diastereoisomeric cyclic duplexes, with both base pairs of the cyclic duplex adopting the same pairing mode[4]), and each one of the diastereoisomers may adopt several conformations, as detailed below.

To form a cyclic duplex, the yet unpaired bases of the linear duplex must be located on the same side of the plane defined by the two paired nucleobases of the linear duplex ('base plane 1': pl-1; *Fig. 1,b*). The orientation of the yet unpaired bases is determined by the angles κ of monoplex 1 and χ/I of monoplex 2. To analyse the formation of the cyclic duplex, one must also consider the angles κ of monoplex 2 and χ/I of monoplex 1, taking into account that the angles κ and χ/I cannot vary independently of each other. We initially assumed a value of $+90^\circ$ or -90° for κ as favourable for the cyclisation[5]).

Cyclisation of the linear duplex generates a second base plane (pl-2), parallel to the first one. Both planes possess diastereotopic faces. Pl-2 is localised on top of one of the two diastereotopic faces of pl-1, and may turn one or the other of its diastereotopic faces towards pl-1, leading to the formation of three diastereoisomeric cyclic duplexes $\underline{\underline{\mathbf{A}}}$, $\underline{\underline{\mathbf{B}}}$, and $\underline{\underline{\mathbf{C}}}$[6]), with $\underline{\underline{\mathbf{A}}}$ and $\underline{\underline{\mathbf{B}}}$ C_2-symmetric and $\underline{\underline{\mathbf{C}}}$ C_1-symmetric, as illustrated for U*[x]A(*) dimers in *Fig. 2*. The duplexes $\underline{\underline{\mathbf{A}}}$ and $\underline{\underline{\mathbf{B}}}$ are characterised by an orientation of the ribosyl units of the two U moieties on one or on the other side of a plane bisecting pl-1 and pl-2, and approximately parallel to the direction of the H-bonds between the nucleobases. In duplex $\underline{\underline{\mathbf{C}}}$, the ribosyl units are oriented on opposite sides.

The three diastereoisomers with *WC* H-bonds are characterised by the sign of the two χ/I angles, as $++$ for $\underline{\underline{\mathbf{A}}}_{WC}$, $--$ for $\underline{\underline{\mathbf{B}}}_{WC}$, and $+-$ (identical to $-+$) for $\underline{\underline{\mathbf{C}}}_{WC}$ (*Fig. 2* and *Table 1*), the value of the angles depending on the conformation of each diastereoisomer.

At least one of the two χ angles of the diastereoisomers $\underline{\underline{\mathbf{B}}}_{WC}$ and $\underline{\underline{\mathbf{C}}}_{WC}$ (but not of $\underline{\underline{\mathbf{A}}}_{WC}$) amounts to -60° or -30° (*Fig. 2* and *Table 1*). The conformers with $\chi = -60^\circ$ are energetically disfavoured, involving a destabilising steric interaction of the adenosine moiety with H–C(2′/I). The conformers of the *C(8/I)*-unsubstituted diastereoisomers with $\chi = -30^\circ$ correspond to a minimum that is, however, higher in energy than the one for the classic *syn*- or *anti*-conformers ($\chi = +60 \pm 30^\circ$ or $-120 \pm 30^\circ$).

---

[4]) To simplify the analysis, we first assumed the same pairing mode for both base pairs. The consequences of a different behaviour will be discussed further below.

[5]) This assumption was tested by analysing the data in the *Cambridge* crystal data base for *C(2)*-substituted *N(1)*-alkylated imidazoles (26 compounds; no data were found for *C(8)*-substituted adenosines) and of *C(6)*-substituted uridines (six compounds). Of these, 22 imidazoles are characterised by $\kappa = 90 \pm 30^\circ$, 14 by $\kappa = 180 \pm 30^\circ$. One uridine shows $\kappa = \pm 90 \pm 30^\circ$ and five $\kappa = \pm 180 \pm 30^\circ$. The energy difference between conformers with $\kappa = 90$ and 180° appears to be small, as shown experimentally and computationally for benzyl methyl ether [9] and computationally for benzyl methyl thioether [10].

[6]) There are three rather than four diastereoisomers on account of the symmetry resulting from the self-complementary nature of the dimers. Note that the notation **A** refers to the monoplex and $\underline{\underline{\mathbf{A}}}$ to the cyclic duplex.

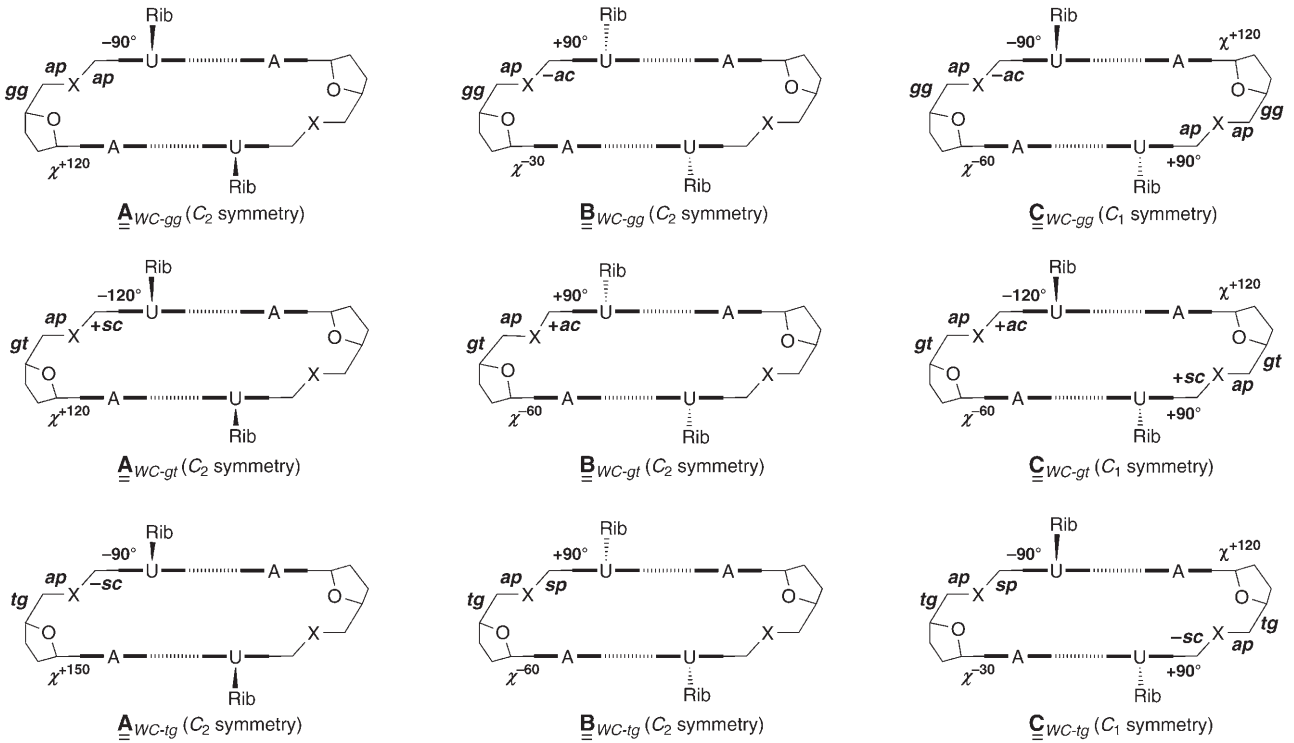

Fig. 2. *Cyclic duplexes of U*[x]A(*) dimers* (x = CH_2, O, or S) *connected by* WC *base pairing: schematic represensation of the staggered conformers resulting from rotation about the C(4′/I)–C(5′/I) bond of the three diastereoisomers showing approximate values for the* χ, η_1/η_2, θ, ι, *and* κ *angles* (large distance of 5–6 Å between the base pairs). Conformational analysis based on *Maruzen* models.

Table 1. *Cyclic Duplexes Derived of U*[x]A(*) Dimers* (x = CH_2, O, or S) *Connected by* WC, *r*WC, H, *or r*H *Base Pairing: Approximate Values of the* χ, η_1/η_2, θ, ι, *and* κ *Angles* (distance of 5–6 Å between the base pairs) *for Conformers Assembled by* Maruzen *Models*

Cyclic duplex	χ [°]	η_1/η_2	θ	ι	κ [°]
$\underline{\underline{\mathbf{A}}}_{WC\text{-}gg}$	+120	*gg*	*ap*	*ap*	−90
$\underline{\underline{\mathbf{A}}}_{WC\text{-}gt}$	+120	*gt*	*ap*	+*sc*	−120
$\underline{\underline{\mathbf{A}}}_{WC\text{-}tg}$	+150	*tg*	*ap*	−*sc*	−90
$\underline{\underline{\mathbf{B}}}_{WC\text{-}gg}$	−30	*gg*	*ap*	−*ac*	+90
$\underline{\underline{\mathbf{B}}}_{WC\text{-}gt}$	−60	*gt*	*ap*	+*ac*	+90
$\underline{\underline{\mathbf{B}}}_{WC\text{-}tg}$	−60	*tg*	*ap*	*sp*	+90
$\underline{\underline{\mathbf{C}}}_{WC\text{-}gg}$	−60/+120	*gg*/*gg*	*ap*/*ap*	−*ac*/*ap*	−90/+90
$\underline{\underline{\mathbf{C}}}_{WC\text{-}gt}$	−60/+120	*gt*/*gt*	*ap*/*ap*	+*ac*/+*sc*	−120/+90
$\underline{\underline{\mathbf{C}}}_{WC\text{-}tg}$	−30/+120	*tg*/*tg*	*ap*/*ap*	*sp*/−*sc*	−90/+90
$\underline{\underline{\mathbf{A}}}_{rWC\text{-}gg}$	−60	*gg*	*ap*	−*ac*	−90
$\underline{\underline{\mathbf{A}}}_{rWC\text{-}gt}$	−60	*gt*	*ap*	+*ac*	−120
$\underline{\underline{\mathbf{A}}}_{rWC\text{-}tg}$	−60	*tg*	*ap*	*sp*	−120
$\underline{\underline{\mathbf{B}}}_{rWC\text{-}gg}$	+120	*gg*	*ap*	*ap*	+90
$\underline{\underline{\mathbf{B}}}_{rWC\text{-}gt}$	+120	*gt*	*ap*	+*sc*	+120
$\underline{\underline{\mathbf{B}}}_{rWC\text{-}tg}$	+120	*tg*	*ap*	−*sc*	+120
$\underline{\underline{\mathbf{C}}}_{rWC\text{-}gg}$	+120/−60	*gg*/*gg*	*ap*/*ap*	*ap*/*ap*	−90/+120
$\underline{\underline{\mathbf{C}}}_{rWC\text{-}gt}$	+90/−60	*gt*/*gt*	*ap*/*ap*	*ap*/−*sc*	−90/+90
$\underline{\underline{\mathbf{C}}}_{rWC\text{-}tg}$	+120/−60	*tg*/*tg*	*ap*/*ap*	*ap*/+*sc*	−90/+60
$\underline{\underline{\mathbf{A}}}_{H\text{-}gg}$	−60	*gg*	*ap*	*ap*	−90
$\underline{\underline{\mathbf{A}}}_{H\text{-}gt}$	−60	*gt*	*ap*	+*sc*	−90
$\underline{\underline{\mathbf{A}}}_{H\text{-}tg}$	−60	*tg*	*ap*	−*sc*	−90
$\underline{\underline{\mathbf{B}}}_{H\text{-}gg}$	+120	*gg*	*ap*	−*ac*	+90
$\underline{\underline{\mathbf{B}}}_{H\text{-}gt}$	+120	*gt*	*ap*	+*ac*	+90
$\underline{\underline{\mathbf{B}}}_{H\text{-}tg}$	+120	*tg*	*ap*	*sp*	+90
$\underline{\underline{\mathbf{C}}}_{H\text{-}gg}$	+120/−30	*gg*/*gg*	*ap*/*ap*	−*ac*/−*ac*	−90/+120
$\underline{\underline{\mathbf{C}}}_{H\text{-}gt}$	+90/−60	*gt*/*gt*	*ap*/*ap*	+*ac*/*ap*	−90/+120
$\underline{\underline{\mathbf{C}}}_{H\text{-}tg}$	+120/−30	*tg*/*tg*	*ap*/*ap*	*sp*/+*ac*	−90/+120
$\underline{\underline{\mathbf{A}}}_{rH\text{-}gg}$	+120	*gg*	*ap*	*ap*	−120
$\underline{\underline{\mathbf{A}}}_{rH\text{-}gt}$	+90	*gt*	*ap*	+*sc*	−120
$\underline{\underline{\mathbf{A}}}_{rH\text{-}tg}$	+150	*tg*	*ap*	−*sc*	−90
$\underline{\underline{\mathbf{B}}}_{rH\text{-}gg}$	−60	*gg*	*ap*	*ap*	+120
$\underline{\underline{\mathbf{B}}}_{rH\text{-}gt}$	−60	*gt*	*ap*	+*sc*	+90
$\underline{\underline{\mathbf{B}}}_{rH\text{-}tg}$	−60	*tg*	*ap*	−*sc*	+60
$\underline{\underline{\mathbf{C}}}_{rH\text{-}gg}$	−60/+120	*gg*/*gg*	*ap*/*ap*	*ap*/−*ac*	−90/+60
$\underline{\underline{\mathbf{C}}}_{rH\text{-}gt}$	−60/+120	*gt*/*gt*	*ap*/*ap*	+*sc*/+*ac*	−90/+60
$\underline{\underline{\mathbf{C}}}_{rH\text{-}tg}$	−30/+150	*tg*/*tg*	*ap*/*ap*	−*sc*/−*sc*	−90/+60
$\underline{\underline{\mathbf{C}}}_{WC/rWC\text{-}gg}$	+120/+120	*gg*/*gg*	*ap*/*ap*	*ap*/*ap*	−90/+90
$\underline{\underline{\mathbf{C}}}_{WC/rWC\text{-}gt}$	+120/+120	*gt*/*gt*	*ap*/*ap*	+*sc*/+*sc*	−90/+90
$\underline{\underline{\mathbf{C}}}_{WC/rWC\text{-}tg}$	+120/+120	*tg*/*tg*	*ap*/*ap*	−*sc*/−*sc*	−90/+90
$\underline{\underline{\mathbf{C}}}_{H/rH\text{-}gg}$	+150/+150	*gg*/*gg*	*ap*/*ap*	*ap*/−*ac*	−90/+120
$\underline{\underline{\mathbf{C}}}_{H/rH\text{-}gt}$	+120/+120	*gt*/*gt*	*ap*/*ap*	+*sc*/+*ac*	−90/+90
$\underline{\underline{\mathbf{C}}}_{H/rH\text{-}tg}$	+120/+120	*tg*/*tg*	*ap*/*ap*	−*sc*/−*sc*	−90/+60

The *C(8/I)*-substituted diastereoisomers with $\chi = -30°$ are destabilised by an interaction of the *C(8/I)*-substituent with H−C(2′/I). Thus, on the basis of the χ angles, the diastereoisomers $\underline{\underline{\mathbf{B}}}_{WC}$ and $\underline{\underline{\mathbf{C}}}_{WC}$ are disfavoured; they are omitted from further considerations.

Turning to the conformers of $\underline{\underline{\mathbf{A}}}_{WC}$, we note that fixing the angles η_1/η_2 has the consequence of restricting the angles θ and ι, as shown in *Fig. 2*, and that at least one synclinal torsion angle is found in all conformers. Their stability can only be evaluated upon specifying the nature of X (*cf. Fig. 1,a*).

The conformers possessing a propane-1,3-diyl group between C(4′/I) and C(6/II) ($X = CH_2$) are destabilised by at least one synclinal arrangement, *i.e.*, by 2×0.85 kcal/mol [11][12]. This destabilisation disfavours the formation of cyclic duplexes, but is compatible with the formation of linear duplexes and higher associates.

Turning to the 2-oxapropane-1,3-diyl-linked conformers ($X = O$), we calculated a conformational energy for $\underline{\underline{\mathbf{A}}}_{WC\text{-}gg}$ of -0.1 kcal/mol (the synclinal arrangement of O−C(5′) and C(3′) amounting to 2×0.45 kcal/mol [13], the synclinal arrangement of O−C(5′) and O−C(4′) to 2×0.35 kcal/mol [13], and the $\sigma_{C-H}/\sigma^*_{C-O}$ interactions to 4×-0.425 kcal/mol[7])). The enforced antiperiplanar angles θ and ι correspond to the preferred conformation of Et_2O [17][18].

The conformational energy of the $\underline{\underline{\mathbf{A}}}_{WC\text{-}gt}$ conformer is 1.45 kcal/mol (synclinal arrangements of O−C(5′) with C(3′) (2×0.45 kcal/mol), $\sigma_{C-H}/\sigma^*_{C-O}$ interactions (2×-0.425 kcal/mol), and synclinal ι (2×0.7 kcal/mol [17])).

The conformational energy of $\underline{\underline{\mathbf{A}}}_{WC\text{-}tg}$ is 2.3 kcal/mol (synclinal arrangement of O−C(5′) and C(3′) (2×0.45 kcal/mol) and synclinal ι (2×0.7 kcal/mol)).

According to this analysis of the oxymethylene-linked dimers, only $\underline{\underline{\mathbf{A}}}_{WC\text{-}gg}$ should form a (*WC*-paired) cyclic duplex. The *gg*-conformation is compatible with a high-*syn*-orientation of the nucleobase, but hardly with a classic *syn*-orientation, this combination leading to an unfavourable steric interaction between the nucleobase and the substituent at C(5′).

An evaluation of the relative stability of all conformers of the thiomethylene-linked analogues ($X = S$) that form cyclic duplexes requires information about the relative stability of the rotamers of butane analogues characterised by the S−C−C−O, the S−C−C−C, or the C−C−S−C connectivity, corresponding to the angles η_1, η_2, and θ/ι, respectively. According to *ab initio* calculations for 1-methoxy-2-(methylsulfanyl)-ethane, the antiperiplanar conformation of the S−C−C−O fragment is favoured over a synclinal conformation by 0.13 kcal/mol, close to the experimental value of 0.17 kcal/mol [19]. We used the average value of 0.15 kcal/mol. According to *ab initio* calculations, the antiperiplanar conformation of the S−C−C−C fragment in MeSPr is preferred by 0.6 kcal/mol over the synclinal conformation [17]. *Ab initio* calculations also suggest that the *ap*/*sc*-conformation of the two C−S−C−C fragments of Et_2S (corresponding to the angles θ and ι) is preferred over the *ap*/*ap*-conformation by 0.2 kcal/mol, with one of the angles 180° and the other one 71° [20].

The $\underline{\underline{\mathbf{A}}}_{WC\text{-}gg}$ conformer ($X = S$) is thus destabilised by 2 kcal/mol (synclinal η_1 (2×0.2 kcal/mol), synclinal η_2 (2×0.6 kcal/mol), and antiperiplanar θ and ι (2×0.2 kcal/mol)).

---

[7]) This value for a $\sigma_{C-H}/\sigma^*_{C-O}$ interaction was calculated on the basis of a *gg*/*gt*/*tg* 57:29:14 equilibrium of *ribo*-configured pyrimidine nucleosides [14] using the above mentioned increments [15]. For calculations of the attractive *gauche* effect of ethylene glycols, see [16].

The $\underline{\underline{\mathbf{A}}}_{WC\text{-}gt}$ conformer is disfavoured by 0.4 kcal/mol (synclinal η_1 (2×0.2 kcal/mol); the antiperiplanar η_2 and ι as well as the synclinal θ angles correspond to the preferred conformation of MeSPr and Et_2S).

The $\underline{\underline{\mathbf{A}}}_{WC\text{-}tg}$ conformer is destabilised by 1.2 kcal/mol (synclinal η_2 (2×0.6 kcal/mol)).

According to this analysis, $\underline{\underline{\mathbf{A}}}_{WC\text{-}gt}$ is the preferred conformer of a cyclic duplex of the thiomethylene-linked U*[s]A$^{(*)}$ dimers linked by *WC* base pairs.

The relative stability of the U*[x]A$^{(*)}$ (x = CH_2, O, or S) duplexes that are linked by r*WC*, *H*, or r*H* base pairs was analysed in the same way as described above for the duplexes linked by *WC* base pairs (*Table 1*). All conformers of two out of the three diastereoisomers of each constitutionally isomeric cyclic duplex are destabilised by unfavourable χ and/or ι angles, and only one conformer of the remaining diastereoisomers appears to be favourable. The preferred diastereoisomers are $\underline{\underline{\mathbf{B}}}_{rWC}$, $\underline{\underline{\mathbf{B}}}_{H}$, and $\underline{\underline{\mathbf{A}}}_{rH}$. $\underline{\underline{\mathbf{B}}}_{H}$ is the least stable one on account of an ι angle of ± 120 to $\pm 150^\circ$ for $\underline{\underline{\mathbf{B}}}_{H\text{-}gg}$ and $\underline{\underline{\mathbf{B}}}_{H\text{-}gt}$, and one of *ca.* 0° for $\underline{\underline{\mathbf{B}}}_{H\text{-}tg}$, corresponding to an eclipsed conformation.

Again, all analogues with X = CH_2 are disfavoured. Of the analogues with X = O, the *gg*-conformer is preferred also in the r*WC*, *H*, and r*H* base-paired cyclic duplexes. Similarly, for X = S, the *gt*-conformer is favoured independently of the type of base pairing.

A priori, cyclic duplexes possessing two different base-pairing types cannot be excluded. However, *Maruzen* models show that cyclic duplexes combining a *WC*- and a *H*-type base pair cannot be formed. This is due to the strongly differing distances in pl-1 and pl-2 between the ribosylated N-atom of one base and the C-atom carrying the linker of the other base (*e.g.*, between C(6) of U and N(9) of A). This distance amounts to 8.9–9.5 Å in the *WC*-type base pairs and to 5.6–6.0 Å in the *H*-type base pairs. Cyclic duplexes combining a *WC* and a r*WC* base pair, or a *H* and a r*H* base pair appear feasible. Replacing a *WC* by a r*WC* base pair, or a *H* by a r*H* base pair leads to a change of the sign and value of the χ and κ angles. Effecting this operation on the C_2-symmetric diastereoisomers $\underline{\underline{\mathbf{A}}}$ and $\underline{\underline{\mathbf{B}}}$ results in constitutionally isomeric C_1-symmetric diastereosiomers of which all contain one unfavourable χ angle (-60 to -30°). $\underline{\underline{\mathbf{C}}}$ is transformed into two constitutionally isomeric diastereoisomers possessing either two negative or two positive χ angles. Two of these diastereoisomers ($\underline{\underline{\mathbf{C}}}_{WC/rWC}$ and $\underline{\underline{\mathbf{C}}}_{H/rH}$, *Table 1*) are favourable, possessing high-*syn* χ angles of 120–150°.

Inspection of *Maruzen* models does not allow to predict the relative stability of the constitutionally isomeric cyclic duplexes $\underline{\underline{\mathbf{A}}}_{WC}$, $\underline{\underline{\mathbf{B}}}_{rWC}$, $\underline{\underline{\mathbf{B}}}_{H}$, $\underline{\underline{\mathbf{A}}}_{rH}$, $\underline{\underline{\mathbf{C}}}_{WC/rWC}$, and $\underline{\underline{\mathbf{C}}}_{H/rH}$.

We also evaluated the relative stability of the cyclic duplexes of the sequence isomeric A*[s]U$^{(*)}$ dimers, similarly as we proceeded for the U*[s]A$^{(*)}$ dimers (*Table 2*). According to these considerations, the relative stability of the isomeric cyclic duplexes is sequence-independent, as *e.g.* in the A*[s]U$^{(*)}$ series, $\underline{\underline{\mathbf{D}}}_{WC\text{-}gt}$, $\underline{\underline{\mathbf{E}}}_{rWC\text{-}gt}$, $\underline{\underline{\mathbf{D}}}_{H\text{-}gt}$, $\underline{\underline{\mathbf{D}}}_{rH\text{-}gt}$, $\underline{\underline{\mathbf{E}}}_{WC/rWC\text{-}gt}$, and $\underline{\underline{\mathbf{E}}}_{H/rH\text{-}gt}$ are favoured.

Although we did not consider the different C–O and C–S bond lengths (1.41–1.44 Å *vs.* 1.79–1.84 Å), and the different C–O–C and C–S–C bond angles (110–114° *vs.* 98–105°), the above conformational analysis suggests that cyclic duplexes of oxymethylene-linked dimers adopt a *gg*-, and those of thiomethylene-linked dimers a *gt*-conformation about the C(4′/I)–C(5′/I) bond.

However, all favourable conformers of the cyclic duplexes of the oxymethylene and thiomethylene analogues (*Tables 1* and *2*) are characterised by a distance of 5–6 Å between pl-1 and pl-2 and a small twist angle ($< 20^\circ$). This is a large distance for π-

Table 2. *Cyclic Duplexes Derived of A*[x]U$^{(*)}$ Dimers* (x = CH_2, O, or S) *Connected by* WC, *r*WC, H, *or r*H *Base Pairing: Approximate Values of the* χ, η_1/η_2, θ, ι, *and* κ *Angles* (distance of 5–6 Å between the base pairs) *for Conformers Assembled by* Maruzen *Models* (only conformers possessing positive χ angles)

Cyclic duplex	χ [°]	η_1/η_2	θ	ι	κ [°]
$\underline{\underline{\mathbf{D}}}_{WC\text{-}gg}$	+90	*gg*	*ap*	*ap*	−90
$\underline{\underline{\mathbf{D}}}_{WC\text{-}gt}$	+90	*gt*	*ap*	+*sc*	−90
$\underline{\underline{\mathbf{D}}}_{WC\text{-}tg}$	+90	*tg*	*ap*	−*sc*	−90
$\underline{\underline{\mathbf{E}}}_{rWC\text{-}gg}$	+90	*gg*	*ap*	*ap*	+60
$\underline{\underline{\mathbf{E}}}_{rWC\text{-}gt}$	+60	*gt*	*ap*	+*sc*	+60
$\underline{\underline{\mathbf{E}}}_{rWC\text{-}tg}$	+120	*tg*	*ap*	−*sc*	+60
$\underline{\underline{\mathbf{D}}}_{H\text{-}gg}$	+120	*gg*	*ap*	−*ac*	+90
$\underline{\underline{\mathbf{D}}}_{H\text{-}gt}$	+120	*gt*	*ap*	+*ac*	+90
$\underline{\underline{\mathbf{D}}}_{H\text{-}tg}$	+150	*tg*	*ap*	*sp*	+90
$\underline{\underline{\mathbf{D}}}_{rH\text{-}gg}$	+120	*gg*	*ap*	+*ac*	−90
$\underline{\underline{\mathbf{D}}}_{rH\text{-}gt}$	+120	*gt*	*ap*	*sp*	−90
$\underline{\underline{\mathbf{D}}}_{rH\text{-}tg}$	+120	*tg*	*ap*	−*ac*	−60
$\underline{\underline{\mathbf{E}}}_{rWC/rWC\text{-}gg}$	+120/+120	*gg*/*gg*	*ap*/*ap*	*ap*/*ap*	+60/−120
$\underline{\underline{\mathbf{E}}}_{WC/rWC\text{-}gt}$	+90/+90	*gt*/*gt*	*ap*/*ap*	+*sc*/+*sc*	+60/−120
$\underline{\underline{\mathbf{E}}}_{WC/rWC\text{-}tg}$	+90/+120	*tg*/*tg*	*ap*/*ap*	−*sc*/−*sc*	+90/−60
$\underline{\underline{\mathbf{E}}}_{H/rH\text{-}gg}$	+150/+120	*gg*/*gg*	*ap*/*ap*	+*sc*/−*sc*	−90/+60
$\underline{\underline{\mathbf{E}}}_{H/rH\text{-}gt}$	+120/+120	*gt*/*gt*	*ap*/*ap*	−*sc*/*ap*	−90/+60
$\underline{\underline{\mathbf{E}}}_{H/rH\text{-}tg}$	+150/+150	*tg*/*tg*	*ap*/*ap*	*ap*/+*sc*	−90/+60

stacking [21]. The distance may be reduced by increasing the twist angle. This can be effected by changing the value of the χ, θ, ι, and κ angles, without directly affecting the favourable η_1/η_2 angles. The most probable torsion angles to respond to an increase of the twist angle are χ and κ, with χ increasingly approaching the value of the classic *syn*-conformation and κ the antiperiplanar conformation. The classic *syn*-conformation appears to destabilise the *gg*-conformer, while there is no obvious destabilising consequence of an antiperiplanar κ. Increasing the twist angle may also lead to some unfavourable non-bonding interactions between the ribosyl units in the cyclic duplex that were, however, not considered. The above conformational analysis is thus only valid as long as such interactions remain negligible, and must be modified for cyclic duplexes on account of the more extensive base stacking and an increased twist angle.

2. *Association of the U*[o]A$^{(*)}$ Dimers.* The tendency of U*[o]A$^{(*)}$ dimers to form cyclic duplexes had already been analysed on the basis of the concentration dependence of the chemical shift of H–N(3) ('shift/concentration curve', SCC) [7]. The SCCs reflect the combination of the equilibria between monoplex, duplexes, and/or linear associates [3], while the transformation of the intermediate linear duplexes to cyclic duplexes is concentration independent. The only criterion used so far to evidence cyclic duplexes of oxymethylene-linked dinucleosides is the constant value of δ(H–N(3)) at a concentration above 15–20 mM (formation of a plateau in the SCC). It is difficult to conceive that aggregation not leading to cyclic duplexes should be restricted to forming linear duplexes and not continue to generate higher associates.

The detailed analysis of the pairing of ethynylene-linked dimers [3] taught us the value of additional criteria, *viz.* the values of δ(H–N(3)) extrapolated to zero and to

infinite concentration, and the curvature of the SCC between 1 and *ca.* 10 mM (steepness of the ascent) that is correlated with the formation of a plateau. This correlation is taken to reflect the combination of the equilibria between monoplex and linear duplexes, and between linear and cyclic duplexes. The tendency to form linear duplexes should indeed not vary significantly for individual monoplexes considering the absence of unfavourable steric interactions.

A steady increase of the SCC in combination with a weak bending at concentrations between 1 and *ca.* 10 mM was taken as criterion for the formation of mainly linear duplexes and higher associates. The value of δ(H–N(3)) extrapolated to a dinucleoside concentration of 0 mM corresponds to the (not observable) chemical-shift value for H–N(3) of the monoplex, a value that must be close to the one of the weakly associating monomer (*ca.* 7.70 ppm [5][22]). The values of δ(H–N(3)) extrapolated to infinite concentration evidence the type of base pairing, *WC*-type base pairing resulting in a larger value for δ(H–N(3), $c=\infty$) than *H*-type base pairing (typically, $\Delta\delta=$ 0.8 ppm [3][23]).

The SCCs of the oxymethylene analogues **1**–**6** are shown in *Fig. 3*. Only the SCC of diol **6** forms a plateau; the SCCs of the other dinucleosides show a more or less pronounced steady increase of δ(H–N(3), most typically for the fully protected dimer **3**. As expected, the SCC of **3** shows also the weakest bending at low concentrations. δ(H–N(3)) for **3** extrapolated to a concentration of 0 mM is 8.5 ppm, sufficiently close to the 7.70 ppm assumed for the monoplex to conclude that the association of **3** favours the monoplex. This conclusion is in agreement with the rather low association constant ($K_{ass}=970$ M^{-1}), as determined by graphical analysis of the SCC [7]. The plateau-forming SCC of **6** should show the strongest bending at low concentrations. However, numerical analysis led to a poor fitting with a too low value of 6.01 ppm for δ(H–N(3), $c=0$ mM) and a K_{ass} of 70000 ± 4500000 M^{-1}. The fitting was much improved by adding a value of 7.70 ppm for a concentration of 0.0001 mM. Numerical analysis then led to a δ(H–N(3), $c=0$ mM) of 7.66 ± 0.06 ppm and to a K_{ass} of 40300 ± 13400 M^{-1}. The SCCs of the remaining dimers **1**, **2**, **4**, and **5** are of an intermediate type. Assuming, as mentioned above, that the tendency of the individual monoplexes to form linear associates does not differ significantly, we interpret the SCCs of the intermediate type as reflecting the competition between the formation of linear duplexes, cyclic duplexes, and higher associates. The δ(H–N(3), $c=0$ mM) values for **4** (12.0 ppm), **1** (11.4 ppm), **2** (10.3 ppm), and **5** (9.2 ppm) are larger than the one for **3**; they are considered to express a decreasing proportion of cyclic duplexes. The large δ(H–N(3), $c=0$ mM) values for **4** and **1**, suggesting a weak bending, are considered an artefact resulting from exchange of H–N(3) with residual H_2O in $CDCl_3$, an exchange that is most strongly felt at low concentrations, and leads to an increasingly strong upfield shift for H–N(3)[8]).

---

[8]) Graphical and numerical analysis of the SCC of **4** led to a K_{ass} value of 280 [7] and of 260 ± 58 M^{-1}, respectively. These values are too low considering $K_{ass}=970$ M^{-1} of **3**. The error induced by the H/H exchange may partly be corrected by adding a value of 7.70 ppm for a concentration of 0.0001 mM. This leads to an increased association constant for **4** ($K_{ass}=13300\pm2150$ M^{-1}). K_{ass} of the other duplexes are similarly corrected, for **1** from 1890 to 18400 ± 2350 M^{-1}, for **2** from 2500 to 12300 ± 1240 M^{-1}, for **5** from 3220 to 6820 ± 660 M^{-1}, and for **3** from 970 to 1610 ± 110 M^{-1}. These values reflect well the bending of the curves.

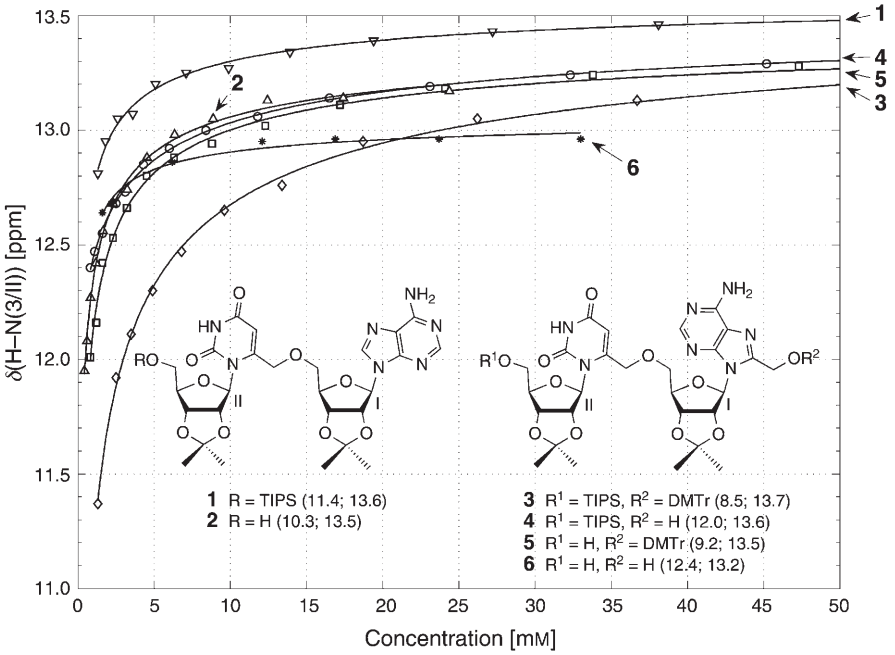

Fig. 3. *SCCs for H–N(3) of the U*[o]A(*) dimers* **1**, **3**–**5** (0.8–50 mM), **2** (0.8–25 mM), *and* **6** (1–35 mM) *in $CDCl_3$ solutions* (solid lines: fitted curve). The extrapolated δ(H–N(3/II), $c = 0$ mM and ∞) values [ppm] are given in parentheses.

The same δ(H–N(3), $c = \infty$) value is found for all dinucleosides (13.5–13.7 ppm), with the exception of **6** (13.2 ppm). The ROESY spectrum of **1** (15 mM) reveals a *ca.* 1:1 mixture of *WC*- and *H*-type base-paired associates. The known dependence of δ(H–N(3)) on the type of base pairing suggests that the cyclic duplex of **6** is characterised by *H*-type H-bonding[9]).

A *ca.* 8:1:1 distribution of the *gg*/*gt*/*tg* conformers of the *C(8)*-unsubstituted dimers **1** and **2** is suggested by J(4′,5′a/I) and J(4′,5′b/I) values (**1**: 2.8 and 2.7, **2**: 3.3 and 2.7 Hz). The chemical shifts for H–C(2′/I) of **1** (5.66 ppm) and **2** (5.68 ppm) evidence the predominance of a *syn*-conformation, in keeping with the assumption that **1** and **2** form cyclic duplexes to a rather large extent. A *ca.* 6:1:3 distribution of the *gg*/*gt*/*tg* conformers of the *C(8/I)*-substituted dimer **4** is indicated by J(4′,5′a/I) and J(4′,5′b/I) values (4.6 and 3.4 Hz, resp.). The large preference of the *gg*-conformer is in keeping with the rather large proportion of cyclic duplexes possessing a high-*syn*-orientation of the adenine moiety. A *ca.* 1:1:1 ratio of the *gg*/*gt*/*tg* conformers of the *C(8/I)*-substituted dimers **3**, **5**, and **6** is suggested by J(4′,5′a/I) and J(4′,5′b/I) values (**3**: 5.3 and

[9]) This interpretation is supported by a difference of 0.4 ppm between δ(H–N(3), $c = \infty$) of **6** and **1** (*WC*/*H ca.* 1:1), considering a typical chemical-shift difference of 0.8 ppm for the two types of base pairing [3][23].

4.9, **5**: 5.7 and 4.5, **6**: 5.7 and 4.5 Hz). The lower population of the *gg*-conformation of **3** and **5** is thought to reflect the steric interaction of the substituent at C(5′/I) with the adenine moiety adopting a classic *syn*-orientation in the linear duplexes. Similarly, the population of the *tg*- and *gt*-conformations are favoured by such an interaction in the cyclic duplexes of **6** and by an improved base stacking resulting from increasing the twist angle.

3. *Synthesis of the U*[s]A(*) and A*[s]U(*) Dimers.* For the synthesis of the desired thiomethylene-linked dinucleosides **27**–**38** (*Scheme 2*, *vide infra*), we required the C(5′)-*S*-acetates **9**, **15**, **19**, and **25**, the methanesulfonate **12**, and the bromide **22** (*Scheme 1*). The C(5′)-*O*-acetates **10**, **16**, **20**, and **26** were prepared to obtain reference compounds for the conformational analysis of the C(5′)-*S*-acetates. All these compounds were synthesized from the uridine-derived isopropylidene acetal **7** [24] and the adenosine-derived analogue **17** [24].

Scheme 1

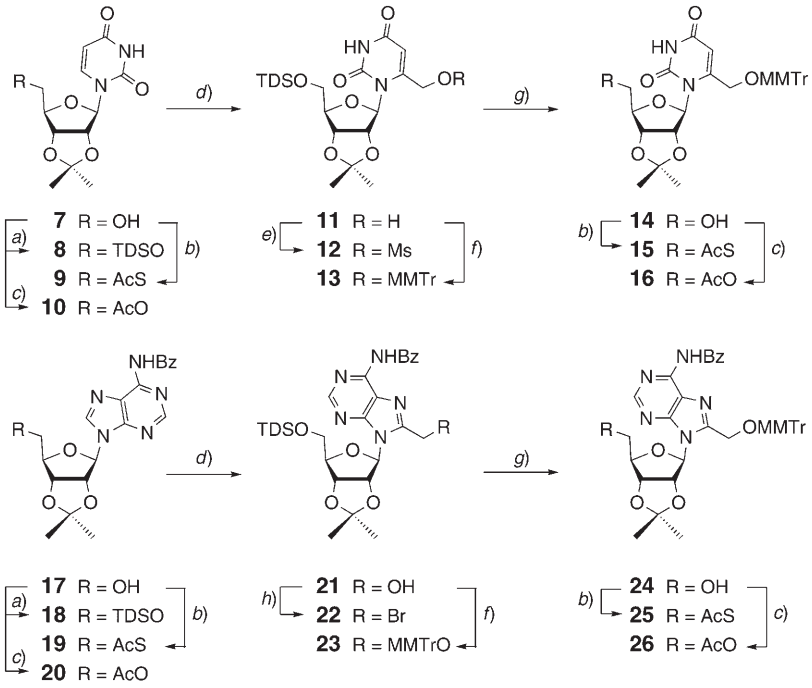

TDS = Thexyl(dimethyl)silyl (thexyl = 1,1,2-trimethylpropyl), MMTr = (monomethoxy)trityl (=(4-methoxyphenyl)(diphenyl)methyl). *a*) TDSCl, 1*H*-imidazole, DMF; >98% of **8**; 95% of **18**. *b*) 1. TsCl, 4-(dimethylamino)pyridine (DMAP), CH_2Cl_2 or TsCl, pyridine; 2. AcSK, DMF, 80°; 70% of **9**; 75% of **15**; 68% of **19**; 77% of **25**. *c*) Ac_2O, pyridine; 61% of **10**; 81% of **16**; 45% of **20**; 77% of **26**. *d*) 1. LDA (Lithium diisopropylamide), THF, −78°, then DMF; 2. $NaBH_4$, AcOH, EtOH; 80% of **11**; 72% of **21**. *e*) MsCl (Ms = methylsulfonyl), $(i\text{-}Pr)_2EtN$, CH_2Cl_2; 61%. *f*) MMTrCl, $(i\text{-}Pr)_2EtN$, CH_2Cl_2; 80% of **13**; 83% of **23**. *g*) $Bu_4NF \cdot 3\,H_2O$, 4-Å mol. sieves, THF; 84% of **14**; 82% of **24**. *h*) 1. Ms_2O, $EtN(i\text{-}Pr)_2$, CH_2Cl_2 2. LiBr, CH_2Cl_2; 61%.

The isopropylidenated uridine **7** was transformed into the 'thexyl(dimethyl)silyl' (TDS; thexyl = 1,1,2-trimethylpropyl) ether **8** (> 98%; *Scheme 1*) according to [25]. Deprotonation of **8** with excess LDA [26], followed by formylation with DMF [27][28], hydrolysis, and reduction [29] of the resulting aldehyde [7] yielded 80% of the hydroxymethylated uridine **11**. Mesylation of **11** yielded 82% of **12**, while 4-monomethoxytritylation gave 80% of **13** that was desilylated [30] to the alcohol **14** (84%). The desired C(5′)-*S*-acetates **9** [31] (70%) and **15** (75%) were obtained by substitution of the crude C(5′)-*O*-*p*-toluenesulfonates obtained from **7** and **14** with excess potassium thioacetate in DMF [32]. The C(5′)-*O*-acetates **10** [33] and **16** [34] were obtained from **7** and **14**, respectively.

Similarly, silylation of the isopropylidenated adenosine **17** afforded **18** (95%) that was hydroxymethylated to **21** (68%; *Scheme 1*). The alcohol **21** was transformed, by mesylation and treatment with LiBr, into the bromo derivative **22** (61%). Monomethoxytritylation of **21** yielded 83% of **23** that was desilylated in 82% to the alcohol **24**. The crude C(5′)-*O*-tosylates derived from **17** and **24** were converted with AcSK in DMF into the desired C(5′)-*S*-acetates **19** (68%) and **25** (77%), respectively. Acetylation of **17** and **24** gave the C(5′)-*O*-acetates **20** [34] and **26**.

The C(5′)-*S*-acetates **9**, **15**, **19**, and **25** were transformed to the corresponding thiolates by treatment with MeONa in MeOH (*Scheme 2*). These conditions led also to the (desired) *N*-debenzoylation of the adenosines **19** and **25**. Nucleophilic substitution of the uridine-derived methanesulfonate **12** by the thiolates resulting from the adenosine-derived C(5′)-*S*-acetates **19** and **25** yielded the U*[s]A$^{(*)}$ dimers **27** (85%) and **29** (62%), respectively. The sequence isomeric A*[s]U$^{(*)}$ dimers **33** (77%) and **35** (75%) were obtained by nucleophilic substitution of the bromomethylated adenosine **22** by the thiolates derived from the uridine C(5′)-*S*-acetates **9** and **15**, respectively. The U*[s]A$^{(*)}$ dimers **27** and **29**, as well as the A*[s]U$^{(*)}$ dimers **33** and **35** were desilylated with $(HF)_3 \cdot Et_3N$ in THF to yield 58–93% of the alcohols **28**, **30**, **34**, and **36**, respectively. The fully protected U*[s]A$^{(*)}$ dimer **29** was detritylated ($Et_3SiH/Cl_2CHCOOH$ [35]) to yield 87% of the silyl ether **31**, that was desilylated to the diol **32** (80%). Similarly, the sequence-isomeric fully protected A*[s]U$^{(*)}$ dimer **35** was transformed into the silyl ether **37** (67%) and further into the diol **38** (78%).

4. *Association of the U*[s]A$^{(*)}$ and A*[s]U$^{(*)}$ Dimers in $CHCl_3$ Solution.* The association of the U*[s]A$^{(*)}$ and A*[s]U$^{(*)}$ dimers was studied by ^{1}H-NMR and circular dichroism (CD) spectroscopy, similarly as previously described for ethynylene- [3], (*Z*)-ethenylene- [5], and oxymethylene-linked dimers [7]. Vapour-pressure osmometry (VPO) was used in a few cases to determine the stoichiometry of the association.

In the following sections, we discuss the conformation of the uridine and adenosine monomers and the self-association of the U*[s]A$^{(*)}$ and A*[s]U$^{(*)}$ dimers. We also discuss NMR parameters of the U*[s]A$^{(*)}$ and A*[s]U$^{(*)}$ dimers that are hardly affected by association.

4.1. *Conformation of the Uridine and Adenosine Monomers.* The expected *anti*-orientation of the *C(6)*-unsubstituted, C(5′)-*O*-silylated uridine derivative **8** is evidenced by the upfield shift of H–C(2′) (4.73 ppm, *Table 6* in the *Exper. Part*). The *gg*-rotamer is strongly favoured, as evidenced by small *J*(4′,5′a) and *J*(4′,5′b) values

Scheme 2

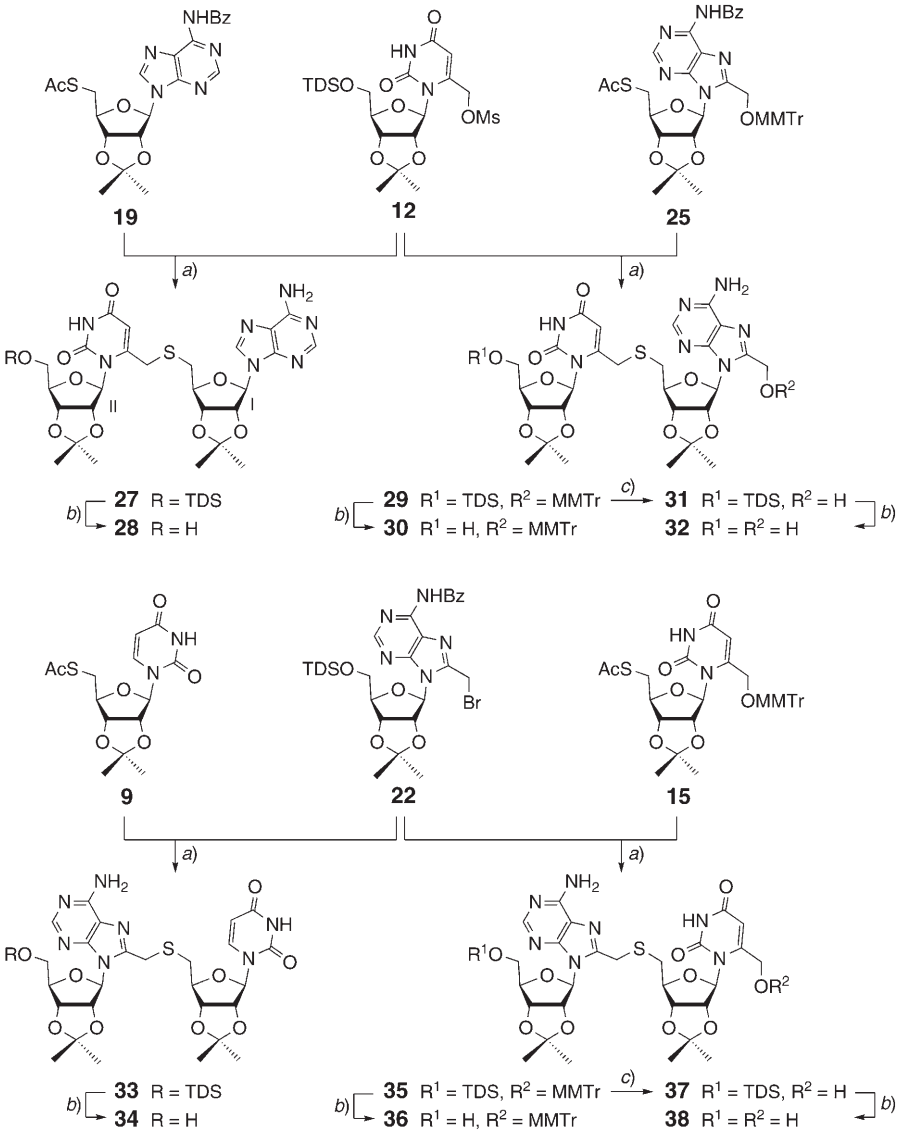

TDS = Thexyl(dimethyl)silyl (thexyl = 1,1,2-trimethylpropyl), MMTr = (monomethoxy)trityl. *a*) MeONa, MeOH; 85% of **27**; 62% of **29**; 77% of **33**; 75% of **35**. *b*) $(HF)_3 \cdot Et_3N$, THF; 58% of **28**; 83% of **30**; 80% of **32**; 58% of **34**; 93% of **36**; 78% of **38**. *c*) Cl_2CHCO_2H, Et_3SiH, CH_2Cl_2; 87% of **31**; 67% of **37**.

of 2.4 and 3.6 Hz, suggesting a 91:7:2 *gg*/*gt*/*tg* rotamer distribution[10]). A *ca.* 1:1 (*S*)/(*N*) equilibrium of the furanose ring conformation is derived from $J(1',2')/J(3',4') = 0.83$. Surprisingly, a substantial population of the *syn*-conformation is suggested for the *C(6)*-unsubstituted uridine C(5′)-*S*-acetate **9** and of the corresponding *O*-acetate **10** by the downfield shift of H–C(2′) resonating at 5.00–5.01 ppm. This is in keeping with a *ca.* 3:1 *syn*/*anti* equilibrium for both **9** and **10**, as derived from the relative intensity of the NOE peaks for H–C(1′) and H–C(2′)/H–C(3′) obtained upon irradiation of H–C(6) [42]. The higher population of the *syn*-conformation of **9** and **10** is correlated with a lower population of the *gg*-conformation. This is shown by $J(4',5'a)$ and $J(4',5'b)$ values of **9** (both 6.6 Hz) and **10** (3.7 and 7.2 Hz). The coupling constants evidence a *gg*/*gt*/*tg* rotamer distribution for the *S*-acetate **9** of 15:45:45, *i.e.*, an equal proportion of the *gt*- and *tg*-conformers, while the *gg*/*gt*/*tg* rotamer distribution of *ca.* 20:60:20 for the *O*-acetate **10**[11]) shows a preference for the *gt*-rotamer. Both **9** and **10** prefer the (*N*)-conformation more strongly than **8**.

An even higher population of the *syn*-conformation is expected for the *C(6)*-substituted uridines **11**–**15** and evidenced by the downfield shift for H–C(2′) (5.19–5.23 ppm) typical for a classic *syn*-conformation [3]. This decreases the population of the *gg*-conformation of the *S*-acetate **15** and the *O*-acetate **16** even further, as evidenced by a slight increase of $J(4',5'a)$ and $J(4',5'b)$ values ($\Delta J \leq 0.6$ Hz) upon substitution at C(6). The calculated *gg*/*gt*/*tg* rotamer distributions of 1:49:50 for **15** and of 12:72:16 for **16** are in agreement with a *gauche* effect in ethylene glycols, but not in the corresponding monothio analogues. The silyl ethers **11**–**13** prefer the *gg*-conformation (20–25%) more strongly than the *S*- and *O*-acetates **15** and **16**, respectively, as it was observed for the 6-unsubstituted analogues **8**–**10**. The alcohol **14** forms a partially persistent H-bond to O=C(2) leading to a larger population of the *gg*-rotamer, as indicated by the calculated *gg*/*gt*/*tg* ratio of 60:20:20. The partial persistence of the H-bond is suggested by the broad *s* at 3.25 ppm for HO–C(5′). The C(5′)-*O*- and C(5′)-*S*-protected **11**–**13**, **15**, and **16** prefer the (*N*)-conformation more strongly than the alcohol **14**.

---

[10]) The rotamer distribution was calculated for the C(5′)-oxy and C(5′)-thio nucleosides according to *Eqns. 1–3*, where P_{gg}, P_{gt}, and P_{tg} represent the mole fractions of the *gg*, *gt*, and *tg* rotamers, resp.

C(5′)-*O*-derivatives	C(5′)-*S*-derivatives	
$2.2\ P_{gg} + 2.0\ P_{gt} + 10.6\ P_{tg} = J(4'/5'_{pro\text{-}S})$	$4.7\ P_{gg} + 2.1\ P_{gt} + 11.6\ P_{tg} = J(4'/5'_{pro\text{-}S})$	(1)
$1.8\ P_{gg} + 9.6\ P_{gt} + 4.4\ P_{tg} = J(4'/5'_{pro\text{-}R})$	$1.8\ P_{gg} + 11.6\ P_{gt} + 3.1\ P_{tg} = J(4'/5'_{pro\text{-}R})$	(2)
$P_{gg} + P_{gt} + P_{tg} = 1$	$P_{gg} + P_{gt} + P_{tg} = 1$	(3)

The coefficients in *Eqns. 1* and *2* correspond to $^3J(4',5'a)$ and $^3J(4',5'b)$ of the staggered conformers. They were derived by MM3* minimisation of the staggered conformers of methyl 2,3-*O*-isopropylidene-5-(*O* or *S*)-methyl-β-D-ribofuranoside and calculation of the vicinal coupling constants using the *Haasnoot–Altona* equation [36] implemented in Macromodel 6.0 [37]. The H_a–C(5′) signal of the C(5′)-*O*-derivatives appearing at lower field is assigned to $H_{pro\text{-}S}$–C(5′), in agreement with the assignment for U- and A-derived nucleosides [38–40] and for methyl β-D-ribofuranosides [41].

[11]) The relative chemical shift of $H_{pro\text{-}S}$–C(6) and $H_{pro\text{-}R}$–C(6) of glucopyranosides is inverted upon acetylation of HO–C(6) [43]. Apparently, this is not the case in the ribofuranose series.

The *anti*-conformation of the *C(8)*-unsubstituted adenosine-derived silyl ether **18** is evidenced by the typical shift for H–C(2′) of 5.30 ppm (*Table 8* in the *Exper. Part*) [3]. A dominant population of the *gg*-rotamer is deduced from *J*(4′,5′a) and *J*(4′,5′b) of 3.9 and 4.2 Hz, leading to a calculated *gg*/*gt*/*tg* rotamer distribution of 55:25:20. A substantial population of the *syn*-conformation of the C(5′)-*S*- and C(5′)-*O*-acetates **19** and **20**, respectively, is evidenced by the downfield shift for H–C(2′) (5.51–5.52 ppm). In agreement with this, the NOEs for H–C(1′) and H–C(2′)/H–C(3′) resulting from irradiating H–C(8) suggest a *ca.* 85:15 *syn*/*anti* equilibrium for **19** and **20**, *i.e.*, a slightly stronger preference for the *syn*-conformation than of the corresponding uridine-derived *S*- and *O*-acetates **9** and **10**, respectively. Both **19** (*gg*/*gt*/*tg* 2:45:53) and **20** (*gg*/*gt*/*tg* 28:46:26) show a weaker preference for the *gg*-conformation than **18**, a similar result as in the uridine series. Both **19** and **20** show a slightly stronger preference for the (*N*)-conformation than **18**.

The *C(8)*-substituted *S*- and *O*-acetates **25** and **26** prefer a classic *syn*-conformation more strongly than the *C(8)*-unsubstituted **19** and **20**, while the *C(8)*-substituted silyl ethers **22** and **23** adopt completely a classic *syn*-conformation. This is evidenced by a weaker downfield shift for H–C(2′) of **25** and **26** than of **22** and **23** (5.68/5.65 *vs.* 5.84/5.82 ppm; *cf.* [3]). A *ca.* 1:1 *gt*/*tg* rotameric equilibrium is adopted by the *S*-acetate **25** and the silyl ethers **22** and **23**, as evidenced by *J*(4′,5′a) and *J*(4′,5′b) values of 5.7–7.2 Hz. The *O*-acetate **26**, however, shows smaller *J*(4′,5′a) and *J*(4′,5′b) values (4.1 and 6.9 Hz) suggesting a *gg*/*gt*/*tg* 19:57:24 rotameric distribution and evidencing a substantial population of the *gg*-conformation. All these derivatives prefer a (*N*)-conformation.

A *syn*/*anti* equilibrium of *ca.* 4:1 is suggested for the alcohol **21** by $\delta(\text{H}-\text{C}(2'))=5.67$ ppm. This may be rationalized by different intramolecular H-bonds of the conformers. In the *syn*-conformer, $\text{HOCH}_2-\text{C}(8)$ (*t* at 5.10 ppm, $J=6.3$ Hz) forms an intramolecular H-bond to N(7), and in the *anti*-conformer one to O–C(5′). In agreement with this interpretation, **21** shows a substantial population of the *gg*-conformation, as evidenced by *J*(4′,5′a) of 5.7 Hz and *J*(4′,5′b) of 5.1 Hz, suggesting a *gg*/*gt*/*tg* 30:28:42 rotameric distribution.

The alcohol **24** forms a completely persistent intramolecular H-bond to N(3), as evidenced by the exclusive population of the *gg*-rotamer ($J(4',5'a)=J(4',5'b)<1$ Hz), the (*S*)-conformation ($J(1',2')/J(3',4')=2.8$), and the typical *J*(5′,OH) couplings (2.1 and 11.1 Hz; *cf.* [3][44]). H–C(2′) of **24** resonates at an unusually high field (5.29 ppm) for a classic *syn*-conformer. This shift reflects the (*S*)- and a non-classic *syn*-conformation, as suggested by the crystal structure of 8-(hydroxymethyl)-2′,3′-*O*-isopropylideneadenosine [7] (χ *ca.* $+40$ rather than $+60°$).

These investigations of monomeric uridines and adenosines corroborate the presence of a *gauche* effect for 5′-oxygenated derivatives favouring the *gt*- and especially the *gg*-rotamer, whereas the absence of a *gauche* effect in the 5-sulfanylated analogues leads to an equal population of the *gt*- and the *tg*-rotamers. Noteworthy is the stronger preference for the *gg*-rotamer of the 6-unsubstituted silyl ethers **8** and **18** than of the corresponding *O*- and *S*-acetates **9**, **10**, **19**, and **20**, and the preferred *syn*-conformation of these acetates.

4.2. *Association of the U*[s]A*(*) and A*[s]U*(*) Dimers.* The association of the U*[s]A(*) and A*[s]U(*) dimers **27**–**32** and **33**–**38** was mainly investigated by

analysing the concentration and temperature dependence of the chemical shift for H–N(3) and by the temperature dependence of the CD spectra. To analyse the conformation of cyclic duplexes, we recorded ^{1}H-NMR spectra of the U*[s]A$^{(*)}$ dimers **27**–**32** (*Table 10* in the *Exper. Part*) and of the A*[s]U$^{(*)}$ dimers **33**–**38** (*Table 12* in the *Exper. Part*) in $CDCl_3$ at a concentration in the plateau region of the SCC, with the exception of the A*[s]U$^{(*)}$ dimers **34** and **38** that gelate $CDCl_3$[12]). The ^{1}H-NMR spectrum of **34** was recorded of a 5.9 mM solution in $CDCl_3$ (just below the minimum gelation concentration), while the ^{1}H-NMR spectrum of **38** was obtained in CD_3OD solution where solvation strongly disfavours the formation of duplexes. The assignment of the signals is based on selective homodecoupling experiments, and corroborated by DQF-COSY, HSQC, and HMBC spectra of **31** and **37**.

4.2.1. *Association of the U*[s]A$^{(*)}$ Dimers.* The SCCs of the U*[s]A$^{(*)}$ dimers **27**–**32** were determined for 0.8–50-mM solutions in $CDCl_3$ and are depicted in *Fig. 4*.

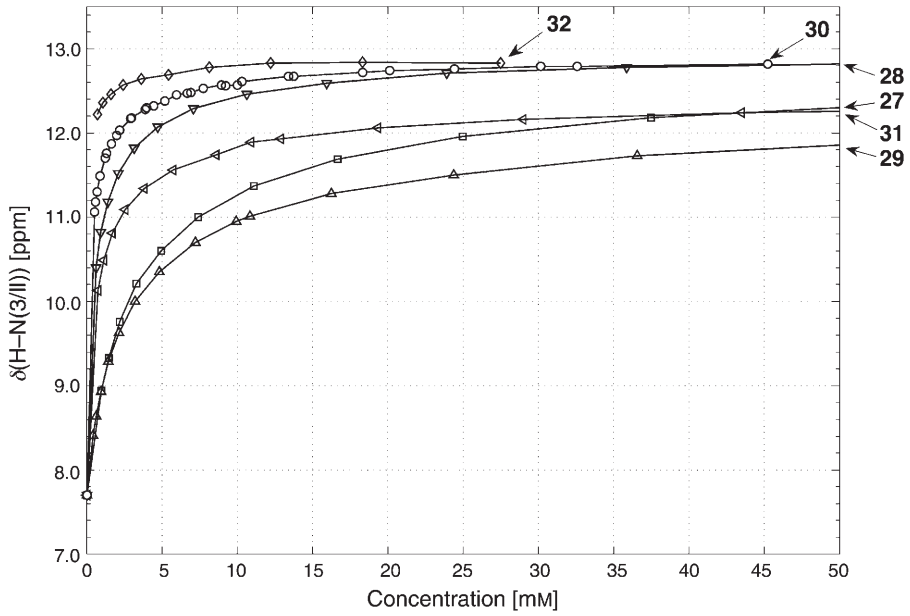

Fig. 4. *Shift/concentration curves* (SCCs) *for H–N(3) of the U*[s]A$^{(*)}$ dimers* **27**–**31** (0.4–50 mM) *and* **32** (0.7–27 mM) *in $CDCl_3$ solution* (including a value of 7.70 ppm for a 0.0001-mM solution)

The SCCs of **28** and **30**–**32** reach a plateau at a concentration of *ca.* 10 mM (**32**), 20 mM (**30**), and 30 mM (**28** and **31**), whereas the SCCs of **27** and **29** do not reach a plateau. The curvature of the SCCs at low concentrations decreases in the order **32**, **30**, **28**, **31**, **29**, and **27**. The extrapolated δ(H–N(3), $c = 0$ mM) values for all compounds are close to 7.7 ppm. Hence, the SCCs of the alcohols **28** and **30**–**32** represent predominantly the equilibria between monoplex and cyclic duplexes, whereas the SCCs of the silyl and/or trityl ethers **27** and **29** represent predominantly the equilibria between monoplex, linear duplexes, and higher linear associates.

---

[12]) The properties of the gels will be published elsewhere.

The δ(H–N(3), $c = 30$ mM) values for **28**, **30**, and **32** are identical (12.8 ppm), and 0.6 ppm larger than that for **31**. For **28**, *WC*- and *H*-type base pairing is evidenced by ROESY cross-peaks of moderate intensity between H–N(3/II) and both H–C(2/I) and H–C(8/I). If substitution at C(8/I) induces an upfield shift for H–N(3/II), similarly as it is the case in the U*[c_y]A$^{(*)}$ series [3], then δ(H–N(3), $c = 30$ mM) of the *C(8/I)*-substituted **30** and **32** evidences that the corresponding cyclic duplexes prefer *WC*-type H-bonding, and this more strongly than the cyclic duplexes of the *C(8/I)*-unsubstituted **28**. In the ROESY spectrum of **30**, a strong cross-peak between H–N(3) and H–C(2/I), and the absence of cross-peaks between H–N(3) and CH_2–C(8/I) evidence *WC*-type base pairing. A strong preference for *H*-type base pairing is indicated for **31** by δ(H–N(3), $c = 30$ mM) = 12.2 ppm. In contradistinction, the ROESY spectrum of **31** suggests a predominant *WC*-type base pairing of the duplexes, as inferred from a strong cross-peak between H–N(3) and H–C(2/I), and only a weak cross-peak between H–N(3) and CH_2–C(8/I) (the ratio of the peak volumes is *ca.* 10:3). The upfield shift for H–N(3) of **31** must then be due to the strongly persistent intramolecular H-bond of $HOCH_2$–C(8/I) to N(7/I), which is evidenced by the downfield shift of the OH signal (5.20 ppm) and its independence on concentration. A *WC*- rather than *H*-type base pairing of **27**–**32** is suggested by the chemical shift for H–C(2/I) resonating at 8.28–8.38 ppm.

The SCCs of *Fig. 4* were analysed numerically by the method proposed by *Gutowsky* and *Saika* [45], including a value of 7.70 ppm for a 0.0001-mM solution. Including this value reduces the variance of K_{ass} (*cf.* also [5]). The SCC of the diol **32** was obtained from an oversaturated solution. After the spontaneous crystallisation of **32**, we could no longer obtain solutions exceeding a concentration of 2 mM of **32** in $CDCl_3$. The SCC of **32** could thus only be measured once and no *van't Hoff* analysis was carried out. The diol **32** ($K_{ass} = 28100$ M^{-1}) shows the strongest association, followed by the alcohols **30** (4294 M^{-1}), **28** (1529 M^{-1}), and **31** (1259 M^{-1}; *Table 3*). The fully *O*-protected **27** and **29** form linear associates, and associate only weakly, as expressed by K_{ass} values of 198 M^{-1} and 227 M^{-1}, respectively.

Thermodynamic parameters of **27**–**31** were determined by *van't Hoff* analysis of the ^{1}H-NMR spectra recorded for *ca.* 5-mM solutions in $CDCl_3$ in intervals of *ca.* 10° and in the temperature range of 7 to 50° (*Table 3*). Typical $-\Delta H$ values of 6–7 and of 5–6 kcal/mol were found for a *WC*- and *H*-type base pair of ethynylene-linked dimers [3]. The $-\Delta H$ values of 14.8 and 13.9 kcal/mol for **31** and **30**, respectively, agree well with a *WC*-type cyclic duplex, and the smaller $-\Delta H$ value of 12.5 kcal/mol for **28** agrees with a mixture of *WC*- and *H*-type cyclic duplexes. The even smaller ΔH values of **27** (8.9 kcal/mol) and **29** (10.0 kcal/mol) confirm the formation of only linear associates.

The chemical shift values for H–C(2′/I) of **29**–**31** (5.46–5.57 ppm; *Table 10* in the *Exper. Part*) and of the diol **32** (5.65 ppm) are distinctly smaller than those for *syn*-2′,3′-*O*-isopropylideneadenosines (5.70–5.80 ppm [3]). The upfield shift for the *C(8/I)*-unsubstituted S-linked dimer **27** may be rationalised by assuming a *syn*/*anti* equilibrium that is compatible with the formation of linear associates, and was similarly postulated above for the monomeric *S*-acetate **19**.

The *C(8/I)*-unsubstituted alcohol **28** forms mainly cyclic duplexes. A contribution of an *anti*-conformer is, therefore, improbable, similarly as for the *C(8/I)*-substituted

Table 3. *Association Constants* K_{ass} *as Calculated from the Concentration Dependence of* δ*(HN(3)) in* $CDCl_3$ *at 295 K for the U*[s]A(*) Dimers* **27**–**32** *and the A*[s]U(*) Dimers* **33**–**37** (including a value of 7.70 ppm for 0.0001 mM), *and Determination of the Thermodynamic Parameters by* van't Hoff *Analysis of the Temperature Dependence of* δ*(HN(3)) of* **27**–**31** *and* **33**–**37** *for* ca. *5-m*M *Solutions in* $CDCl_3$ *at 7–50°*

Dimer	K_{ass} [M^{-1}]	$-\Delta G_{295}$[a]) [kcal/mol]	$-\Delta H$ [kcal/mol]	$-\Delta S$ [cal/mol K]
U*[s]A(*) series				
27	198	3.1	8.9	19.6
28	1529	4.3	12.5	27.4
29	227	3.2	10.0	23.5
30	4294	4.9	13.9	31.1
31	1259	4.2	14.8	36.1
32	28100	6.0		
A*[s]U(*) series				
33	225	3.2	10.7	25.1
34	221	3.2	8.9	19.3
35	1334	4.2	10.9	24.4
36	658	3.8	12.4	28.9
37	3373	4.8	13.8	30.2

[a]) Calculated from K_{ass}.

29–**32**. The upfield shift for H–C(2′/I) of **28**–**32** is rationalized by assuming the formation of cyclic duplexes adopting a high-*syn*-conformation (as suggested by *Maruzen* models). The ribosyl unit I of all dimers **27**–**32** adopts predominantly a (*N*) conformation.

Unit I of the U*[s]A(*) dimers **27**–**32** adopts mainly the *gt*- and *tg*-conformations. The ratio of the conformers is strongly correlated with the nature of the substituent at C(5′) of unit II. The alcohols **28**, **30**, and **32** adopt the *gt*- or the *tg*-conformation to a larger extent than the silyl ethers **27**, **29**, and **31**, as evidenced by *J*(4′,5′a/I) (9.3–9.9 *vs.* 7.3–7.5 Hz; *Table 10* in the *Exper. Part*), *J*(4′,5′b/I) (3.0–3.6 *vs.* 5.0–5.7 Hz), and $\Delta\delta(H_a-C(5'/I)/H_b-C(5'/I))$ (0.36–0.59 *vs.* $\leq$0.08 ppm) values. The signals of the diastereotopic H–C(5′/I) were assigned on the basis of the relative volumes of the ROESY cross-peaks between H–C(3′/I) and either H_a–C(5′/I), or H_b–C(5′/I). A volume ratio of 1:1[13]) is calculated by assuming that the more deshielded H_a–C(5′/I) is $H_{pro\text{-}R}$ and by considering only the main *gt*-rotamer (*Fig. 5*). This ratio agrees rather well with the experimental ratio of 1:1.2. The assignment of the more deshielded H_a–C(5′/I) to $H_{pro\text{-}R}$ leads to a *gg*/*gt*/*tg* ratio of *ca.* 10:80:10 for the alcohols **28**, **30**, and **32**, and to one of *ca.* 10:55:35 for the silyl ethers **27**, **29**, and **31**, respectively. The converse assignment of the more deshielded H–C(5′/I) to $H_{pro\text{-}S}$ may be excluded, as it suggests a *tg*-conformation and a ROESY cross-peak between H–C(3′/I) and exclusively H_a–C(5′/I), and leads to a calculated volume ratio of 1:0.

---

[13]) For this qualitative estimation of the volume ratio, we assume that the distances between H–C(3′/II) and either H_{gg}–C(5′/II) or H_{gt}–C(5′/II) are identical, although MM3* modeling suggested a slightly shorter distance for H_{gg}–C(5′/II) (2.57 *vs.* 2.85 Å).

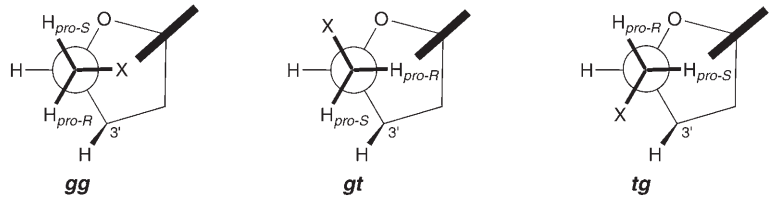

Fig. 5. *Staggered conformations about the C(4′)–C(5′) bond of C(5′)–O and C(5′)–S nucleosides* (X = OR or SR): *evaluation of short distances between H–C(3′) and either* $H_{pro\text{-}R}$–C(5′) *and* $H_{pro\text{-}S}$–*C(5′)*. Note the proximity of X and the nucleobase in the *gg* conformer, suggesting that the χ angle depends on the population of *gg*/*gt*/*tg* conformations.

The CD spectra of 1-mM solutions of **27**–**31** in $CHCl_3$ are characterised by a positive *Cotton* effect around 260 nm and by the absence of exciton splittings (*Fig. 6*). The ellipticities of these dimers are in the order of 10–40 mdeg, slightly weaker than the ellipticities that are typical for cyclic duplexes of ethynylene-linked dimers [3]. The CD spectra of the dimers **28**, **30**, and **31** that form cyclic duplexes show a decrease of the ellipticity with increasing temperature, denoting a moderate extent of π-stacking of their bases in the cyclic duplexes. The ellipticity of **27** and **29** is much less temperature-dependent, in agreement with a poor π-stacking of linear associates.

An UV melting curve, recorded at 260 nm for a 21-μM solution of the strongly associating diol **32** in $CHCl_3$ ($K_{ass} = 28100\ M^{-1}$) showed a melting temperature of 2° (*Fig. 7*). The hypochromicity at lower temperature evidences π-stacking and confirms the formation of cyclic duplexes in $CHCl_3$ solution.

The ^{1}H-NMR spectra of an oversaturated 20-mM solution of **32** in $CDCl_3$ evidence at least three different cyclic duplexes. The spectra show coalescence of the H–N(3) signals at 0° and the appearance of three H–N(3) *singlet*s at 14.52, 13.24, and *ca.* 12.45 ppm at −40°. The first two signals are quite sharp and of similar intensity, whereas the last one is broad and weak. They are assigned to a *WC*-type base-paired cyclic duplex (14.52 ppm), to a *H*-type base-paired cyclic duplex (12.45 ppm), and to a duplex (13.24 ppm) with either *WC*- or *H*-type base pairing. Overlapping signals below 9 ppm and line broadening prevent a thorough conformational analysis.

The π-stacking of the cyclic duplexes of **30** and **31** indicates that the distance of 5–6 Å between the base pairs, as suggested by *Maruzen* modeling, is reduced in reality. As the concomitant increase of the twist angle leads to a clash of the uridine ribosyl units in the $\underline{\underline{\mathbf{B}}}_{rWC\text{-}gt}$, but not in the $\underline{\underline{\mathbf{A}}}_{WC\text{-}gt}$ duplex, we restricted a refined modeling to $\underline{\underline{\mathbf{A}}}_{WC\text{-}gt}$, using the AMBER* programme (*Fig. 1*). Energy minimisation for this conformer led to a reduced distance of 3.25 Å between the base pairs and to a change of the high-*syn*-conformation of unit I to a classic *syn*-conformation, whereas the *WC* base pairing and the *gt*-conformation are retained (*Fig. 8* and *Table 4*). The θ and ι angles were only slightly altered, while the κ angle is increased to *ca.* −165° without, however, leading to a significant destabilisation [10]. The duplex fragment of **31**·**31** correponds to a right-handed helix with 6–7 base pairs per turn, and appears to be the main species among the cyclic duplexes of **31**.

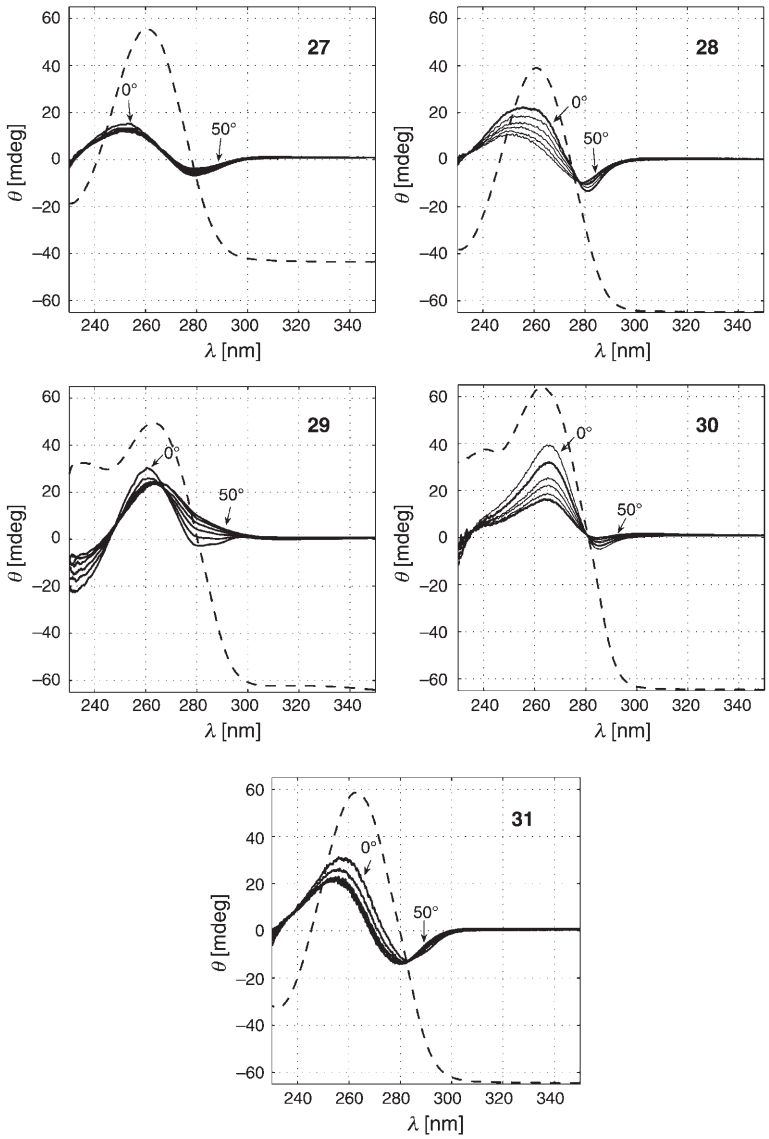

Fig. 6. *Temperature-dependent CD* (solid lines, in 10° steps from 0 to 50°) *and UV spectra* (dashed lines, arbitrary scale) *of the U*[s]A(*) dimers* **27**–**31** *for 1-mM solutions in* $CDCl_3$ (1-mm cell)

Unfortunately, attempts to obtain crystals of cyclic duplexes of U*[s]A(*) dimers failed. The diol **32** forms linear associates in the crystalline state (*Fig. 9,a*)[14]). Reverse

[14]) The crystallographic data have been deposited with the *Cambridge Crystallographic Data Centre* as deposition No. CCDC-600037. These data can be obtained free of charge *via* http://www.ccdc.cam.ac.uk/cgi-bin/catreq.cgi (or from the *Cambridge Crystallographic Data Centre*, 12 Union Road, Cambridge CB2 1EZ (fax: +44(1223)336033; e-mail: deposit@ccdc.cam.ac.uk).

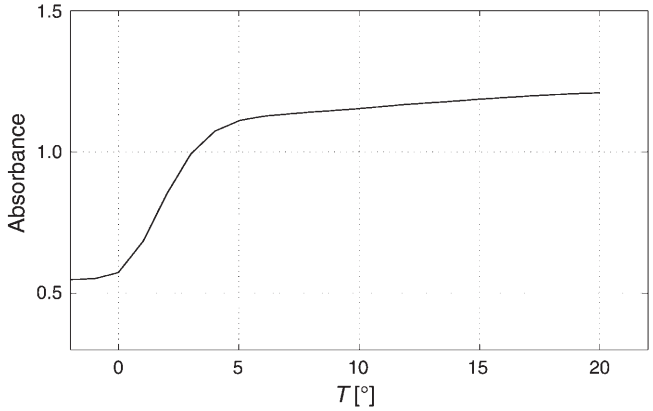

Fig. 7. *UV Melting curve* (at 260 nm) *of a 21-μM solution of the diol* **32** *in* $CHCl_3$

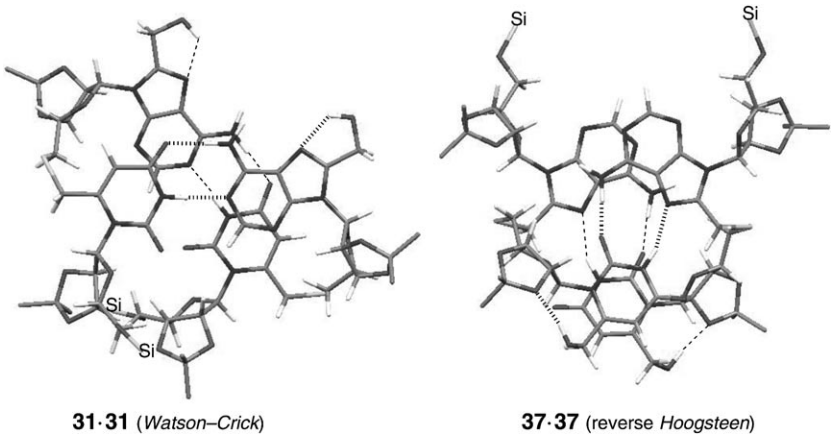

Fig. 8. *AMBER*-Modeled cyclic duplexes connected by* Watson–Crick (*i.e.*, **31**·**31**) *and reverse* Hoogsteen (*i.e.*, **37**·**37**) *base pairing*. For enhanced visibility, the substituents at Si-atoms and the isopropylidene H-atoms are omitted. Hashed and dashed lines indicate H-bonds of the base pair in the fore- and the background, respectively.

Hoogsteen base pairing leads to corrugated ribbons (*Fig. 9*, *b*, and *Table 5*). The ribbons are connected to each other by C(8/I)CH_2OH···N(3/I) H-bonds (*Fig. 9*, *c*). HO–C(5′/II) is not involved in intermolecular H-bonding, but forms an intramolecular bifurcated H-bond to O–C(4′/II) and O=C(2/II) (see [7] for a similar case). As expected, both nucleobases adopt a classic *syn*-conformation ($\chi = 66.4$ and 65.7°). The linking unit is characterised by a *gg*-conformation ($\eta_1 = 61.6°$, $\eta_2 = 178.8°$), *gauche* θ and κ angles (−85.2 and −77.1°, resp.), and an antiperiplanar ι angle (164.1°). On the basis of conformational analysis, the formation of a cyclic duplex would require interchanging the values of θ and ι. The ribose ring of unit I adopts a ^2E, and the ribose ring of unit II an $^OT_4$ conformation. There is no π-stacking in crystalline **32**; U and A are almost orthogonally arranged.

Table 4. *Selected Distances* [Å] *and Torsion Angles* [°] *for the* AMBER*-*Modeled Cyclic Duplexes Connected by* Watson–Crick (**31**·**31**) *and Reverse* Hoogsteen (**37**·**37**) *Base Pairs* (values related to the two base pairs or to the two dimers)

	31·**31** (*WC*)	**37**·**37** (r*H*)
Distance N(3)H···N(1 or 7)	1.76, 1.78	2.06, 2.16
Distance NH···O=C(4 or 2)	1.72, 1.70	1.66, 1.64
Distance OH···N(7)	1.91, 1.91	–, –
Distance OH···O(2′)	–, –	1.89, 1.87
Distance between base pairs	3.25	3.25
Twist *t* (residues per turn; helix sense)	+53 (6.8; right-handed)	−59 (6.1; left-handed)
χ/I	+67, +56	+46, +48
η_1	+77, +64	+80, +78
η_2	−165, −177	−162, −164
θ	−150, −148	−80, −80
ι	+71, +63	−68, −61
κ	−167, −162	−53, −47

4.2.2. *Association of the A*[s]U(*) Dimers.* The SCCs for H–N(3) were determined of 0.8–50-mM solutions of the A*[s]U(*) dimers **33** and **35**–**37**, and of 0.8–6-mM solutions of **34** in $CDCl_3$ (*Fig. 10*). The SCC of **38** could not be determined, since the solution formed a gel already at the low concentration of 2 mM.

All SCCs in *Fig. 10* reflect equilibria between the monoplex, linear associates, and/or cyclic duplexes. The SCC of the alcohol **37** with a free $HOCH_2$–C(6/I) approximates a plateau at a concentration of 15 mM, where VPO shows a degree of association of 1.8. Hence, this SCC reflects equilibria between the monoplex and mostly cyclic duplexes. The SCCs of **35** and **36** show a flattening above 30 mM, evidencing equilibria between monoplex, cyclic duplexes, and linear associates. This interpretation is corroborated by the apparent molecular mass for **36** at 26 mM, showing a degree of association of only 1.6. An even lower degree of association of 1.3 was determined for a 27-mM solution of **35**. A continuous increase of the SCC of **33** at concentrations >15 mM reveals equilibria between monoplex and linear associates. Identical SCCs of **33** and **34** at concentrations below 6 mM suggest similar equilibria also for **34**. In agreement with this interpretation, a considerable amount of these *C(6/I)*-unsubstituted dimers adopt an *anti*-conformation that is only compatible with the formation of linear associates, as evidenced by the upfield shift for H–C(2′/I) of **33** and **34** (see below).

At a concentration of 30 mM, δ(H–N(3/I) decreases from 12.2 ppm for **35** to 11.5 ppm for **36** and to 11.2 ppm for **37**. This suggests a large proportion of *WC*-type base-paired cyclic duplexes of **35** and a large proportion of *H*-type base-paired cyclic duplexes of **37**. Indeed, a cross-peak in the ROESY spectrum of **35** (7 mM) between H–N(3/I) and H–C(2/II) reveals a *WC*-type H-bonding. The *H*-type base pairing of **37** (15 mM) is evidenced by a cross-peak between H–N(3/I) and H_aC–C(8/II) resonating at 4.11 ppm and by the absence of a cross-peak between H–N(3/I) and H–C(2/II). The δ(H–N(3/I)) value of 11.2 ppm of **36** suggests an equilibrium of *WC*- and *H*-type cyclic duplexes, but the ROESY spectrum of **36** evidences only *WC*-type H-bonding, showing a cross-peak between H–N(3/I) and H–C(2/II) but none between H–N(3/I) and CH_2–C(8/II), as expected for a *H*-type cyclic duplex.

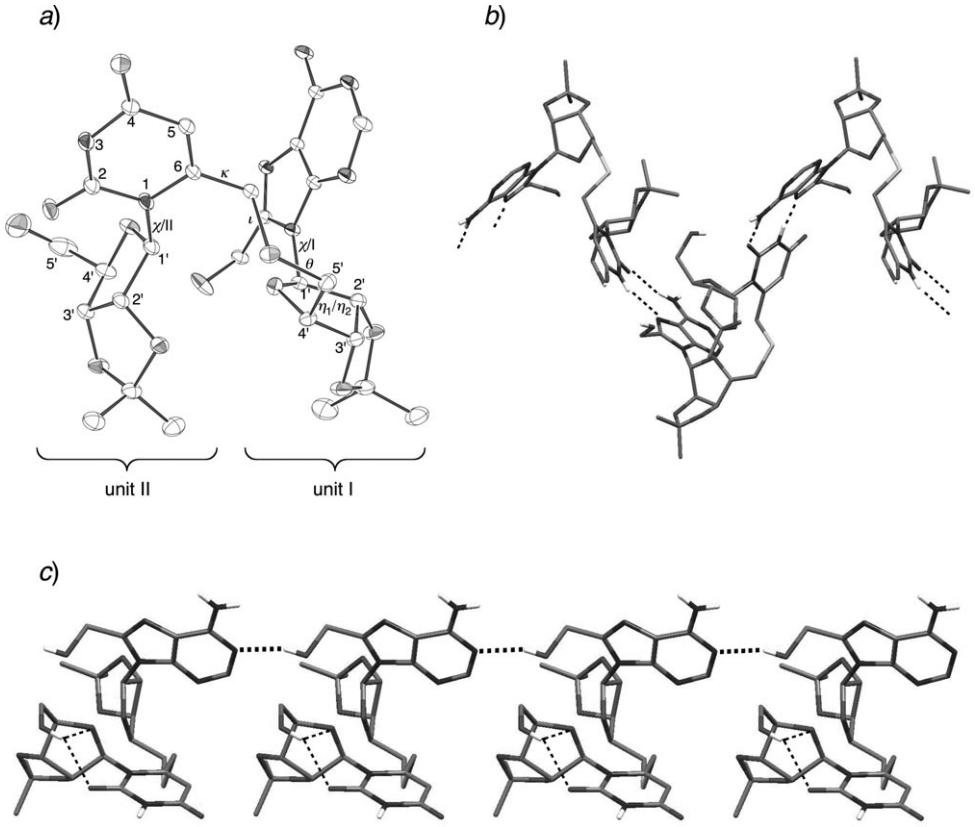

Fig. 9. *Crystal structure of* **32**: a) *ORTEP representation* (heavy atoms only) *of one molecule.* b) *Corrugated ribbon structure with r*H *base pairing* (dashed lines). c) *Inter-ribbon H-bonds between C(8/I)–CH$_2$OH and N(1/I)* (bold dashed line), *and bifurcated intramolecular H-bonds of HO–C(5′/II)* (narrow dashed lines).

The hydroxymethylated dimer **37** associates most strongly ($K_{ass} = 3373\ M^{-1}$), followed by **35** ($1334\ M^{-1}$), and **36** ($658\ M^{-1}$; *Table 3*). Small K_{ass} values of the *C(6/I)*-unsubstituted **33** ($225\ M^{-1}$), and **34** ($221\ M^{-1}$) suggest the formation of mainly linear duplexes. The $-\Delta H$ values determined by *van't Hoff* analysis of δ(H–N(3/I)) reflect cyclic *H*-type base-paired duplexes for **37** (13.8 kcal/mol), linear and cyclic *WC*-type base-paired duplexes for **35** (10.9 kcal/mol) and **36** (12.4 kcal/mol), and linear associates for **33** (10.7 kcal/mol) and **34** (8.9 kcal/mol).

A *ca.* 1:1 *syn*/*anti* orientation of the uracil moiety, similarly as observed for the C(5′)-*S*-acetyl monomer **9** is revealed by the chemical shift for H–C(2′/I) of the *C(6/I)*-unsubstituted dimers **33** (4.96 ppm) and **34** (5.01 ppm; *Table 12* in the *Exper. Part*). Conversely, a *syn*-conformation is revealed for the *C(6/I)*-substituted dimers **35** and **36**, H–C(2′/I) resonating at 5.17 and 5.19 ppm, respectively[15]). The variance of δ(H–C(2/

[15]) The slight upfield shift of H–C(2′/I) of **37** ($\Delta\delta = 0.1$ ppm) and the downfield shift of H–C(1′/I) ($\Delta\delta \approx 0.3$ ppm) must be due to close contacts in the *H*-type base-paired duplexes.

Table 5. *Distances* [Å] *and Bond Angles* [°] (N–H–O or N–H–N) *of Intermolecular H-Bonds, and Selected Torsion Angles* [Å] *of Crystalline* **32**

	H···X Distance [Å]	Bond angle [°]
N(6/I)–H···O=C(2/II)	2.03	173.0
N(7/I)···H–N(3/II)	2.13	161.7
C(8/I)CH_2O–H···N(7/I)	1.98	161.5
	Short notation	Torsion angle [°]
O(4′/I)–C(1′/I)–N(9/I)–C(4/I)	χ/I	+66.4
O(4′/II)–C(1′/II)–N(1/II)–C(2/I)	χ/II	+65.7
O(4′/I)–C(4′/I)–C(5′/I)–S	η_1	+61.6
C(3′/I)–C(4′/I)–C(5′/I)–S	η_2	+178.8
C(4′/I)–C(5′/I)–S–CH_2	θ	−85.2
C(5′/I)–S–CH_2–C(6/II)	ι	+164.1
S–CH_2–C(6/II)–N(1/II)	κ	−77.1
N(9/I)–C(8/I)–CH_2–O		+61.2
C(1′/I)–C(2′/I)–C(3′/I)–C(4′/I)		−29.0
C(2′/I)–C(3′/I)–C(4′/I)–O(4′/I)		+21.0
C(3′/I)–C(4′/I)–O(4′/I)–C(1′/I)		−3.3
C(1′/II)–C(2′/II)–C(3′/II)–C(4′/II)		+10.6
C(2′/II)–C(3′/II)–C(4′/II)–O(4′/II)		−24.1
C(3′/II)–C(4′/II)–O(4′/II)–C(1′/II)		+29.5

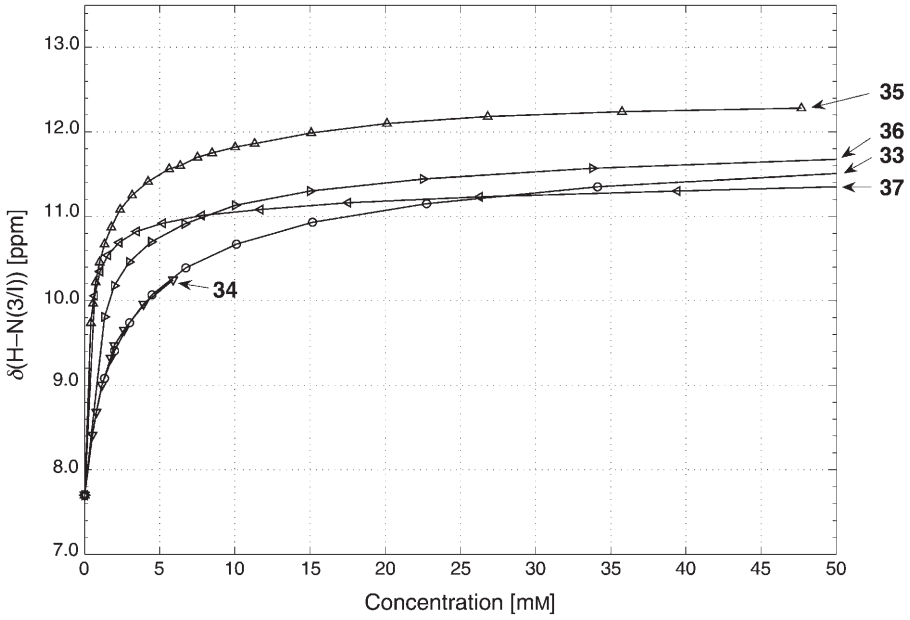

Fig. 10. *SSCs for H–N(3/I) of the A*[s]U′*) dimers* **33** *and* **35**–**37** (0.4–50 mM) *and* **34** (0.8–6 mM) *in $CDCl_3$ solution* (including a value of 7.70 ppm for a 0.0001-mM solution)

II)) of **33**–**37** (8.22–8.38 ppm) is small, and does not seem sufficiently sensitive to the *syn*/*anti* conformation to be of diagnostic value. The OH group of **37** gives rise to a broad *s* at 1.75–2.25 ppm, evidencing at best a weakly persistent H-bond to an etheral O-atom. The ribose moiety of unit I of **33**–**37** prefers a (*N*)-conformation. The relative chemical shifts of H–C(2/II) agree with a *WC*-type base pairing of **35** (8.38 ppm) and a *H*-type base pairing of **37** (8.22 ppm).

CD Spectra of the A*[s]U$^{(*)}$ dimers **33**–**37** were recorded of 1-mM solutions in $CHCl_3$ in the temperature range between 0 and 50° (*Fig. 11*). A positive *Cotton* effect at 270–280 nm is observed for the completely *O*-protected dimers **33** and **35**, whereas a negative *Cotton* effect characterizes the alcohols **34**, **36**, and **37**. No evidence of π-stacking is found for **33**, forming linear associates, and for **35** and **36**, forming a mixture of linear associates and cyclic *WC*-type base-paired duplexes. π-Stacking is, however, evidenced for **37** that forms cyclic *H*-type base-paired duplexes ($\theta \leq 50$ mdeg; a strong temperature dependence). Surprisingly, an even larger ellipticity (θ up to -60 mdeg) and a similar temperature dependence is observed for **34** which gelates $CHCl_3$ at concentrations above 6 mM. The similar shape of the CD curves of **37** and **34** suggests that **34** also forms (in part) cyclic duplexes possessing *H*-type base pairs.

A *ca.* 10:45:45 *gg*/*gt*/*tg* equilibrium of the *C(6/I)*-unsubstituted alcohol **34** is suggested by the equal *J*(4′,5′a/I) and *J*(4′,5′b/I) values (6.2 Hz). Substitution at C(6/I) leads to a preferred *syn*-conformation that disfavoures the *gg*-conformer. This is evidenced by the larger *J*(4′,5′a/I) and *J*(4′,5′b/I) values of the *C(6/I)*-substituted alcohol **36** (both 7.2 Hz) that characterize a *ca.* 1:1 *gt*/*tg* equilibrium. The *J*(4′,5′a/I) value of **35** and **37** is distinctly larger than *J*(4′,5′b/I) (8.4 and 8.2 *vs.* 5.7 and 4.0 Hz, resp.), in keeping with either a *gt*/*tg* or *tg*/*gt* ratio of *ca.* 2:1. On the basis of the small $\Delta\delta(H_a{-}C(5'/I)/H_b{-}C(5'/I))$ of ≤ 0.10 ppm, we assigned the more deshielded $H_a{-}C(5'/I)$ to $H_{pro\text{-}R}$. This assignment is corroborated by the *ca.* 1:2 volume ratio of the cross-peaks between H–C(3′/I), and both $H_a{-}C(5'/I)$ and $H_b{-}C(5'/I)$ in the ROESY spectrum of **35**. This ratio is in agreement with the expected 2:3 ratio for a 2:1 *gt*/*tg* mixture (with $H_a{-}C(5'/I)$ as $H_{pro\text{-}R}$; *Fig. 5*); the expected ratio for the opposite assignment is 3:1. Similarly to the U*[s]A$^{(*)}$ series, silylation of HO–C(5′/II) leads to a stronger preference for the *gt*-conformation of unit I.

In contradistinction to the sequence-isomeric **31**, the cyclic duplexes of the *C(6/I)*-hydroxymethylated dimer **37** prefer *H*-type base pairing and show strong π-stacking. According to *Maruzen* modeling, reduction of the distance between the base pairs is feasible for the $\underline{\underline{\mathbf{D}}}_{rH\text{-}gt}$-conformer, but not for the $\underline{\underline{\mathbf{D}}}_{H\text{-}gt}$-conformer (*Table 2*). AMBER* Minimisation of $\underline{\underline{\mathbf{D}}}_{rH\text{-}gt}$ led to a cyclic duplex **37**·**37** with a distance of 3.23 Å between the base pairs (*Fig. 8* and *Table 4*). The *gt*-conformation and a *gauche* ι angle are maintained, while the χ angle of unit I is changed from high-*syn* to *ca.* $+50°$, and the θ angle is changed from 180 to $-80°$. The OH group is involved in an intramolecular H-bond to O–C(2′/I), similarly as it was already observed in a r*H* base-paired A*[c_y]U$^{(*)}$ cyclic duplex [5]. Probably, this H-bond is responsible for the preferred r*H* base pairing. The **37**·**37** duplex forms the beginning of a right-handed helix with six base pairs per turn. Interestingly, the axis of the helix goes through the centre of the U pyrimidine ring, leading to a stronger π-stacking than in the *WC* base-paired **31**·**31**.

Thus, the experimental findings are in agreement with the results of the conformational analysis, and, while both oxymethylene and thiomethylene-linked

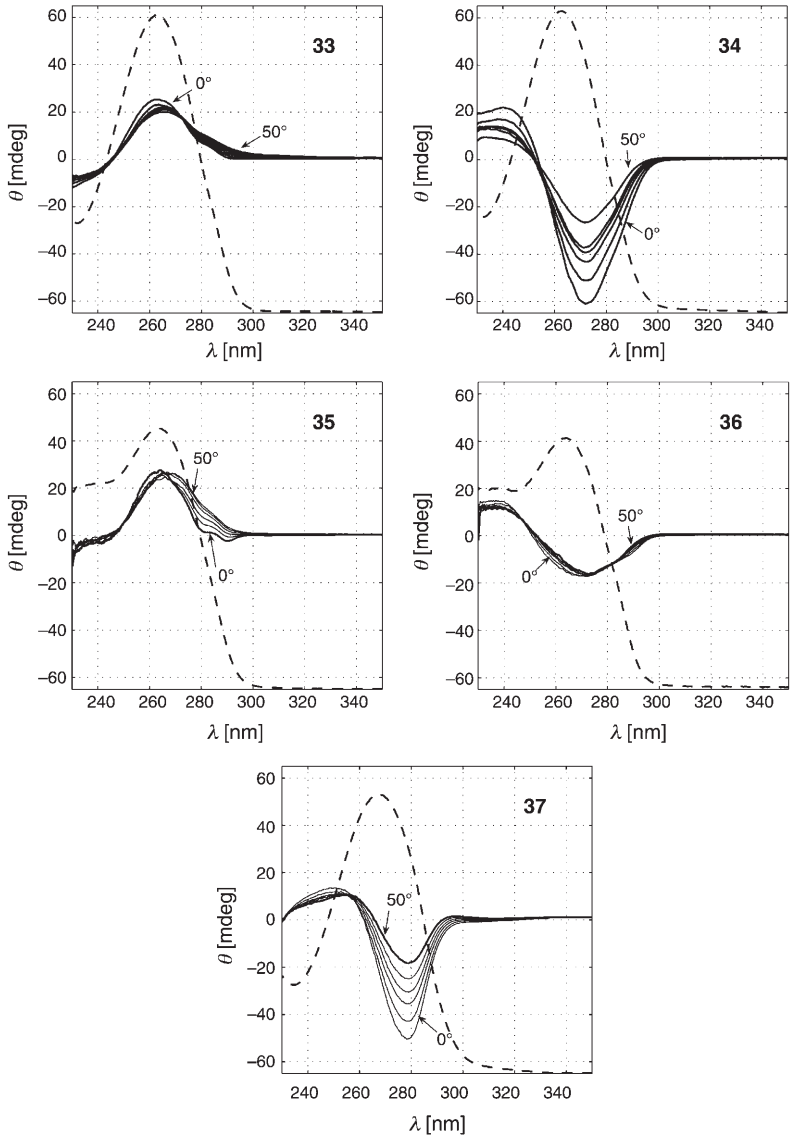

Fig. 11. *Temperature-dependent CD* (solid lines, in 10° steps from 0 to 50°) *and UV spectra* (dashed lines, arbitrary scale) *of the A*[s]U(*) dimers* **33**–**37** *for 1-mM solutions in* $CDCl_3$ (1-mm cell)

self-complementary dimers may pair, their cyclic duplexes adopt different conformations.

4.2.3. *^{1}H-NMR Parameters of U*[s]A(*) and A*[s]U(*) Dimers That Are Little Influenced by Association.* The ribosyl unit II of the U*[s]A(*) dimers **27**–**32** that is not directly involved in the formation of cyclic duplexes prefers an (*N*)-conformation ($J(1',2')/J(3',4') = 0.22-0.36$). The downfield shift for H–C(2′/II) of **27**–**29** and **31**

(5.16–5.28 ppm) evidences a classic *syn*-conformation. The upfield shift for H–C(2′/II) of the alcohols **30** and **32** (5.04 and 5.11 ppm) is rationalized by an intramolecular H-bond to O=C(2/II) and/or O–C(4′/II). The C(5′/II)-*O*-silyl ethers **27**, **29**, and **31** prefer the *gt*-conformation over the similarly populated *gg*- and *tg*-conformations (J(4′,5′a/II) = 5.4–5.8, J(4′,5′b/II) = 7.2–7.9 Hz), while the alcohol **28** prefers strongly the *gg*-conformation, as evidenced by J(4′,5′a/II) = J(4′,5′b/II) = 3.9 Hz. A *ca.* 1:1 *gg*/*tg* equilibrium of **30** and **32** is suggested by the observation that J(4′,5′a/II) is larger than J(4′,5′b/II) (6.0 and 6.9 *vs.* 2.4 and 2.7 Hz, resp.), but this interpretation rests on the correct assignment of the more deshielded H_a–C(5′/II) to $H_{pro\text{-}S}$ [38–41]. This assignment should be revised for **27**–**32**, and the relative chemical shifts of $H_{pro\text{-}R}$ and $H_{pro\text{-}S}$ should be inverted. The preference for the *tg*- over the *gt*-conformation is not in agreement with the *gauche* effect that favours the *gt*-conformation. Also, only HO–C(5′/II) of the *gt*, but not of the *tg*-conformer can form an intramolecular H-bond to O–C(4′/II). In a *gt*-conformation, $H_{pro\text{-}R}$–C(5′/II), usually resonating at higher field, is in close contact to O=C(2/II) (see *Fig. 5*), and this may well lead to a downfield shift and to an inversion of the relative chemical shifts of $H_{pro\text{-}R}$–C(5′/II) and $H_{pro\text{-}S}$–C(5′/II)[16]). This revised assignment is in agreement with a 1.7:1 ratio of the volumes of the cross-peaks between H–C(3′/II), and either H_a–C(5′/II) or H_b–C(5′/II) in the ROESY spectrum of **30**. This ratio is in agreement with the 2:1 volume ratio that is predicted if one assumes H_a–C(5′/II) to be $H_{pro\text{-}R}$ and a 1:1 *gg*/*gt* equilibrium (see *Fig. 5*), while a 1:1 volume ratio is predicted if one assumes H_b–C(5′/II) to be $H_{pro\text{-}R}$ and a 1:1 *gg*/*tg* equilibrium.

The alcohols **34** and **36** possess a completely persistent intramolecular H-bond to N(3) and show similar characteristics as the monomeric alcohol **24**. Also the silyl ethers **33**, **35**, and **36** show similar characteristics as the monomeric silyl ethers **22** and **23**, with the exception of a stronger downfield shift for H–C(2′/II) of **35** (6.01 ppm) which must be due to either an anisotropy effect or a close contact to a polar substituent in the cyclic duplex.

We thank the *ETH-Zürich* and *F. Hoffmann-La Roche AG*, Basel, for generous support, Mrs. *B. Brandenberg* for recording the 2D-NMR spectra, Mr. *P. Seiler* for the determination of the X-ray structure, and Mr. *M. Schneider* for the VPO measurements.

Experimental Part

General. Solvents were distilled: THF from Na/benzophenone, CH_2Cl_2, MeOH, DMF, pyridine, (i-Pr)$_2$NH, and EtN(i-Pr)$_2$ from CaH_2. Reactions were run under Ar or N_2. Qual. TLC: precoated silica-gel plates (*Merck* silica gel *60 F254*); detection by spraying with 'mostain' and heating. Flash chromatography (FC): silica gel *Merck 60* (0.04–0.063 mm). Optical rotations: 1-dm cell at 25° and 589 nm. The temp.-dependent CD (10° steps from 0° to 50°) and UV spectra (20°) were recorded of 1-mM solns. in $CDCl_3$ in a 1-mm *Suprasil* cell. FT-IR: 1–2% soln. in the indicated solvent or in KBr. ^{1}H- and ^{13}C-NMR spectroscopy: at 300 or 500 MHz and 75 or 125 MHz, resp. MS: matrix-assisted laser desorption ionization time-of-flight mass spectrometry (MALDI-TOF) with 0.05M indol-3-acrylic-acid (IAA) in THF, or with 0.05M α-cyano-4-hydroxycinnamic acid (CCA) in MeCN/EtOH/H_2O, and HR-MALDI-MS with 0.05M 2,5-dihydrobenzoic acid (DHB) in THF.

---

16) This change of the relative chemical shifts of $H_{pro\text{-}R}$–C(5′) and $H_{pro\text{-}S}$–C(5′) should only be observed if there is a large *gt*/*tg* ratio.

General Procedure for NMR Studies. NMR Experiments were performed at 295 K and at 300 MHz in $CDCl_3$ (passed through basic aluminium oxide immediately prior to use). Experiments started at the highest concentration, with stepwise replacement of 0.2 ml of the 0.6 ml soln. with 0.2 ml of $CDCl_3$. The data were analysed by non-linear least-squares fitting using MATLAB (trust-region algorithm); the parameters were K_{ass}, δ(H–N(3), $c = 0$ mM), and δ(H–N(3/I or II), $c = \infty$). The thermodynamic parameters were determined by *van't Hoff* analysis. The uracil δ(H–N(3)) was monitored at 7, 15, 22, 30, 40, and 50°, and at a fixed concentration (typically 5 to 10 mM).

5′-O-[Dimethyl(1,1,2-trimethylpropyl)silyl]-2′,3′-O-isopropylideneuridine (**8**). A suspension of **7** [46] (20.0 g, 70.4 mmol) in DMF (50 ml) was treated with 1*H*-imidazole (9.56 g, 68.1 mmol) and dropwise with 'thexyldimethylsilyl chloride' (TDSCl; dimethyl(1,1,2-trimethyl)silyl chloride; 15.2 ml, 77.4 mmol). The mixture was stirred for 4 h at 23°. Volatiles were removed. A soln. of the residue in CH_2Cl_2 was washed with brine, dried ($MgSO_4$), and evaporated. The residue was dried 24 h under high vacuum to yield **8** (30 g, > 98%). Colourless powder. R_f (AcOEt/cyclohexane 1:1) 0.43. M.p. 56.7–57.7°. $[\alpha]_D^{25} = -18.1$ ($c = 1.0$, $CHCl_3$). IR ($CHCl_3$): 3392*w*, 2961*m*, 2869*w*, 1715*m*, 1694*s*, 1636*w*, 1458*m*, 1386*w*, 1263*m*, 1156*w*, 1127*m*, 1086*m*, 969*w*, 836*m*. ^{1}H-NMR (300 MHz, $CDCl_3$): see *Table 6*; additionally, 9.75 (br. *s*, NH); 1.60 (*sept.*, $J = 6.9$, Me_2CH); 1.55, 1.32 (2*s*, Me_2CO_2); 0.84 (*d*, $J = 6.9$, Me_2CH); 0.82 (*s*, Me_2CSi); 0.10, 0.09 (2*s*, Me_2Si). ^{13}C-NMR (75 MHz, $CDCl_3$): see *Table 7*; additionally, 114.05 (*s*, Me_2CO_2); 33.99 (*d*, Me_2CH); 27.29, 25.37 (2*q*, Me_2CO_2); 25.37 (*s*, Me_2CSi); 20.33, 20.23 (2*q*, Me_2CSi); 18.52, 18.48 (2*q*, Me_2CH); –3.28, –3.46 (2*q*, Me_2Si). HR-MALDI-MS: 449.2074 ($[M+Na]^+$, $C_{20}H_{34}N_2NaO_6Si^+$; calc. 449.2084). Anal. calc. for $C_{20}H_{34}N_2O_6Si$ (426.22): C 56.31, H 8.03, N 6.57; found: C 56.19, H 7.95, N 6.51.

Table 6. *Selected ^{1}H-NMR Chemical Shifts* [ppm] *and Coupling Constants* [Hz] *of Uridine Monomers* **8**–**16** in *$CDCl_3$*

	8	**9**	**10**	**11**	**12**	**13**	**14**	**15**	**16**
H–C(5)	5.67	5.72	5.73	5.81	5.88	5.75	5.79	5.72	5.71
H–C(6)	7.62	7.24	7.27	–	–	–	–	–	–
CH_a–C(6)	–	–	–	4.53	5.11	4.02	4.04	4.01	4.02
CH_b–C(6)	–	–	–	4.47	5.04	3.97	3.95	3.95	3.96
H–C(1′)	5.95	5.55	5.63	5.77	5.58	5.59	5.53	5.60	5.65
H–C(2′)	4.73	5.01	5.00	5.19	5.23	5.20	5.21	5.20	5.19
H–C(3′)	4.67	4.71	4.82	4.79	4.80	4.77	4.99	4.81	4.87
H–C(4′)	4.26	4.17	4.36	4.13	4.10	4.00	4.12	4.03	4.15
H_a–C(5′)	3.87	3.27	4.35	3.83	3.79	3.76	3.85	3.25	4.35
H_b–C(5′)	3.76	3.22	4.27	3.79	3.75	3.71	3.77	3.21	4.21
J(5,6)	8.1	8.1	8.1	–	–	–	–	–	–
J(5,NH)	[a])	1.5	[a])	[a])	[a])	1.5	[a])	2.1	1.9
J(H_a,H_b)	–	–	–	14.5	12.3	12.6	12.6	12.6	12.6
J(1′,2′)	3.0	1.8	2.0	0.9	0.9	0.9	2.1	0.9	0.9
J(2′,3′)	6.3	6.6	6.4	6.5	6.6	6.3	6.6	6.3	6.5
J(3′,4′)	2.7	3.9	3.8	4.6	4.5	4.4	4.2	4.2	4.2
J(4′,5′a)	2.4	6.6	3.7	5.1	5.4	5.4	3.9	6.9	3.4
J(4′,5′b)	3.6	6.6	7.2	6.0	6.9	7.5	3.9	7.2	7.8
J(5′a,5′b)	11.7	13.5	12.6	11.1	10.8	11.4	11.4	13.5	10.5

[a]) Not assigned.

5′-S-Acetyl-2′,3′-O-isopropylidene-5′-thiouridine (**9**). A soln. of **7** [46] (2.00 g, 7.04 mmol) in pyridine (15 ml) under N_2 was cooled to –15°, treated with TsCl (1.47 g, 7.74 mmol), stirred for 1 h at –15° and for 15 h at 23°, diluted with CH_2Cl_2, and washed with 0.1M H_2SO_4, sat. $NaHCO_3$ soln., and brine. The

Table 7. *Selected ^{13}C-NMR Chemical Shifts* [ppm] *of the Uridine Monomers* **8**, **9**, *and* **11**–**16** *in* $CDCl_3$

	8	**9**	**11**	**12**	**13**	**14**	**15**	**16**
C(2)	150.06	149.96	150.39	150.03	150.32	151.18	150.77	150.53
C(4)	163.34	163.68	163.88	163.53	163.29	162.99	163.69	163.27
C(5)	102.19	102.59	101.17	104.58	102.44	103.07	102.97	102.92
C(6)	140.46	142.74	155.48	147.80	152.72	152.31	152.38	152.39
CH_2–C(6)	–	–	60.57	63.81	62.17	62.23	62.29	62.23
C(1′)	91.72	95.18	91.15	92.03	91.93	92.19	92.18	91.97
C(2′)	85.11	84.51	84.10	84.05	84.12	83.35	84.91	84.55
C(3′)	80.23	83.32	81.86	81.92	82.12	80.36	84.29	81.97
C(4′)	86.46	86.49	89.33	89.50	89.21	87.43	87.86	86.50
C(5′)	63.13	31.28	63.93	64.31	64.01	62.69	31.50	64.74

combined org. layers were dried ($MgSO_4$) and taken to dryness at 30°. A soln. of the residue (2.68 g) in DMF (10 ml) was treated with AcSK (2.08 g, 18.2 mmol), stirred for 1 h at 40° and for 2 h at 75°, and freed of volatiles. A soln. of the residue in AcOEt was washed with H_2O and brine, dried ($MgSO_4$), and evaporated. FC (AcOEt/cyclohexane 1:3 → 1:1) gave **9** (1.25 g, 70%). Slightly pink foam. R_f (AcOEt) 0.58. $[\alpha]_D^{25} = +17.5$ ($c = 1.0$, $CHCl_3$). IR ($CHCl_3$): 3388*w*, 3026*w*, 3015*w*, 2938*m*, 1716*s*, 1696*s*, 1634*w*, 1454*m*, 1384*m*, 1271*w*, 1251*w*, 1157*w*, 1132*w*, 1091*m*, 969*w*, 881*w*, 860*m*. ^{1}H-NMR (300 MHz, $CDCl_3$): see *Table 6*; additionally, 10.06 (br. *s*, NH); 7.24 (*d*, $J = 8.1$, H–C(6)); 2.33 (*s*, AcS); 1.51, 1.31 (2*s*, Me_2C). ^{13}C-NMR (75 MHz, $CDCl_3$): see *Table 7*; additionally, 194.43 (*s*, SC=O); 114.43 (*s*, Me_2C); 30.67 (*q*, *Me*C=O); 27.10, 25.29 (2*q*, Me_2C). HR-MALDI-MS: 365.0783 ($[M+Na]^+$, $C_{14}H_{18}N_2NaO_6S^+$; calc. 365.0784).

*5′-*O*-[Dimethyl(1,1,2-trimethylpropyl)silyl]-6-(hydroxymethyl)-2′,3′-*O*-isopropylideneuridine* (**11**). A soln. of $(i\text{-}Pr)_2NH$ (50.3 ml, 359 mmol) in THF (300 ml) was cooled to −70°, treated dropwise with 1.6M BuLi in hexane (220 ml, 352 mmol), stirred for 15 min, warmed to 0°, stirred for 15 min, and cooled again to −70°. A soln. of **8** (30.0 g, 70.4 mmol) in THF (300 ml) was added dropwise. The soln. was stirred at −70° for 1 h, treated dropwise with DMF (135 ml, 1.76 mol), stirred for 2.5 h, treated dropwise with AcOH (42 ml), and allowed to warm to 23°. The mixture was diluted with EtOH (300 ml), treated with $NaBH_4$ (8.5 g, 225 mmol), stirred 30 min. and freed of volatiles. A soln. of the residue in CH_2Cl_2 was washed with H_2O and brine, dried ($MgSO_4$), and evaporated. FC (AcOEt/cyclohexane 1:1) gave **11** (26.0 g, 80%). Colourless foam. R_f (AcOEt/cyclohexane 1:1) 0.23. M.p. 66.3–67.2°. $[\alpha]_D^{25} = +15.0$ ($c = 1.0$, $CHCl_3$). IR ($CHCl_3$): 3607*w*, 3390*w* (br.), 2961*m*, 2870*w*, 1698*s*, 1458*w*, 1383*m*, 1255*w*, 1158*w*, 1083*m*, 973*w*, 877*w*, 837*m*, 767*w*. ^{1}H-NMR (300 MHz, $CDCl_3$): see *Table 6*; additionally, 9.95 (br. *s*, NH); 4.18–3.98 (br. *s*, OH); 1.60 (*sept.*, $J = 6.9$, Me_2CH); 1.53, 1.32 (2*s*, Me_2CO_2); 0.84 (*d*, $J = 6.9$, Me_2CH); 0.82 (*s*, Me_2CSi); 0.09, 0.07 (2*s*, Me_2Si). ^{13}C-NMR (75 MHz, $CDCl_3$): see *Table 7*; additionally, 113.70 (*s*, Me_2CO_2); 34.08 (*d*, Me_2CH); 27.26, 25.35 (2*q*, Me_2CO_2); 25.35 (*s*, Me_2CSi); 20.39, 20.35 (2*q*, Me_2CSi); 18.52 (*q*, Me_2CH); −3.16 (*q*, Me_2Si). MALDI-MS: 479.219 ($[M+Na]^+$, $C_{21}H_{36}N_2NaO_7Si^+$; calc. 479.218).

*5′-*O*-[Dimethyl(1,1,2-trimethylpropyl)silyl]-2′,3′-*O*-isopropylidene-6-[(methylsulfonyloxy)methyl]-uridine* (**12**). A soln. of **11** (0.502 g, 1.1 mmol) in CH_2Cl_2 (15 ml) under N_2 was cooled to −15°, treated dropwise with Et_3N (0.34 ml, 2.4 mmol), stirred for 5 min, and treated dropwise over 10 min. with a soln. of Ms_2O (0.383 g, 2.2 mmol) in CH_2Cl_2 (10 ml). The mixture was stirred for 15 min, diluted with CH_2Cl_2 (30 ml), washed with brine at 0°, dried ($MgSO_4$), and evaporated. FC (AcOEt/cyclohexane 1:4 → 1:1) gave **12** (480 mg, 82%). Colourless foam. R_f (AcOEt/cyclohexane 1:1) 0.30. $[\alpha]_D^{25} = +2.7$ ($c = 1.0$, $CHCl_3$). IR ($CHCl_3$): 3386*w*, 3027*w*, 2961*m*, 1703*s*, 1458*w*, 1377*m*, 1354*m*, 1266*w*, 1178*w*, 1084*m*, 1011*w*, 965*w*, 875*w*, 839*m*. ^{1}H-NMR (300 MHz, $CDCl_3$): see *Table 6*; additionally, 8.61 (br. *s*, NH); 3.16 (*s*, MsO); 1.60 (*sept.*, $J = 6.9$, Me_2CH); 1.54, 1.34 (2*s*, Me_2CO_2); 0.86 (*d*, $J = 6.9$, Me_2CH); 0.83 (*s*, Me_2CSi); 0.09, 0.08 (2*s*, Me_2Si). ^{13}C-NMR (75 MHz, $CDCl_3$): see *Table 7*; additionally, 113.88 (*s*, Me_2CO_2); 38.60 (*q*, MsO); 34.15 (*d*, Me_2CH); 27.29, 25.49 (2*q*, Me_2CO_2); 25.36 (*s*, Me_2CSi); 20.44, 20.39 (2*q*, Me_2CSi); 18.61, 18.57

(2*q*, *Me*$_2$CH); −3.16 (*q*, Me$_2$Si). HR-MALDI-MS: 557.197 ([*M* + Na]$^+$, $C_{22}H_{38}N_2NaO_9SSi^+$; calc. 557.196).

5′-O-[Dimethyl(1,1,2-trimethylpropyl)silyl]-2′,3′-O-isopropylidene-6-{[(4-methoxyphenyl)diphenylmethoxy]methyl}uridine (**13**). A soln. of **11** (8.00 g, 17.6 mmol) in CH_2Cl_2 (50 ml) under N_2 was cooled to 0°, treated dropwise with EtN(i-Pr)$_2$ (5.80 ml, 35.2 mmol), stirred for 10 min, and treated dropwise with a soln. of 4-monomethoxytrityl chloride (10.6 g, 35.2 mmol; → dark green soln.). The mixture was stirred for 20 min at 0° and for 4 h at 23°, diluted with CH_2Cl_2 (200 ml), washed with sat. NH_4Cl soln. and brine, dried ($MgSO_4$), and evaporated. FC (AcOEt/cyclohexane 1:9) gave **13** (10.2 g, 80%). Colourless foam. R_f (AcOEt/cyclohexane 1:4) 0.38. $[\alpha]_D^{25} = -6.0$ ($c = 1.0$, $CHCl_3$). IR ($CHCl_3$): 3389*w*, 3007*w*, 2936*m*, 2868*w*, 1694*s*, 1606*w*, 1510*m*, 1448*m*, 1381*m*, 1253*m*, 1156*w*, 1068*m*, 1034*m*, 978*w*, 878*w*, 833*m*. ^{1}H-NMR (300 MHz, $CDCl_3$): see *Table 6*; additionally, 9.76 (br. *s*, NH); 7.50–7.23 (*m*, 12 arom. H); 6.89–6.81 (*d*, $J = 8.7$, 2 arom. H); 3.81 (*s*, MeO); 1.60 (*sept.*, $J = 6.9$, Me$_2$C*H*); 1.43, 1.30 (2*s*, Me$_2$CO$_2$); 0.85 (*d*, $J = 6.9$ *Me*$_2$CH); 0.83 (*s*, Me$_2$CSi); 0.07, 0.06 (2*s*, Me$_2$Si). ^{13}C-NMR (75 MHz, $CDCl_3$): see *Table 7*; additionally, 158.82, 143.13, 142.98, 134.04 (4*s*); 130.26 (2*d*); 128.13 (2*d*); 128.02 (4*d*); 127.96 (2*d*); 127.32 (2*d*); 113.33 (2*d*); 113.33 (*s*, Me$_2$*C*O$_2$); 88.22 (*s*, Ph$_2$*C*); 55.27 (*q*, MeO); 34.14 (*d*, Me$_2$*C*H); 27.28, 25.52 (2*q*, *Me*$_2$CO$_2$); 25.37 (*s*, Me$_2$*C*Si); 20.46, 20.42 (2*q*, *Me*$_2$CSi); 18.59, 18.55 (2*q*, *Me*$_2$CH); −3.14, −3.16 (2*q*, Me$_2$Si). HR-MALDI-MS: 751.3378 ([*M* + Na]$^+$, $C_{41}H_{52}N_2NaO_8Si^+$; calc. 751.3391).

2′,3′-O-Isopropylidene-6-{[(4-methoxyphenyl)diphenylmethoxy]methyl}uridine (**14**). A suspension of **13** (2.00 g, 2.75 mmol) and 4-Å mol. sieves in THF (20 ml) was stirred for 15 min at 23°, treated dropwise with a soln. of $Bu_4NF \cdot 3\,H_2O$ (2.60 g, 8.25 mmol) in THF (10 ml), stirred for 4 h at 23°, and filtered. Evaporation and FC (AcOEt/cyclohexane 1:1 → 4:1) gave **14** (1.35 g, 84%). Colourless foam. R_f (AcOEt/cyclohexane 1:1) 0.12. $[\alpha]_D^{25} = -22.1$ ($c = 1.0$, $CHCl_3$). IR ($CHCl_3$): 3606*w*, 3476*w*, 3389*w*, 3019*w*, 2957*m*, 2937*w*, 1697*s*, 1629*w*, 1608*w*, 1510*w*, 1449*w*, 1384*m*, 1248*w*, 1156*w*, 1103*m*, 1070*m*, 1035*w*, 978*w*, 838*w*. ^{1}H-NMR (300 MHz, $CDCl_3$): see *Table 6*; additionally, 8.81 (br. *s*, NH); 7.49–7.42 (*m*, 4 arom. H); 7.37–7.23 (*m*, 8 arom. H); 6.85 (*d*, $J = 8.7$, 2 arom. H); 3.79 (*s*, MeO); 3.21 (br. *s*, OH); 1.38, 1.29 (2*s*, Me$_2$C). ^{13}C-NMR (75 MHz, $CDCl_3$): see *Table 7*; additionally, 158.83, 143.08, 142.93, 133.96 (4*s*); 130.24 (2*d*); 128.09 (2*d*); 128.02 (4*d*); 127.97 (2*d*); 127.33 (2*d*); 113.92 (*s*, Me$_2$*C*); 113.34 (2*d*); 88.24 (*s*, Ph$_2$*C*); 55.27 (*q*, MeO); 27.31, 25.33 (2*q*, *Me*$_2$C). HR-MALDI-MS: 609.2215 ([*M* + Na]$^+$, $C_{33}H_{34}N_2NaO_8^+$; calc. 609.2213).

5′-S-Acetyl-2′,3′-O-isopropylidene-6-{[(4-methoxyphenyl)diphenylmethoxy]methyl}-5′-thiouridine (**15**). A soln. of **14** (1.50 g, 2.5 mmol) in CH_2Cl_2 (1 ml) under N_2 was cooled to 0°, treated with a soln. of DMAP (625 mg, 5.1 mmol) in CH_2Cl_2 (2 ml), stirred for 5 min, treated with TsCl (729 mg, 3.8 mmol), stirred for 1 h at 0° and for 1 h at 10°, and poured into a sat. NH_4Cl soln. After extraction with AcOEt, the combined org. layers were washed with brine, dried ($MgSO_4$), and evaporated at 30°. A soln. of the residue in DMF (4 ml) was treated with AcSK (2.80 g, 25 mmol), stirred for 1 h at 40° and for 2 h at 75°, and evaporated. A soln. of the residue in AcOEt was washed with H_2O and brine, dried ($MgSO_4$), and evaporated. FC (AcOEt/cyclohexane 1:3 → 1:1) gave **15** (1.20 g, 75%). Slightly pink foam. R_f (AcOEt/cyclohexane 1:1) 0.26. $[\alpha]_D^{25} = +0.04$ ($c = 1.0$, $CHCl_3$). IR ($CHCl_3$): 3388*w*, 3017*m*, 2932*w*, 2835*w*, 1695*s*, 1608*w*, 1511*m*, 1449*m*, 1384*m*, 1301*w*, 1255*w*, 1157*w*, 1093*m*, 1068*m*, 1035*m*, 979*w*, 909*w*, 878*w*, 838*w*. ^{1}H-NMR (300 MHz, $CDCl_3$): see *Table 6*; additionally, 8.42 (br. *s*, NH); 7.49–7.43 (*m*, 4 arom. H); 7.37–7.25 (*m*, 8 arom. H); 6.85 (*d*, $J = 8.7$, 2 arom. H); 3.81 (*s*, MeO); 2.34 (*s*, AcS); 1.41, 1.29 (2*s*, Me$_2$C). ^{13}C-NMR (75 MHz, $CDCl_3$): see *Table 7*; additionally, 193.63 (*s*, S–C=O); 158.84, 143.10, 142.94, 133.96 (4*s*); 130.27 (2*d*); 128.12 (2*d*); 128.02 (4*d*); 127.98 (2*d*); 127.33 (2*d*); 113.56 (*s*, Me$_2$*C*); 113.34 (2*d*); 88.23 (*s*, Ph$_2$*C*); 55.26 (*q*, MeO); 30.65 (*q*, *Me*C=O); 27.13, 25.36 (2*q*, *Me*$_2$C). HR-MALDI-MS: 667.2089 ([*M* + Na]$^+$, $C_{35}H_{36}N_2NaO_8S^+$; calc. 667.2085).

5′-O-Acetyl-2′,3′-O-isopropylidene-6-{[(4-methoxyphenyl)diphenylmethoxy]methyl}uridine (**16**). A soln. of **14** (150 mg, 0.26 mmol) in pyridine (1 ml) under N_2 was treated with Ac_2O (47 µl, 0.52 mmol) and stirred for 48 h at 24°. The soln. was diluted with AcOEt (50 ml), washed with sat. NH_4Cl soln. and brine, dried ($MgSO_4$), and evaporated. FC (AcOEt/cyclohexane 1:3 → 1:1) gave **16** (132 mg, 81%). White foam. R_f (AcOEt/cyclohexane 7:3) 0.63. $[\alpha]_D^{25} = -6.3$ ($c = 1.0$, $CHCl_3$). IR ($CHCl_3$): 3408*w*, 3063*w*, 3018*m*, 2936*w*, 1741*m*, 1709*m*, 1614*s*, 1589*m*, 1510*m*, 1462*m*, 1449*m*, 1427*m*, 1374*m*, 1252*s*, 1180*m*, 1156*w*, 1072*s*, 1037*m*, 978*w*, 900*w*, 864*w*, 835*w*. ^{1}H-NMR (300 MHz, $CDCl_3$): see *Table 6*; additionally, 9.24 (br. *s*, NH); 7.45–7.49 (*m*, 4 arom. H); 7.23–7.38 (*m*, 8 arom. H); 6.83–6.88 (*m*, 2 arom. H); 3.81 (*s*, MeO); 2.07

(*s*, AcO); 1.44, 1.31 (2*s*, Me_2C). ^{13}C-NMR (75 MHz, $CDCl_3$): see *Table 7*; additionally, 170.60 (*s*, O–C=O); 158.98, 143.19, 143.01, 134.02 (4*s*); 130.36 (2*d*); 128.19 (4*d*); 128.07 (2*d*); 128.01 (2*d*); 127.40 (2*d*); 113.56 (*s*, Me_2C); 113.36 (2*d*); 88.25 (*s*, Ph_2C); 55.29 (*q*, MeO); 20.83 (*q*, *Me*C=O); 27.11, 25.30 (2*q*, Me_2C). HR-MALDI-MS: 651.2322 ($[M+Na]^+$, $C_{35}H_{36}N_2NaO_9^+$; calc. 651.2313), 667.2054 ($[M+K]^+$, $C_{35}H_{36}KN_2O_9^+$; calc. 667.2052).

N^6-*Benzoyl-5′*-O-*[dimethyl(1,1,2-trimethylpropyl)silyl]-2′,3′*-O-*isopropylideneadenosine* (**18**). A suspension of **17** [24] (10.0 g, 24.3 mmol) in DMF (10 ml) was treated with 1*H*-imidazole (4.80 g, 26.8 mmol) and dropwise with TDSCl (5.30 ml, 26.8 mmol). The mixture was stirred for 6 h at 23°. DMF was evaporated *i.v.* A soln. of the residue in CH_2Cl_2 was washed with brine, dried ($MgSO_4$), and evaporated. Drying for 24 h under vacuum afforded **18** (12.8 g, 95%). Colourless powder. R_f (AcOEt/cyclohexane 7:3) 0.41. $[\alpha]_D^{25} = -57.4$ ($c = 1.0$, $CHCl_3$). IR ($CHCl_3$): 3408*w*, 2961*m* (br.), 2868*w*, 1709*m*, 1673*w*, 1612*m*, 1586*m*, 1502*w*, 1478*w*, 1456*s*, 1385*w*, 1327*w*, 1258*m*, 1156*w*, 1130*w*, 1090*m*, 837*w*. ^{1}H-NMR (300 MHz, $CDCl_3$): see *Table 8*; additionally, 9.04 (br. *s*, NH); 8.03–8.00 (*m*, 2 arom. H); 7.62–7.47 (*m*, 3 arom. H); 1.71, 1.40 (2*s*, Me_2CO_2); 1.53 (*sept.*, $J = 6.9$, Me_2CH); 0.81 (*d*, $J = 6.9$, Me_2CH); 0.77, 0.76 (2*s*, Me_2CSi); 0.04, 0.03 (2*s*, Me_2Si). ^{13}C-NMR (75 MHz, $CDCl_3$): see *Table 9*; additionally, 164.26 (*s*, C=O); 133.60 (*s*); 132.60 (*d*); 128.71 (2*d*); 127.73 (2*d*); 114.10 (*s*, Me_2CO_2); 33.99 (*d*, Me_2CH); 27.26, 25.39 (2*q*, Me_2CO_2); 25.29 (*s*, Me_2CSi); 20.30, 20.23 (2*q*, Me_2CSi); 18.48 (*q*, Me_2CH); −3.31, −3.45 (2*q*, Me_2Si). HR-MALDI-MS: 576.2619 ($[M+Na]^+$, $C_{28}H_{39}N_5NaO_5Si^+$; calc. 576.2618), 554.2780 ($[M+H]^+$, $C_{28}H_{40}N_5O_5Si^+$; calc. 554.2798).

Table 8. *Selected ^{1}H-NMR Chemical Shifts* [ppm] *and Coupling Constants* [Hz] *of Adenosine Monomers* **18**–**26** *in $CDCl_3$*

	18	**19**	**20**	**21**	**22**	**23**	**24**	**25**	**26**
H–C(2)	8.85	8.84	8.82	8.73	8.75	8.79	8.78	8.81	8.79
H–C(8)	8.23	8.12	8.11	–	–	–	–	–	–
CH_a–C(8)	–	–	–	4.98	4.76	4.54	4.52	4.55	4.56
CH_b–C(8)	–	–	–	4.91	4.69	4.49	4.46	4.50	4.50
H–C(1′)	6.22	6.14	6.18	6.30	6.27	6.26	6.17	6.24	6.28
H–C(2′)	5.30	5.52	5.51	5.67	5.84	5.82	5.29	5.68	5.65
H–C(3′)	4.95	4.98	5.07	5.05	5.11	5.05	5.12	5.01	5.08
H–C(4′)	4.46	4.38	4.52	4.24	4.27	4.18	4.48	4.19	4.28
H_a–C(5′)	3.87	3.28	4.36	3.72	3.70	3.78	4.02	3.29	4.38
H_b–C(5′)	3.76	3.19	4.24	3.62	3.60	3.65	3.82	3.15	4.19
$J(H_a,H_b)$	–	–	–	14.6	11.7	12.3	12.3	12.0	12.1
J(1′,2′)	2.4	2.1	2.3	2.1	2.1	2.7	5.1	1.0	2.2
J(2′,3′)	6.3	6.3	6.3	6.6	6.6	6.6	6.0	6.3	6.4
J(3′,4′)	2.4	2.7	3.6	3.6	3.3	3.3	1.8	3.6	4.1
J(4′,5′a)	3.9	7.2	4.3	5.7	6.0	6.6	< 1.0	7.2	4.1
J(4′,5′b)	4.2	6.9	6.1	5.1	5.7	6.3	< 1.0	7.2	6.9
J(5′a,5′b)	11.1	13.8	12.0	11.1	10.8	10.8	12.9	13.8	11.0

5′-S-*Acetyl*-N^6-*benzoyl-2′,3′*-O-*isopropylidene-5′-thioadenosine* (**19**). Under N_2, a soln. of **17** [24] (1.00 g, 2.43 mmol) in pyridine (8 ml) was cooled to −20°, treated with TsCl (508 mg, 2.67 mmol), stirred for 1 h at −20° for 15 h at 23°, diluted with AcOEt, and washed with sat. NH_4Cl soln. and brine. The combined org. layers were dried ($MgSO_4$) and evaporated at 30°. A soln. of the residue (1.12 g) in DMF (4 ml) was treated with AcSK (0.81 g, 7.1 mmol), and stirred for 1 h at 40° and for 2 h at 75°. Volatiles were removed, and a soln. of the residue in AcOEt was washed with H_2O and brine, dried ($MgSO_4$), and evaporated. FC (AcOEt/cyclohexane 1:3 → 1:1) gave **19** (0.87 g, 68%). Slightly pink foam. R_f (AcOEt) 0.42. $[\alpha]_D^{25} = -29.9$ ($c = 1.0$, $CHCl_3$). IR ($CHCl_3$): 3408*w*, 3007*w*, 2928*w*, 1706*s*, 1611*s*, 1586*m*, 1503*w*, 1479*m*, 1456*s*, 1385*w*, 1357*w*, 1328*w*, 1248*m*, 1156*w*, 1134*w*, 1093*m*, 868*m*. ^{1}H-NMR

Table 9. *Selected ^{13}C-NMR Chemical Shifts* [ppm] *of the Adenosine Monomers* **18**, **19**, *and* **21**–**26** *in $CDCl_3$*

	18	**19**	**21**	**22**	**23**	**24**	**25**	**26**
C(2)	152.75	152.47	152.21	152.75	152.26	151.98	152.32	152.36
C(4)	149.40	149.72	148.77	149.43	149.01	149.76	149.16	149.06
C(5)	123.18	123.68	121.15	121.97	121.89	122.55	122.10	122.01
C(6)	151.00	150.93	152.03	151.95	151.97[a])	151.52[a])	151.98[a])	152.00[a])
C(8)	141.40	142.25	154.43	150.15	151.84[a])	151.31[a])	151.58[a])	151.46[a])
CH_2–C(8)	–	–	57.61	21.45	59.58	59.64	59.58	59.52
C(1′)	91.80	90.84	89.83	90.16	90.34	92.31	90.02	89.68
C(2′)	84.79	84.10	83.16	82.82	82.75	82.62	83.88	83.47
C(3′)	81.49	83.44	81.36	81.42	81.75	81.27	83.73	81.54
C(4′)	87.31	85.98	87.29	87.51	87.13	85.64	85.87	84.47
C(5′)	63.28	31.24	62.58	62.61	62.97	63.32	31.31	63.97

[a]) Assignments may be interchanged.

(300 MHz, $CDCl_3$): see *Table 8*; additionally, 8.98 (br. *s*, NH); 8.05–8.00 (*m*, 2 arom. H); 7.65–7.52 (*m*, 3 arom. H); 2.35 (*s*, AcS); 1.61, 1.40 (2*s*, Me_2C). ^{13}C-NMR (75 MHz, $CDCl_3$): see *Table 9*; additionally, 194.17 (*s*, SC=O) 164.47 (*s*, NC=O); 133.39 (*s*); 132.59 (*d*); 128.59 (2*d*); 127.85 (2*d*); 114.57 (*s*, Me_2C); 30.63 (*q*, *Me*C=O); 27.2, 25.4 (2*q*, Me_2C). HR-MALDI-MS: 492.1307 ($[M+Na]^+$, $C_{22}H_{23}N_5NaO_5S^+$; calc. 492.1318).

N^6-*Benzoyl-5′*-O-*[dimethyl(1,1,2-trimethylpropyl)silyl]-8-(hydroxymethyl)-2′,3′*-O-*isopropylidene-adenosine* (**21**). A soln. of $(i\text{-}Pr)_2NH$ (14.6 ml, 104 mmol) in THF (100 ml) was cooled to $-70°$, treated dropwise with 1.6M BuLi in hexane (63.4 ml, 102 mmol), stirred for 15 min, warmed to 0°, stirred for 15 min, cooled to $-70°$, treated dropwise with a soln. of **18** (10.6 g, 19.3 mmol) in THF (100 ml), stirred for 1 h, treated dropwise with DMF (39.5 ml, 508 mmol), stirred for 2.5 h, treated with AcOH (15 ml), and allowed to warm to 23°. The mixture was diluted with EtOH (100 ml), treated with $NaBH_4$ (2.45 g, 64.4 mmol), and stirred for 30 min. Volatiles were evaporated. A soln. of the residue in CH_2Cl_2 was washed with H_2O and brine, dried ($MgSO_4$), and evaporated. FC (AcOEt/cyclohexane 1:2) gave **21** (8.1 g, 72%). Colourless powder. R_f (AcOEt) 0.52. M.p. 139.0–140.0°. $[\alpha]_D^{25} = -16.7$ ($c = 1.0$, $CHCl_3$). IR ($CHCl_3$): 3568*w* (br.), 3408*w* (br.), 2961*m*, 2870*w*, 1709*m*, 1672*w*, 1614*m*, 1590*m*, 1479*m*, 1428*m*, 1386*w*, 1358*w*, 1264*m*, 1158*w*, 1090*m*, 835*w*. ^{1}H-NMR (300 MHz, $CDCl_3$): see *Table 8*; additionally, 9.25 (br. *s*, NH); 8.03–7.98 (*m*, 2 arom. H); 7.58–7.38 (*m*, 3 arom. H); 5.10 (*t*, $J = 6.3$, OH); 1.61, 1.42 (2*s*, Me_2CO_2); 1.53 (*sept.*, $J = 6.9$, Me_2CH); 0.80 (*d*, $J = 6.9$, Me_2CH); 0.76, 0.75 (2*s*, Me_2CSi); −0.034, −0.037 (2*s*, Me_2Si). ^{13}C-NMR (75 MHz, $CDCl_3$): see *Table 9*; additionally, 164.72 (*s*, C=O); 133.39 (*s*); 132.54 (*d*); 128.55 (2*d*); 127.74 (2*d*); 114.26 (*s*, Me_2CO_2); 34.05 (*d*, Me_2CH); 27.21, 25.44 (2*q*, Me_2CO_2); 25.31 (*s*, Me_2CSi); 20.29 (*q*, Me_2CSi); 18.49 (*q*, Me_2CH); −3.29 (*q*, Me_2Si). HR-MALDI-MS: 606.2726 ($[M+Na]^+$, $C_{29}H_{41}N_5NaO_6Si^+$; calc. 606.2724).

N^6-*Benzoyl-8-(bromomethyl)-5′*-O-*[dimethyl(1,1,2-trimethylpropyl)silyl]-2′,3′*-O-*isopropylideneade-nosine* (**22**). A soln. of **21** (1.00 g, 1.76 mmol) in CH_2Cl_2 (5 ml) under N_2 was cooled to $-10°$, treated dropwise with $EtN(i\text{-}Pr)_2$ (640 µl, 4.57 mmol) and MsCl (330 µl, 4.2 mmol), stirred for 10 min at 0° and for 1 h at 23°, diluted with CH_2Cl_2 (50 ml), and washed with sat. NH_4Cl soln. and brine. The combined org. layers were dried ($MgSO_4$) and evaporated. A soln. of the residue in CH_2Cl_2 (2 ml) was treated with LiBr (3.0 g, 35 mmol), stirred for 16 h at 23°, diluted with CH_2Cl_2 (50 ml), washed with H_2O and brine, dried ($MgSO_4$), and evaporated. FC (AcOEt/cyclohexane 1:10 → 1:1) yielded **22** (0.69 g, 61%). R_f (AcOEt/cyclohexane 1:1) 0.47. $[\alpha]_D^{25} = +3.0$ ($c = 1.0$, $CHCl_3$). IR ($CHCl_3$): 3407*w*, 2959*m*, 2929*m*, 1710*m*, 1613*m*, 1589*w*, 1520*w*, 1473*w*, 1427*w*, 1358*w*, 1253*w*, 1089*m*, 832*m*. ^{1}H-NMR (300 MHz, $CDCl_3$): see *Table 8*; additionally, 9.10 (br. *s*, NH); 7.99–7.97 (*m*, 2 arom. H); 7.58–7.38 (*m*, 3 arom. H); 1.39 (*s*, Me_2CO_2); 1.53 (*sept.*, $J = 6.9$, Me_2CH); 0.80 (*d*, $J = 6.9$, Me_2CH); 0.76, 0.75 (2*s*, Me_2CSi); −0.03, −0.04 (2*s*, Me_2Si). ^{13}C-NMR (75 MHz, $CDCl_3$): see *Table 9*; additionally, 164.20 (*s*, C=O); 133.44 (*s*); 132.67

(*d*); 128.69 (2*d*); 127.73 (2*d*); 114.21 (*s*, Me_2CO_2); 34.07 (*d*, Me_2CH); 27.26, 25.47 (2*q*, Me_2CO_2); 25.30 (*s*, Me_2CSi); 20.32 (*q*, Me_2CSi); 18.51 (*q*, Me_2CH); −3.29 (*q*, Me_2Si). HR-MALDI-MS: 648.2024 (100, $[M+H]^+$, $C_{29}H_{41}{}^{81}BrN_5O_5Si^+$; calc. 648.2040), 646.2046 (98, $[M+H]^+$, $C_{29}H_{41}{}^{79}BrN_5O_5Si^+$; calc. 646.2060).

N^6-*Benzoyl-5′*-O-*[dimethyl(1,1,2-trimethylpropyl)silyl]-2′,3′*-O-*isopropylidene-8-{[(4-methoxyphenyl)diphenylmethoxy]methyl}adenosine* (**23**). A soln. of **21** (3.00 g, 5.13 mmol) in dry CH_2Cl_2 (50 ml) under N_2 was treated dropwise with $EtN(i\text{-}Pr)_2$ (1.25 ml, 7.69 mmol), stirred for 10 min at 23°, treated dropwise with a soln. of MMTrCl (2.33 g, 7.69 mmol) in dry CH_2Cl_2 (40 ml, → dark green soln.), stirred for 4 h at 23°, and washed with sat. NH_4Cl soln. and brine. The combined org. layers were dried ($MgSO_4$) and evaporated. FC (AcOEt/cyclohexane 1:3 → 1:1) yielded **23** (3.64 g, 83%). Colourless powder. R_f (AcOEt/cyclohexane 6:4) 0.75. M.p. 130.5–131.3°. $[\alpha]_D^{25} = -17.0$ ($c = 1.0$, $CHCl_3$). IR ($CHCl_3$): 3408*w*, 3065*w*, 3014*m*, 2960*m*, 2869*w*, 1708*m*, 1614*s*, 1588*m*, 1510*m*, 1463*m*, 1427*m*, 1355*m*, 1327*m*, 1299*w*, 1254*w*, 1177*w*, 1098*m*, 832*w*. ^{1}H-NMR (300 MHz, $CDCl_3$): see *Table 8*; additionally, 8.99 (br. *s*, NH); 8.03–7.99 (*m*, 2 arom. H); 7.55–7.24 (*m*, 15 arom. H); 6.85 (*d*, $J = 8.7$, 2 arom. H); 3.77 (*s*, MeO); 1.60 (*sept.*, $J = 6.9$, Me_2CH); 1.42, 1.38 (2*s*, Me_2CO_2); 0.83 (*d*, $J = 6.9$, Me_2CH); 0.80, 0.78 (2*s*, Me_2CSi); 0.01, −0.01 (2*s*, Me_2Si). ^{13}C-NMR (75 MHz, $CDCl_3$): see *Table 9*; additionally, 164.24 (*s*, NC=O); 158.69 (*s*); 143.30 (2*s*); 134.28, 133.82 (2*s*); 132.57 (*d*); 130.44 (2*d*); 128.77 (2*d*); 128.27 (4*d*); 127.91 (4*d*); 127.63 (2*d*); 127.11 (2*d*); 113.98 (*s*, Me_2CO_2); 113.22 (2*d*); 88.03 (*s*, Ph_2C); 55.23 (*q*, MeO); 34.12 (*d*, Me_2CH); 27.32, 25.65 (2*q*, Me_2CO_2); 25.29 (*s*, Me_2CSi); 20.37 (*q*, Me_2CSi); 18.55 (*q*, Me_2CH); −3.30 (*q*, Me_2Si). HR-MALDI-MS: 878.3912 ($[M+Na]^+$, $C_{49}H_{57}N_5NaO_7Si^+$; calc. 878.3920). Anal calc. for $C_{49}H_{57}N_5O_7Si$ (856.10): C 68.75, H 6.71, N 8.18; found: C 68.56, H 6.67, N 8.13.

N^6-*Benzoyl-2′,3′*-O-*isopropylidene-8-{[(4-methoxyphenyl)diphenylmethoxy]methyl}adenosine* (**24**). A suspension of **23** (1.20 g, 1.47 mmol) and 4-Å mol. sieves in THF (10 ml) was stirred for 15 min at 23°, treated dropwise with a soln. of $Bu_4NF \cdot 3\,H_2O$ (1.39 g, 4.41 mmol) in THF (10 ml), stirred for 4 h at 23°, and filtered. Evaporation and FC (AcOEt/cyclohexane 1:1 → 4:1) yielded **24** (0.853 g, 82%). Colourless foam. R_f (AcOEt/cyclohexane 8:2) 0.25. $[\alpha]_D^{25} = -45.1$ ($c = 1.0$, $CHCl_3$). IR ($CHCl_3$): 3396*w* (br.), 3280*w*, 3027*m*, 3014*m*, 2932*w*, 1712*m*, 1614*s*, 1510*w*, 1481*w*, 1463*w*, 1446*w*, 1429*m*, 1360*w*, 1264*w*, 1082*m*, 1034*w*. ^{1}H-NMR (300 MHz, $CDCl_3$): see *Table 8*; additionally, 9.02 (br. *s*, NH); 8.03–8.00 (*m*, 2 arom. H); 7.63–7.24 (*m*, 15 arom. H); 6.84 (*d*, $J = 8.7$, 2 arom. H); 5.74 (br. *d*, $J = 11.1$, OH); 3.77 (*s*, MeO); 1.35, 1.32 (2*s*, Me_2C). ^{13}C-NMR (75 MHz, $CDCl_3$): see *Table 9*; additionally, 164.38 (*s*, NC=O); 158.73, 143.29, 143.25, 134.21, 133.54 (5*s*); 132.66 (*d*); 130.42 (2*d*); 128.69 (2*d*); 128.24 (4*d*); 127.93 (4*d*); 127.76 (2*d*); 127.16 (2*d*); 114.26 (*s*, Me_2C); 113.26 (2*d*); 88.19 (*s*, Ph_2C); 55.24 (*q*, MeO); 27.63, 25.38 (2*q*, Me_2C). HR-MALDI-MS: 736.2735 ($[M+Na]^+$, $C_{41}H_{39}N_5NaO_7^+$; calc. 736.2742).

5′-S-*Acetyl*-N^6-*benzoyl-2′,3′*-O-*isopropylidene-8-{[(4-methoxyphenyl)diphenylmethoxy]methyl}-5′-thioadenosine* (**25**). A soln. of **24** (840 mg, 1.17 mmol) in CH_2Cl_2 (1 ml) under N_2 was cooled to −10°, treated with a soln. of DMAP (283 mg, 2.34 mmol) in CH_2Cl_2 (2 ml), stirred for 5 min at 0°, treated with TsCl (246 mg, 1.29 mmol), and stirred 1 h at 0° and for 1 h at 10°. The mixture was diluted with AcOEt, washed with sat. NH_4Cl soln. and brine, dried ($MgSO_4$), and evaporated at 30°. A soln. of the residue in DMF (4 ml) was treated with AcSK (1.35 g, 12 mmol), stirred at 40° for 1 h and at 75° for 2 h. DMF was evaporated, and a soln. of the residue in AcOEt was washed with H_2O and brine, dried ($MgSO_4$), and evaporated. FC (AcOEt/cyclohexane 1:3 → 1:1) gave **25** (697 mg, 77%). Slightly pink foam. R_f (MeOH/CH_2Cl_2 5:95) 0.46. $[\alpha]_D^{25} = -14.4$ ($c = 1.0$, $CHCl_3$). IR ($CHCl_3$): 3411*w*, 3007*m*, 2930*m*, 2855*w*, 1706*m*, 1614*s*, 1590*m*, 1509*m*, 1462*m*, 1427*m*, 1375*m*, 1365*m*, 1329*w*, 1299*w*, 1156*w*, 1071*m*, 1035*m*, 978*w*, 909*w*, 867*w*. ^{1}H-NMR (300 MHz, $CDCl_3$): see *Table 8*; additionally, 8.97 (br. *s*, NH); 8.04–7.97 (*m*, 2 arom. H); 7.63–7.21 (*m*, 15 arom. H); 6.85 (*d*, $J = 8.7$, 2 arom. H); 3.77 (*s*, MeO); 2.32 (*s*, AcS); 1.50, 1.37 (2*s*, Me_2C). ^{13}C-NMR (75 MHz, $CDCl_3$): see *Table 9*; additionally, 194.32 (*s*, SC=O); 164.47 (*s*, NC=O); 158.71 (*s*); 143.20 (2*s*); 134.17, 133.69 (2*s*); 132.55 (*d*); 130.44 (2*d*); 128.69 (2*d*); 128.26 (4*d*); 127.92 (4*d*); 127.73 (2*d*); 127.14 (2*d*); 114.40 (*s*, Me_2C); 113.30 (2*d*); 88.07 (*s*, Ph_2C); 55.23 (*q*, MeO); 30.62 (*q*, *Me*C=O); 27.24, 25.58 (2*q*, Me_2C). HR-MALDI-MS: 794.2622 ($[M+Na]^+$, $C_{43}H_{41}N_5NaO_7S^+$; calc. 794.2618).

5′-O-*Acetyl*-N^6-*benzoyl-2′,3′*-O-*isopropylidene-8-{[(4-methoxyphenyl)diphenylmethoxy]methyl}adenosine* (**26**). A soln. of **25** (150 ml, 0.33 mmol) in pyridine (1 ml) under N_2 was treated with Ac_2O (60 µl, 0.66 mmol) and stirred for 48 h at 24°. The soln. was diluted with AcOEt (50 ml), washed with sat. NH_4Cl

soln. and brine, dried ($MgSO_4$), and evaporated. Crystallisation from CH_2Cl_2/hexane afforded **26** (193 mg, 77%). Colourless needles. R_f (AcOEt/cyclohexane 7:3) 0.63. $[\alpha]_D^{25} = -10.4$ ($c = 1.0$, $CHCl_3$). IR ($CHCl_3$): 3388*w*, 3018*m*, 1696*s*, 1607*w*, 1510*m*, 1449*w*, 1383*m*, 1298*w*, 1253*m*, 1181*w*, 1157*w*, 1069*m*, 1037*m*, 979*w*, 906*w*, 876*w*, 834*w*. ^{1}H-NMR (300 MHz, $CDCl_3$): see *Table 8*; additionally, 8.92 (br. *s*, NH); 8.00–8.03 (*m*, 2 arom. H); 7.50–7.65 (*m*, 15 arom. H); 7.22–7.42 (*m*, arom. H); 6.84–6.87 (*m*, arom. H); 3.78 (*s*, MeO); 2.02 (*s*, AcS); 1.52, 1.38 (2*s*, Me_2C). ^{13}C-NMR (75 MHz, $CDCl_3$): see *Table 9*; additionally, 170.36 (*s*, OC=O); 164.23 (*s*, NC=O); 158.72 (*s*); 143.24 (2*s*); 134.16, 133.71 (2*s*); 132.61 (*d*); 130.45 (2*d*); 128.77 (2*d*); 128.25 (4*d*); 127.91 (4*d*); 127.66 (2*d*); 127.13 (2*d*); 114.58 (*s*, Me_2C); 113.23 (2*d*); 88.07 (*s*, Ph_2C); 55.25 (*q*, MeO); 27.34, 25.64 (2*q*, Me_2C); 20.87 (*q*, *Me*C=O). HR-MALDI-MS: 756.3011 ($[M+H]^+$, $C_{43}H_{42}N_5O_8^+$; calc. 755.2955), 778.2833 ($[M+Na]^+$, $C_{43}H_{41}N_5NaO_8^+$; calc. 778.2847).

5′-O-[Dimethyl(1,1,2-trimethylpropyl)silyl]-2′,3′-O-isopropylideneuridine-6-methyl-(6¹ → 5′-S)-2′,3′-O-isopropylidene-5′-thioadenosine (**27**). A soln. of **12** (200 mg, 0.37 mmol) and **19** (175 mg, 0.37 mmol) in O_2-free dry MeOH (2 ml) was treated with a soln. of MeONa (80 mg, 1.48 mmol) in O_2-free dry MeOH (2 ml), stirred for 14 h at r.t., and evaporated. A soln. of the residue in CH_2Cl_2 was washed with brine, dried ($MgSO_4$), and evaporated. FC (CH_2Cl_2/MeOH 24:1) gave **27** (238 mg, 85%). Colourless powder. R_f (CH_2Cl_2/MeOH 19:1) 0.29. M.p. 134.1–135.1°. $[\alpha]_D^{25} = -35.7$ ($c = 1.0$, $CHCl_3$). IR ($CHCl_3$): 3408*w*, 3365*w*, 3187*w*, 3026*w*, 2960*m*, 2868*w*, 1697*s*, 1633*m*, 1473*w*, 1378*m*, 1331*w*, 1254*w*, 1157*w*, 1082*m*, 982*w*, 909*w*, 871*m*, 835*m*. ^{1}H-NMR (300 MHz, $CDCl_3$): see *Table 10*; additionally, 7.98 (*s*, H–C(8/I)); 1.52 (*sept.*, $J = 6.9$, Me_2CH); 1.61, 1.54, 1.38, 1.34 (4*s*, 2 Me_2CO_2); 0.83 (*d*, $J = 6.9$, Me_2CH); 0.80, 0.79 (2*s*, Me_2CSi); 0.05, 0.04 (2*s*, Me_2Si). ^{13}C-NMR (75 MHz, $CDCl_3$): see *Table 11*; additionally, 114.47, 113.41 (2*s*, 2 Me_2CO_2); 34.16 (*d*, Me_2CH); 27.44, 27.24, 25.61, 25.47 (4*q*, 2 Me_2CO_2); 25.40 (*s*, Me_2CSi); 20.48, 20.44 (2*q*, Me_2CSi); 18.62, 18.58 (2*q*, Me_2CH); −3.09 (*q*, Me_2Si). HR-MALDI-MS: 784.3122 (100, $[M+Na]^+$, $C_{34}H_{51}N_7NaO_7SSi^+$; calc. 784.3136), 762.3300 (33, $[M+H]^+$; $C_{34}H_{52}N_7O_7SSi^+$; calc. 762.3316). Anal. calc. for $C_{34}H_{51}N_7O_7SSi$ (761.32): C 53.59, H 6.75, N 12.87; found: C 53.59, H 6.72, N 12.69.

2′,3′-O-Isopropylideneuridine-6-methyl-(6¹ → 5′-S)-2′,3′-O-isopropylidene-5′-thioadenosine (**28**). In a polyethylene flask, a soln. of **27** (100 mg, 0.13 mmol) in THF (1.5 ml) was treated with $(HF)_3 \cdot Et_3N$ (210 µl, 1.3 mmol), stirred for 2 d at 23°, poured into brine, and extracted with CH_2Cl_2. The combined org. layers were washed with sat. $NaHCO_3$ soln. and brine, dried ($MgSO_4$) and evaporated. FC (CH_2Cl_2/MeOH/NH_4OH 100:0:0 → 92:8:1) gave **28** (47 mg, 58%). Colourless foam. R_f (CH_2Cl_2/MeOH/NH_4OH 95:5:1) 0.23. $[\alpha]_D^{25} = -42.5$ ($c = 1.0$, $CHCl_3$). IR ($CHCl_3$): 3483*w*, 3402*w*, 3323*w* (br.), 3189*w*, 2994*m*, 2938*w*, 1704*s*, 1641*m*, 1601*w*, 1475*w*, 1427*w*, 1384*m*, 1332*w*, 1297*w*, 1157*m*, 1095*m*, 1071*m*, 982*w*, 909*w*, 871*m*. ^{1}H-NMR (300 MHz, $CDCl_3$): see *Table 10*; additionally, 7.98 (*s*, H–C(8/I)); 4.72–4.54 (br. *s*, HO–C(5′/II)); 1.58, 1.52, 1.36, 1.31 (4*s*, 2 Me_2C). ^{13}C-NMR (75 MHz, $CDCl_3$): see *Table 11*; additionally, 114.52, 114.16 (2*s*, 2 Me_2CO_2); 27.56, 27.23, 25.58, 25.51 (4*q*, 2 Me_2CH). HR-MALDI-MS: 642.1961 (100, $[M+Na]^+$, $C_{26}H_{33}N_7NaO_9S^+$; calc. 642.1953), 620.2142 (20, $[M+H]^+$, $C_{26}H_{34}N_7O_9S^+$; calc. 620.2133).

5′-O-[Dimethyl(1,1,2-trimethylpropyl)silyl]-2′,3′-O-isopropylideneuridine-6-methyl-(6¹ → 5′-S)-2′,3′-O-isopropylidene-8-[[(4-methoxyphenyl)diphenylmethoxy]methyl]-5′-thioadenosine (**29**). A soln. of **25** (50 mg, 0.065 mmol) and **12** (35 mg, 0.065 mmol) in O_2-free dry MeOH (2 ml) was treated with a soln. of MeONa (14 mg, 0.26 mmol) in O_2-free dry MeOH (2 ml), stirred for 14 h at 23°, and evaporated. A soln. of the residue in CH_2Cl_2 was washed with brine, dried ($MgSO_4$), and evaporated. FC (MeOH/CH_2Cl_2 1:24) gave **29** (43 mg, 62%). Colourless powder. R_f (MeOH/CH_2Cl_2 1:19) 0.26. M.p. 140.1–141.1°. $[\alpha]_D^{25} = -33.6$ ($c = 1.0$, $CHCl_3$). IR ($CHCl_3$): 3398*w*, 3325*w*, 3194*w*, 2985*w*, 2960*m*, 2868*w*, 1698*s*, 1640*m*, 1607*w*, 1449*w*, 1376*m*, 1330*w*, 1232*m*, 1157*m*, 1088*s*, 1067*s*, 836*m*. ^{1}H-NMR (300 MHz, $CDCl_3$): see *Table 10*; additionally, 7.52–7.20 (*m*, 12 arom. H); 6.85 (*d*, $J = 8.7$, 2 arom. H); 1.53 (*sept.*, $J = 6.9$, Me_2CH); 1.53 (6 H), 1.37, 1.36 (3*s*, 2 Me_2CO_2); 0.80 (*d*, $J = 6.9$ Me_2CH); 0.78, 0.77 (2*s*, Me_2CSi); 0.02, 0.01 (2*s*, Me_2Si). ^{13}C-NMR (75 MHz, $CDCl_3$): see *Table 11*; additionally, 158.67, 143.45, 143.38, 134.46 (4*s*); 130.40 (2*d*); 128.38 (2*d*); 128.32 (4*d*); 127.88 (4*d*); 127.13 (2*d*); 114.28, 113.24 (2*s*, 2 Me_2CO_2); 113.24 (2*d*); 87.89 (*s*, Ph_2C); 55.25 (*q*, MeO); 34.12 (*d*, Me_2CH); 27.42, 27.33, 25.66, 25.61 (4*q*, 2 Me_2CO_2); 25.31 (*s*, Me_2CSi); 20.41 (*q*, Me_2CSi); 18.56 (*q*, Me_2CH); −3.17 (*q*, Me_2Si). HR-MALDI-MS: 1086.445 (100, $[M+Na]^+$, $C_{55}H_{69}N_7NaO_{11}SSi^+$; calc. 1086.4443), 1064.481 (68, $[M+H]^+$, $C_{55}H_{70}N_7O_{11}SSi^+$; calc. 1064.4623). Anal. calc. for $C_{55}H_{69}N_7O_{11}SSi$ (1063.45): C 62.07, H 6.53, N 9.21; found: C 62.12, H 6.31, N 9.02.

Table 10. *Selected ^{1}H-NMR Chemical Shifts* [ppm] *and Coupling Constants* [Hz] *of the U*[s]A$^{(*)}$ Dimers* **27**–**32** *in $CDCl_3$*

	27 25 mM	**28** 60 mM	**29** 50 mM	**30** 50 mM	**31**[a]) 50 mM	**32** 15 mM
Adenosine unit (I)						
H_2N–C(6/I)	6.72	7.04	6.74	6.80	7.09	6.71
H–C(2/I)	8.36	8.31	8.38	8.34	8.28	8.28
H–C(8/I)	7.98	7.98	–	–	–	–
CH_a–C(8/I)	–	–	4.60	4.53	4.98	4.98
CH_b–C(8/I)	–	–	4.43	4.45	4.93	4.93
H–C(1′/I)	6.08	6.05	6.19	6.16	6.33	6.28
H–C(2′/I)	5.46	5.45	5.54	5.49	5.57	5.65
H–C(3′/I)	5.15	5.08	5.14	5.09	5.19	5.16
H–C(4′/I)	4.46	4.52	4.33	4.48	4.44	4.56
H_a–C(5′/I)	2.94	3.12	2.95	3.33	2.89	3.13
H_b–C(5′/I)	2.86	2.76	2.90	2.74	2.85	2.72
$J(H_a,H_b$/I)	–	–	11.7	12.0	14.3	14.2
J(1′,2′/I)	1.5	1.2	1.8	1.2	< 1.0	< 1.0
J(2′,3′/I)	6.3	6.3	6.6	6.3	6.3	6.3
J(3′,4′/I)	3.9	3.0	4.4	3.6	3.8	3.0
J(4′,5′a/I)	7.5	9.3	7.5	9.9	7.3	9.9
J(4′,5′b/I)	5.7	3.6	5.7	3.0	5.0	3.3
J(5′a,5′b/I)	14.4	14.1	14.10	14.4	14.1	14.4
Uridine unit (II)						
H–N(3/II)	11.88	12.88	11.75	12.87	12.30	12.68
H–C(5/II)	5.22	5.42	5.13	5.45	5.27	5.48
CH_a–C(6/II)	3.60	3.66	3.56	3.68	3.57	3.72
CH_b–C(6/II)	3.48	3.36	3.44	3.28	3.51	3.30
H–C(1′/II)	5.79	5.63	5.74	5.52	5.78	5.61
H–C(2′/II)	5.28	5.16	5.18	5.04	5.25	5.11
H–C(3′/II)	4.83	4.93	4.83	4.86	4.80	4.86
H–C(4′/II)	4.11	4.18	4.08	4.09	4.11	4.25
H_a–C(5′/II)	3.78	3.92–3.80	3.72	3.86	3.76	3.96
H_b – C(5′/II)	3.74	3.92–3.80	3.67	3.77	3.72	3.82
$J(H_a,H_b$/II)	14.9	15.6	15.0	15.0	15.0	16.2
J(1′,2′/II)	< 1.0	1.5	< 1.0	1.2	< 1.0	1.5
J(2′,3′/II)	6.3	6.6	6.3	6.6	6.3	6.3
J(3′,4′/II)	4.4	4.8	4.2	4.5	4.4	4.2
J(4′,5′a/II)	5.4	3.9	5.4	6.0	5.8	6.9
J(4′,5′b/II)	7.5	3.9	7.2	2.4	7.9	2.7
J(5′a,5′b/II)	10.8	[b])	10.5	12.3	10.7	12.6

[a]) Assignments based on a HSQC and a HMBC spectrum. [b]) Not assigned.

*2′,3′-*O*-Isopropylideneuridine-6-methyl-(6^1 → 5′-*S*)-2′,3′-*O*-isopropylidene-8-{[(4-methoxyphenyl)diphenylmethoxy]methyl}adenosine* (**30**). A soln. of **29** (52 mg, 0.05 mmol) in THF (1 ml) in a polyethylene flask was treated with $(HF)_3 \cdot Et_3N$ (80 µl, 0.5 mmol), stirred 2 d at 23°, poured into brine, and extracted with AcOEt. The combined org. layers were washed with sat. $NaHCO_3$ soln. and brine, dried ($MgSO_4$), and evaporated. FC (CH_2Cl_2/MeOH/NH_4OH 100:0:0 → 92:8:1) gave **30** (37 mg, 83%). Colourless foam. R_f (CH_2Cl_2/MeOH/NH_4OH 95:5:1) 0.26. $[\alpha]_D^{25} = -14.9$ ($c = 1.0$, $CHCl_3$). IR ($CHCl_3$): 3478*w*, 3405*w*, 3321*w*, 3194*w*, 3011*w*, 2935*m*, 2847*w*, 1703*s*, 1638*m*, 1607*w*, 1510*m*, 1448*m*, 1383*m*,

Table 11. *Selected ^{13}C-NMR Chemical Shifts* [ppm] *of the U*[s]A$^{(*)}$ Dimers* **27**–**32** *in $CDCl_3$*

	27	**28**	**29**	**30**	**31**[a])	**32**
C(2/I)	153.00	153.12	152.60	152.18	152.67	152.21
C(4/I)	148.61	148.58	148.28	148.32	149.63	149.19
C(5/I)	120.04	119.76	118.86	118.24	118.04	118.04
C(6/I)	156.07	156.24	155.85	155.59	155.71	155.48
C(8/I)	140.01	140.65	149.88	149.32	151.14	149.19
CH_2–C(8/I)	–	–	59.15	58.88	56.98	56.97
C(1′/I)	90.73	91.39	89.65	90.89	89.68	91.24
C(2′/I)	84.04[b])	84.26[b])	83.92[b])	84.12[b])	84.07	84.04[b])
C(3′/I)	84.31[b])	84.73[b])	84.31[b])	84.77[b])	84.69	85.02[b])
C(4′/I)	89.44[c])	90.31[c])	89.46[c])	90.21[c])	89.61	89.93[c])
C(5′/I)	33.19	33.42	32.96	32.98	32.87	33.29
C(2/II)	151.03[d])	151.11[d])	151.10[d])	150.46[d])	151.37	150.93[d])
C(4/II)	162.78	163.27	162.52	162.55	163.19	163.21
C(5/II)	103.99	103.96	104.02	103.77	104.06	103.24
C(6/II)	151.25[d])	152.11[d])	151.10[d])	151.94[d])	151.45	151.66[d])
CH_2–C(6/II)	33.16	32.96	32.88	32.51	31.59	32.46
C(1′/II)	91.35	91.39	91.32	90.99	91.39	91.24
C(2′/II)	84.31[b])	84.36[b])	84.31[b])	84.35[b])	84.24	84.52[b])
C(3′/II)	82.16	80.98	82.23	80.13	82.09	80.85
C(4′/II)	89.31[c])	88.87[c])	89.21[c])	89.07[c])	89.43	89.93[c])
C(5′/II)	63.96	63.13	63.89	63.32	63.92	63.14

[a]) Assignments based on a HSQC and a HMBC spectrum. [b]) [c]) [d]) Assignments may be interchanged.

1330*w*, 1300*w*, 1254*m*, 1157*m*, 1095*m*, 1067*s*, 867*w*, 836*w*. ^{1}H-NMR (300 MHz, $CDCl_3$): see *Table 10*; additionally, 7.53–7.20 (*m*, 12 arom. H); 6.85 (*d*, $J = 8.7$, 2 arom. H); 4.49 (br. *s*, HO–C(5′/II)); 3.79 (*s*, MeO); 1.52, 1.45, 1.35, 1.30 (4*s*, 2 Me_2C). ^{13}C-NMR (75 MHz, $CDCl_3$): see *Table 11*; additionally, 158.66 (*s*); 143.39 (2*s*); 134.42 (*s*); 130.40 (2*d*); 128.32 (6*d*); 127.90 (4*d*); 127.08 (2*d*); 113.85, 113.77 (2*s*, 2 Me_2C); 113.26 (2*d*); 87.82 (*s*, Ph_2C); 55.26 (*q*, MeO); 27.32, 27.21, 25.53, 25.43 (4*q*, 2 Me_2C). HR-MALDI-MS: 944.327 ($[M+Na]^+$, $C_{47}H_{52}N_7NaO_{11}S^+$; calc. 944.326).

*5′-*O*-[Dimethyl(1,1,2-trimethylpropyl)silyl]-2′,3′-*O*-isopropylideneuridine-6-methyl-(6^1 → 5′-*S*)-8-(hydroxymethyl)-2′,3′-*O*-isopropylidene-5′-thioadenosine* (**31**). A soln. of **29** (200 mg, 0.18 mmol) in CH_2Cl_2 (2 ml) was treated with Cl_2CHCO_2H (200 µl, 2.4 mmol) and Et_3SiH (240 µl, 1.5 mmol), stirred for 15 min at 23°, poured in a sat. $NaHCO_3$ soln., and extracted with AcOEt. The combined org. layers were washed with brine, dried ($MgSO_4$), and evaporated. FC (CH_2Cl_2/MeOH/NH_4OH 100 : 0 : 0 → 92 : 8 : 1) gave **31** (124 mg, 87%). Colourless powder. R_f (CH_2Cl_2/MeOH/NH_4OH 90 : 10 : 1) 0.46. M.p. 144.2–146°. $[\alpha]_D^{25} = -38.0$ ($c = 1.0$, $CHCl_3$). IR ($CHCl_3$): 3473*w*, 3389*w* (br.), 3336*w*, 3195*w* (br.), 2961*m*, 2869*w*, 1697*s*, 1639*m*, 1445*w*, 1377*m*, 1330*w*, 1297*w*, 1265*m*, 1157*m*, 1088*s*, 866*m*, 836*m*. ^{1}H-NMR (500 MHz, $CDCl_3$; assignments based on DQFCOSY, HSQC, and HMBC spectra): see *Table 10*; additionally, 5.20 (*s*, $HOCH_2$–C(8/I)); 1.57 (*sept.*, $J = 6.9$, Me_2CH); 1.61, 1.38 (2*s*, Me_2CO_2/I); 1.54, 1.34 (2*s*, Me_2CO_2/II); 0.83 (*d*, $J = 6.9$, Me_2CH); 0.80, 0.79 (2*s*, Me_2CSi); 0.05, 0.04 (2*s*, Me_2Si). ^{13}C-NMR (125 MHz, $CDCl_3$; assignments based on DQFCOSY, HSQC, and HMBC spectra): see *Table 11*; additionally, 114.25 (*s*, Me_2CO_2/I); 113.48 (*s*, Me_2CO_2/II); 34.12 (*d*, Me_2CH); 27.40, 25.59 (2*q*, Me_2CO_2/II); 27.19, 25.41 (2*q*, Me_2CO_2/I); 25.34 (*s*, Me_2CSi); 20.36, 20.33 (2*q*, Me_2CSi); 18.50, 18.46 (2*q*, Me_2CH); −3.27, −3.31 (2*q*, Me_2Si). HR-MALDI-MS: 814.323 (100, $[M+Na]^+$, $C_{55}H_{69}N_7NaO_{11}SSi^+$; calc. 814.324), 792.343 (50, $[M+H]^+$, $C_{55}H_{70}N_7O_{11}SSi^+$; calc. 792.342).

*2′,3′-*O*-Isopropylideneuridine-6-methyl-(6^1 → 5′-*S*)-2′,3′-*O*-isopropylidene-8-(hydroxymethyl)-5′-thioadenosine* (**32**). A soln. of **31** (40 mg, 0.05 mmol) in THF (1 ml) in a polyethylene flask was treated with $(HF)_3 \cdot Et_3N$ (80 µl, 0.5 mmol), stirred for 2 d at 23°, poured on brine, and extracted with AcOEt. The

org. phase was separated, washed with sat. $NaHCO_3$ soln. and brine, dried ($MgSO_4$), and evaporated. FC (AcOEt/MeOH/NH_4OH 100:0:0 → 92:8:1) gave **32** (26 mg, 80%). Colourless powder. R_f (CH_2Cl_2/MeOH/NH_4OH 90:10:1) 0.20. M.p. 182.6–186.7°. $[\alpha]_D^{25} = -48.5$ ($c = 1.0$, $CHCl_3$). UV ($CHCl_3$): 262 (28592). IR ($CHCl_3$): 3473*w*, 3398*w*, 3330*w*, 3200*w*, 3014*m*, 2938*w*, 1702*s*, 1641*m*, 1445*w*, 1384*m*, 1331*w*, 1300*w*, 1249*w*, 1157*m*, 1091*m*, 1068*m*, 908*w*, 867*w*. ^{1}H-NMR (300 MHz, 45°, $CDCl_3$): see *Table 10*; additionally, 11.48 (br. *s*, H–N(3)); 6.71 (br. *s*, H_2N–C(6/I)); 4.56 (br. *s*, HO–C(5′/II); 4.11 (br. *s*, $HOCH_2$–C(8/I)); 1.61, 1.53, 1.39, 1.32 (4*s*, 2 Me_2C). ^{13}C-NMR (75 MHz, $CDCl_3$): see *Table 11*; additionally, 113.96, 113.85 (2*s*, 2 Me_2*C*); 27.27, 27.14, 25.47, 25.31 (4*q*, 2 *Me*$_2$C). HR-MALDI-MS: 672.2065 (100, $[M+Na]^+$, $C_{27}H_{35}N_7NaO_{10}S^+$; calc. 672.2064), 650.2244 (66, $[M+H]^+$, $C_{27}H_{36}N_7O_{10}S^+$; calc. 650.2244).

X-Ray Analysis of **32**[14]). Colourless crystals of **32** were obtained by crystallisation from MeOH/CH_2Cl_2. Crystal data at 220 K for $C_{27}H_{35}N_7O_{10}S$ (649.68); monoclinic $P2_1$; $a = 9.3842(2)$, $b = 17.2829(3)$, $c = 10.0657(2)$ Å, $\beta = 107.263(1)°$. $V = 1558.98(5)$ Å^3; $Z = 2$; $D_{calc} = 1.384$ Mg/m^3. *Bruker-Nonius Kappa-CCD* with MoK_α radiation ($\lambda = 0.7107$ Å). The structure was solved by direct methods [47] and refined by full-matrix least-squares analysis [48] including an isotropic extinction correction. All heavy atoms were refined anisotropically (H-atoms isotropic, whereby H-positions are based on stereochemical considerations). $R = 0.0306$, $R_w = 0.0725$ for 442 parameters and 6193 reflections with $I > 2\sigma(I)$ and $\tau <$ 27.48°.

5′-O-*[Dimethyl(1,1,2-trimethylpropyl)silyl]-2′,3′*-O-*isopropylideneadenosine-8-methyl-(8′ → 5′*-S*)-2′,3′*-O-*isopropylidene-5′-thiouridine* (**33**). A soln. of **22** (200 mg, 0.33 mmol) and **9** (114 mg, 0.33 mmol) in O_2-free dry MeOH (2 ml) was treated with a soln. of MeONa (71.9 mg, 1.33 mmol) in O_2-free dry MeOH (2 ml), and stirred for 14 h at 23°. Volatiles were removed. A soln. of the residue in CH_2Cl_2 was washed with brine, dried ($MgSO_4$), and evaporated. FC (MeOH/CH_2Cl_2 3:97) yielded **33** (194 mg, 77%). Colourless powder. R_f (MeOH/CH_2Cl_2 1:19) 0.34. M.p. 133.4–134.4°. $[\alpha]_D^{25} = -72.2$ ($c = 1.0$, $CHCl_3$). IR ($CHCl_3$): 3406*w*, 3308*w*, 3199*w*, 2960*m*, 2869*w*, 1679*s*, 1635*m*, 1455*w*, 1376*m*, 1330*w*, 1238*w*, 1157*w*, 1087*m*, 932*w*, 835*w*. ^{1}H-NMR (300 MHz, $CDCl_3$): see *Table 12*; additionally, 7.28 (*d*, $J = 8.1$, H–C(6/I)); 1.52 (*sept.*, $J = 6.9$, Me_2CH); 1.59, 1.49, 1.39, 1.25 (4*s*, 2 Me_2CO_2); 0.79 (*d*, $J = 6.9$, *Me*$_2$CH); 0.75, 0.74 (2*s*, Me_2CSi); −0.05, −0.07 (2*s*, Me_2Si). ^{13}C-NMR (75 MHz, $CDCl_3$): see *Table 13*; additionally, 114.73, 113.95 (2*s*, Me_2CO_2); 34.28 (*d*, Me_2CH); 27.40, 27.26, 25.62, 25.41 (4*q*, 2 *Me*$_2$$CO_2$); 25.41 (*s*, Me_2CSi); 20.49 (*q*, *Me*$_2$CSi); 18.66 (*q*, *Me*$_2$CH); −3.27 (*q*, Me_2Si). HR-MALDI-MS: 784.3129 (100, $[M+Na]^+$, $C_{34}H_{51}N_7NaO_7SSi^+$; calc. 784.3136), 762.3308 (42, $[M+H]^+$, $C_{34}H_{52}N_7O_7SSi^+$; calc. 762.3316). Anal. calc. for $C_{34}H_{51}N_7O_7SSi$ (761.32): C 53.59, H 6.75, N 12.87; found: C 53.52, H 6.91, N 12.65.

2′,3′-O-*Isopropylideneadenosine-8-methyl-(8′ → 5′*-S*)-2′,3′*-O-*isopropylidene-5′-thiouridine* (**34**). A soln. of **33** (110 mg, 0.14 mmol) in THF (1 ml) in a polyethylene flask was treated with $(HF)_3 \cdot Et_3N$ (230 µl, 1.43 mmol), stirred for 2 d at 23°, poured into brine, and extracted with CH_2Cl_2. The combined org. layers were washed with sat. $NaHCO_3$ soln. and brine, dried ($MgSO_4$), and evaporated. FC (CH_2Cl_2/MeOH/NH_4OH 100:0:0 → 92:8:1) gave **34** (52 mg, 58%). Colourless foam. R_f (CH_2Cl_2/MeOH/NH_4OH 95:5:1) 0.23. $[\alpha]_D^{25} = -35.4$ ($c = 1.0$, DMSO). IR (KBr): 3343*w* (br.), 3203*w*, 2987*m*, 2931*m*, 2870*w*, 1694*s* (br.), 1638*s* (br.), 1578*w*, 1455*w*, 1427*m*, 1382*s*, 1334*w*, 1305*w*, 1260*m*, 1216*m*, 1156*w*, 1081*s*, 972*w*, 852*m*. ^{1}H-NMR (300 MHz, $CDCl_3$): see *Table 12*; additionally, 7.24 (*d*, $J = 8.1$, H–C(6/I)); 1.62, 1.52, 1.38, 1.29 (4*s*, 2 Me_2C). ^{13}C-NMR (75 MHz, (D_6)DMSO): see *Table 13*; additionally, 114.04, 113.90 (2*s*, 2 Me_2*C*); 27.80, 27.45, 25.91, 25.65 (4*q*, 2 *Me*$_2$C). HR-MALDI-MS: 642.1950 ($[M+Na]^+$, $C_{26}H_{33}N_7NaO_9S^+$; calc. 642.1958).

5′-O-*[Dimethyl(1,1,2-trimethylpropyl)silyl]-2′,3′*-O-*isopropylideneadenosine-8-methyl-(8′ → 5′*-S*)-2′,3′*-O-*isopropylidene-6-{[(4-methoxyphenyl)diphenylmethoxy]methyl}-5′-thiouridine* (**35**). A soln. of **15** (151 mg, 0.25 mmol) and **22** (163 mg, 0.25 mmol) in O_2-free dry MeOH (2 ml) was treated with a soln. of MeONa (55 mg, 1 mmol) in O_2-free dry MeOH (2 ml), stirred for 14 h at 23°, and evaporated. A soln. of the residue in CH_2Cl_2 was washed with NH_4Cl soln. and brine, dried ($MgSO_4$), and evaporated. FC (MeOH/CH_2Cl_2 1:24) gave **35** (200 mg, 75%). Colourless powder. R_f (MeOH/CH_2Cl_2 1:19) 0.23. M.p. 141.1–142.1°. $[\alpha]_D^{25} = -113.6$ ($c = 1.0$, $CHCl_3$). IR ($CHCl_3$): 3386*w* (br.), 3305*w*, 3201*w*, 2961*m*, 2869*w*, 1679*s*, 1636*m*, 1609*m*, 1510*w*, 1448*m*, 1375*m*, 1330*w*, 1299*w*, 1254*w*, 1157*w*, 1089*m*, 980*w*, 908*w*, 875*w*, 836*m*. ^{1}H-NMR (300 MHz, $CDCl_3$): see *Table 12*; additionally, 7.52–7.23 (*m*, 12 arom. H); 6.85 (*d*, $J =$

Table 12. *Selected ^{1}H-NMR Chemical Shifts* [ppm] *and Coupling Constants* [Hz] *of the A*[s]U$^{(*)}$ Dimers* **33**–**37** *in $CDCl_3$, and Dimer* **38** *in CD_3OD*

	33 77 mM	**34** 6 mM[c])	**35** 25 mM	**36** 29 mM	**37**[a]) 12 mM	**38**[b])
Uridine unit (I)						
H–N(3/I)	11.68	10.25	12.02	11.53	11.13	–
H–C(5/I)	5.71	5.72	5.61	5.55	5.47	5.77
CH_a–C(6/I)	–	–	4.06	4.13	4.61	4.48
CH_b–C(6/I)	–	–	4.01	4.02	4.41	4.40
H–C(1′/I)	5.58	5.54	5.68	5.64	5.98	5.76
H–C(2′/I)	4.96	5.01	5.17	5.19	5.085	5.20
H–C(3′/I)	4.70	4.75	4.83	4.88	4.86	4.81
H–C(4′/I)	4.23–4.18	4.25	4.10	4.06	4.29	4.13
H_a–C(5′/I)	3.00–2.88	3.01	2.95	2.90	2.99	2.96
H_b–C(5′/I)	3.00–2.88	2.94	2.85	2.90	2.92	2.89
$J(H_a,H_b/I)$	–	–	[d])	15.0	14.3	14.7
J(1′,2′/I)	< 1.0	1.9	< 1.0	< 1.0	< 1.0	1.5
J(2′,3′/I)	6.3	6.5	6.6	6.6	6.1	6.3
J(3′,4′/I)	4.2	3.9	3.9	3.6	4.5	3.9
J(4′,5′a/I)	[d])	6.2	8.4	7.2	8.2	6.9
J(4′,5′b/I)	[d])	6.2	5.7	7.2	4.0	7.2
J(5′a,5′b/I)	[d])	13.5	12.9	[d])	14.4	13.8
Adenosine unit (II)						
H_2N–C(6/II)	6.89	6.54	7.13	6.99	7.10–6.85	–
H–C(2/II)	8.31	8.27	8.38	8.26	8.22	8.12
CH_a–C(8/II)	4.21	4.14	3.96	3.93	4.11	4.11
CH_b–C(8/II)	4.09	3.97	3.88	3.82	4.00	4.11
H–C(1′/II)	6.28	6.12	6.39	6.11	6.39	6.28
H–C(2′/II)	5.89	5.26	6.01	5.25	5.91	5.52
H–C(3′/II)	5.10	5.10	5.12	5.08	5.093	5.08
H–C(4′/II)	4.23–4.18	4.52	4.24	4.51	4.23	4.32
H_a–C(5′/II)	3.63	4.02	3.57	3.96	3.58	3.77
H_b–C(5′/II)	3.52	3.71–3.82	3.46	3.765	3.49	3.66
$J(H_a,H_b/II)$	14.4	14.5	12.3	12.0	14.8	[d])
J(1′,2′/II)	< 1.0	5.3	< 1.0	5.1	1.5	3.3
J(2′,3′/II)	6.0	5.4	6.0	6.0	6.2	6.0
J(3′,4′/II)	3.0	< 1.0	3.0	< 1.0	3.2	3.0
J(4′,5′a/II)	6.6	< 1.0	6.9	< 1.0	6.6	3.6
J(4′,5′b/II)	6.3	< 1.0	6.6	< 1.0	6.3	4.2
J(5′a,5′b/II)	10.2	15.0	10.5	11.7	10.5	12.3

[a]) Assignments based on a HSQC and a HMBC spectrum. [b]) In CD_3OD. [c]) Gel formation at concentrations > 6 mM. [d]) Not assigned.

8.7, 2 arom. H); 3.81 (*s*, MeO); 1.52 (*sept.*, $J = 6.9$, Me_2CH); 1.61, 1.42, 1.39, 1.24 (4*s*, 2 Me_2CO_2); 0.80 (*d*, $J = 6.9$ Me_2CH); 0.75, 0.74 (2*s*, Me_2CSi); −0.05, −0.08 (2*s*, Me_2Si). ^{13}C-NMR (75 MHz, $CDCl_3$): see *Table 13*; additionally, 158.86, 143.12, 142.98, 134.06 (4*s*); 130.27 (2*d*); 128.19 (4*d*); 127.98 (4*d*); 127.37 (2*d*); 113.58, 113.51 (2*s*, 2 Me_2CO_2); 113.35 (2*d*); 88.24 (*s*, Ph_2C); 55.35 (*q*, MeO); 34.15 (*d*, Me_2CH); 27.27, 27.12, 25.54, 25.31 (4*q*, 2 Me_2CO_2); 25.27 (*s*, Me_2CSi); 20.37 (*q*, Me_2CSi); 18.58 (*q*, Me_2CH); −3.27 (*q*, Me_2Si). HR-MALDI-MS: 1086.4445 ($[M+Na]^+$, $C_{55}H_{69}N_7NaO_{11}SSi^+$; calc. 1086.4443).

Table 13. *Selected ^{13}C-NMR Chemical Shifts* [ppm] *of the A*[s]U$^{(*)}$ Dimers* **33** *and* **35**–**37** *in $CDCl_3$, Dimer* **34** *in (D_6)DMSO, and Dimer* **38** *in CD_3OD*

	33	**34**	**35**	**36**	**37**[a])	**38**
C(2/I)	151.15	150.92	152.40[b])	151.65[b])	152.15	152.07
C(4/I)	164.08	163.87	[c])	163.17	162.87	165.46
C(5/I)	103.25	102.67	103.73	103.44	102.92	101.35
C(6/I)	142.85	143.37	151.44[b])	151.51[b])	153.82	156.42
CH_2–C(6/I)	–	–	62.39	62.31	61.44	60.65
C(1′/I)	95.66	92.49	92.56	92.29	91.49	92.13
C(2′/I)	84.70	84.14	85.04	84.55	84.76	85.71
C(3′/I)	83.82	83.36	84.79	84.48	84.31	85.16
C(4′/I)	90.27	89.91	90.02	92.12	90.60	91.75
C(5′/I)	34.56	33.87	35.23	34.40	33.49	34.81
C(2/II)	152.90	153.00	152.15	152.13	151.77	152.88
C(4/II)	150.80	150.47	150.50	149.65	150.56	150.74
C(5/II)	118.56	118.61	118.36	118.60	118.15	118.97
C(6/II)	155.65	156.34	155.37	155.62	154.78	156.80
C(8/II)	149.60	148.69	149.52	148.78	149.93	150.21
CH_2–C(8/II)	28.40	28.32	29.26	28.43	29.71	28.84
C(1′/II)	88.28	87.04	88.24	87.79	89.99	89.54
C(2′/II)	83.20	83.11	82.89	82.70	83.08	84.17
C(3′/II)	82.40	81.91	82.33	81.63	82.09	82.49
C(4′/II)	87.06	85.91	87.86	85.62	88.10	87.62
C(5′/II)	63.10	62.16	62.96	63.30	62.92	63.18

[a]) Assignments based on a HSQC and a HMBC spectrum. [b]) Assignments may be interchanged. [c]) Not assigned.

*2′,3′-*O*-Isopropylideneadenosine-8-methyl-(8^1 → 5′-*S*)-2′,3′-*O*-isopropylidene-6-{[(4-methoxyphenyl)diphenylmethoxy]methyl}-5′-thiouridine* (**36**). A soln. of **35** (75 mg, 0.07 mmol) in THF (1 ml) in a polyethylene flask was treated with $(HF)_3 \cdot Et_3N$ (100 µl, 0.6 mmol), stirred for 2 d at 23°, poured into brine, and extracted with AcOEt. The combined org. layers were separated, washed with sat. $NaHCO_3$ soln. and brine, dried ($MgSO_4$), and evaporated. FC (CH_2Cl_2/MeOH/NH_4OH 100:0:0 → 92:8:1) gave **36** (60 mg, 93%). Colourless foam. R_f (CH_2Cl_2/MeOH/NH_4OH 93:7:1) 0.20. $[\alpha]_D^{25} = -72.0$ ($c = 1.0$, $CHCl_3$). IR ($CHCl_3$): 3473*w*, 3389*w* (br.), 3316*w*, 3194*w* (br.), 3020*m*, 2934*w*, 2856*w*, 1697*s*, 1638*m*, 1607*m*, 1510*w*, 1449*m*, 1375*m*, 1333*w*, 1300*w*, 1266*m*, 1155*m*, 1083*s*, 1035*m*, 909*w*, 872*w*, 852*w*, 836*m*. ^{1}H-NMR (300 MHz, $CDCl_3$): see *Table 12*; additionally, 7.46–7.23 (*m*, 12 arom. H); 6.84 (*d*, $J = 8.7$, 2 arom. H); 6.58 (br. *d*, $J = 11.1$, HO–C(5′/II)); 3.80 (*s*, MeO); 1.62, 1.39, 1.36, 1.27 (4*s*, 2 Me_2C). ^{13}C-NMR (75 MHz, $CDCl_3$): see *Table 13*; additionally, 158.81, 143.04, 142.93, 134.02 (4*s*); 130.19 (2*d*); 128.14 (4*d*); 127.99 (4*d*); 127.33 (2*d*); 113.87, 113.69 (2*s*, 2 Me_2C); 113.32 (2*d*); 88.20 (*s*, Ph_2C); 55.30 (*q*, MeO); 27.85, 27.10, 25.46, 25.34 (4*q*, 2 Me_2C). HR-MALDI-MS: 944.3271 ($[M + Na]^+$, $C_{47}H_{52}N_7O_{11}S^+$; calc. 944.3265).

*5′-*O*-[Dimethyl(1,1,2-trimethylpropyl)silyl]-2′,3′-*O*-isopropylideneadenosine-8-methyl-(8^1 → 5′-*S*)-6-(hydroxymethyl)-2′,3′-*O*-isopropylidene-5′-thiouridine* (**37**). A soln. of **35** (50 mg, 0.05 mmol) in CH_2Cl_2 (1 ml) was treated with Cl_2CHCO_2H (50 µl, 0.6 mmol) and Et_3SiH (60 µl, 0.4 mmol), stirred for 15 min at 23°, poured into sat. $NaHCO_3$ soln., and extracted with AcOEt. The combined org. layers were washed with brine, dried ($MgSO_4$), and evaporated. FC (CH_2Cl_2/MeOH/NH_4OH 100:0:0 → 90:10:1) gave **37** (25 mg, 67%). Colourless powder. R_f (AcOEt) 0.32. M.p. 137.3–139°. $[\alpha]_D^{25} = -103.0$ ($c = 1.0$, $CHCl_3$). IR ($CHCl_3$): 3398*w* (br.), 3324w, 3191*w* (br.), 2985*m*, 2960*m*, 2868*w*, 1697*s*, 1646*m*, 1609*m*, 1455*w*, 1384*m*, 1375*m*, 1331*w*, 1222*m*, 1157*w*, 1089*m*, 875*m*, 836*m*. ^{1}H-NMR (500 MHz, $CDCl_3$; assignments based on DQFCOSY, HSQC, and HMBC spectra): see *Table 12*; additionally, 2.25–1.75 (br. *s*, *H*OCH_2–C(6/I)); 1.52 (*sept.*, $J = 6.9$, Me_2CH); 1.61, 1.43 (2*s*, Me_2CO_2/II); 1.53, 1.30 (2*s*, Me_2CO_2/I); 0.785 (*d*, $J = 6.9$,

Me$_2$CH); 0.740, 0.727 (2*s*, Me$_2$CSi); −0.05, −0.07 (2*s*, Me$_2$Si). ^{13}C-NMR (125 MHz, $CDCl_3$; assignments based on DQFCOSY, HSQC, and HMBC spectra): see *Table 13*; additionally, 114.25 (*s*, Me$_2$*C*O$_2$/I); 113.74 (*s*, Me$_2$*C*O$_2$/II); 34.03 (*d*, Me$_2$*C*H); 27.28, 25.49 (2*q*, *Me*$_2$CO$_2$/II); 27.21, 25.39 (2*q*, *Me*$_2$CO$_2$/I); 25.19 (*s*, Me$_2$*C*Si); 20.25, 20.24 (*q*, *Me*$_2$CSi); 18.42, 18.39 (2*q*, *Me*$_2$CH); −3.51 (*q*, Me$_2$Si). HR-MALDI-MS: 814.3220 (59, $[M+Na]^+$, $C_{35}H_{53}N_7NaO_{10}SSi^+$; calc. 814.3242), 792.3425 (100, $[M+H]^+$, $C_{35}H_{54}N_7O_{10}SSi^+$; calc. 792.3422).

*2′,3′-*O*-Isopropylideneadenosine-8-methyl-(8^1 → 5′-*S*)-6-(hydroxymethyl)-2′,3′-*O*-isopropylidene-5′-thiouridine* (**38**). A soln. of **37** (40 mg, 0.04 mmol) in CH_2Cl_2 (500 µl) was treated with Cl_2CHCO_2H (50 µl, 0.6 mmol) and Et_3SiH (55 µl, 0.35 mmol), stirred for 15 min at 23°, poured into sat. $NaHCO_3$ soln., and extracted with AcOEt. The combined org. layers were washed with brine, dried ($MgSO_4$), and evaporated. FC (CH_2Cl_2/MeOH/NH_4OH 95 : 5 : 0 → 90 : 10 : 1) gave **38** (22 mg, 78%). Colourless powder. R_f (CH_2Cl_2/MeOH/NH_4OH 90 : 10 : 1) 0.33. $[\alpha]_D^{25} = -26.9$ ($c = 1.0$, MeOH). UV ($CHCl_3$): 260 (18775). IR (KBr): 3345*s*, 3213*m*, 2987*w*, 2937*w*, 1699*s* (br.), 1643*s*, 1578*w*, 1453*m*, 1377*s*, 1333*w*, 1302*w*, 1214*s*, 1157*m*, 1085*s*, 1035*m*, 873*w*, 852*w*. ^{1}H-NMR (300 MHz, CD_3OD): see *Table 12*; additionally, 1.61, 1.40, 1.37, 1.26 (4*s*, 2 Me$_2$C). ^{13}C-NMR (75 MHz, CD_3OD): see *Table 13*; additionally, 114.85, 113.31 (2*s*, 2 Me$_2$*C*); 27.53, 27.14, 25.42, 25.18 (4*q*, 2 *Me*$_2$C). HR-MALDI-MS: 672.2069 (100, $[M+Na]^+$, $C_{47}H_{52}N_7O_{11}S^+$; calc. 672.2064), 650.2233 (22, $[M+Na]^+$, $C_{47}H_{52}N_7O_{11}S^+$; calc. 650.2244).

REFERENCES

[1] X. Zhang, B. Bernet, A. Vasella, *Helv. Chim. Acta* **2007**, *90*, 891.
[2] A. Vasella, *Chimia* **2005**, *59*, 785.
[3] X. Zhang, B. Bernet, A. Vasella, *Helv. Chim. Acta* **2006**, *89*, 2861.
[4] X. Zhang, B. Bernet, A. Vasella, *Helv. Chim. Acta* **2007**, *90*, 792.
[5] X. Zhang, B. Bernet, A. Vasella, *Helv. Chim. Acta* **2007**, *90*, 864.
[6] A. J. Matthews, P. K. Bhardwaj, A. Vasella, *Chem. Commun.* **2003**, 950.
[7] A. J. Matthews, P. K. Bhardwaj, A. Vasella, *Helv. Chim. Acta* **2004**, *87*, 2273.
[8] J. L. Sessler, R. Z. Wang, *J. Am. Chem. Soc.* **1996**, *118*, 9808.
[9] K. Shin-ya, O. Takahashi, Y. Katsumoto, K. Ohno, *J. Mol. Struct.* **2007**, *827*, 155.
[10] O. Takahashi, Y. Kohno, K. Saito, M. Nishio, *Chem.–Eur. J.* **2003**, *9*, 756.
[11] E. L. Eliel, S. H. Wilen, L. N. Mander, 'Stereochemistry of Organic Compounds', John Wiley & Sons, New York, 1994, p. 696.
[12] H. Booth, J. R. Everett, *J. Chem. Soc., Chem. Commun.* **1976**, 278.
[13] J. F. Stoddart, 'Stereochemistry of Carbohydrates', Wiley-Interscience, New York, 1971, p. 67.
[14] D. B. Davies, *Prog. Nucl. Magn. Reson. Spectrosc.* **1978**, *12*, 135.
[15] S. Eppacher, Ph. D. Thesis No. 15088, ETH-Zürich, 2003.
[16] Y. Sasanuma, K. Sugita, *Polym. J.* **2006**, *38*, 983.
[17] P. Vansteenkiste, E. Pauwels, V. Van Speybroeck, M. Waroquier, *J. Phys. Chem., A* **2005**, *109*, 9617.
[18] I. Kanesaka, R. G. Snyder, H. L. Strauss, *J. Chem. Phys.* **1986**, *84*, 395.
[19] M. Črnugelj, D. Dukhan, J.-L. Barascut, J.-L. Imbach, J. Plavec, *J. Chem. Soc., Perkin Trans. 2* **2000**, 255.
[20] D. F. Plusquellic, R. D. Suenram, B. Maté, J. O. Jensen, A. C. Samuels, *J. Chem. Phys.* **2001**, *115*, 3057.
[21] W. Saenger, 'Principles of Nucleic Acid Structure', Springer-Verlag, Berlin, 1984, p. 14.
[22] A. Dunger, H.-H. Limbach, K. Weisz, *Chem.–Eur. J.* **1998**, *4*, 621.
[23] A. Dunger, H.-H. Limbach, K. Weisz, *J. Am. Chem. Soc.* **2000**, *122*, 10109.
[24] S. Chladek, J. Smrt, *Collect. Czech. Chem. Commun.* **1964**, *29*, 214.
[25] H. Wetter, K. Oertle, *Tetrahedron Lett.* **1985**, *26*, 5515.
[26] H. Tanaka, I. Nasu, T. Miyasaka, *Tetrahedron Lett.* **1979**, 4755.
[27] H. Hayakawa, K. Haraguchi, H. Tanaka, T. Miyasaka, *Chem. Pharm. Bull.* **1987**, *35*, 72.
[28] W. Czechtizky, A. Vasella, *Helv. Chim. Acta* **2001**, *84*, 594; W. Czechtizky, A. Vasella, *Helv. Chim. Acta* **2001**, *84*, 1000.
[29] M. P. Groziak, R. Lin, *Tetrahedron* **2000**, *56*, 9885.

[30] M. C. Pirrung, S. W. Shuey, D. C. Lever, L. Fallon, *Bioorg. Med. Chem. Lett.* **1994**, *4*, 1345.
[31] B. Bannister, F. Kagan, *J. Am. Chem. Soc.* **1960**, *82*, 3363; G. Guillerm, D. Guillerm, C. Witkowski-Vandenplas, *Nucleosides Nucleotides Nucleic Acids* **2001**, *20*, 685.
[32] J. Baddiley, G. A. Jamieson, *J. Chem. Soc.* **1955**, 1085.
[33] D. M. Brown, A. Todd, S. Varadarajan, *J. Chem. Soc.* **1956**, 2388.
[34] Y. Maki, K. Kameyama, M. Suzuki, M. Sako, K. Hirota, *J. Chem. Res., Synop.* **1984**, 388.
[35] V. T. Ravikumar, A. H. Krotz, D. L. Cole, *Tetrahedron Lett.* **1995**, *36*, 6587.
[36] C. A. G. Haasnoot, F. A. A. M. De Leeuw, C. Altona, *Tetrahedron* **1980**, *36*, 2783.
[37] F. Mohamadi, N. G. J. Richards, W. C. Guida, R. Liskamp, M. Lipton, C. Caufield, G. Chang, T. Hendrickson, W. C. Still, *J. Comput. Chem.* **1990**, *11*, 440.
[38] M. Remin, D. Shugar, *Biochem. Biophys. Res. Commun.* **1972**, *48*, 636.
[39] R. G. S. Ritchie, A. S. Perlin, *Carbohydr. Res.* **1977**, *55*, 121.
[40] F. E. Hruska, D. J. Wood, T. N. McCaig, A. A. Smith, A. Holy, *Can. J. Chem.* **1974**, *52*, 497.
[41] G. D. Wu, A. S. Serianni, R. Barker, *J. Org. Chem.* **1983**, *48*, 1750.
[42] H. Rosemeyer, G. Toth, B. Golankiewicz, Z. Kazimierczuk, W. Bourgeois, U. Kretschmer, H. P. Muth, F. Seela, *J. Org. Chem.* **1990**, *55*, 5784.
[43] V. S. Rao, A. S. Perlin, *Can. J. Chem.* **1983**, *61*, 2688.
[44] H. Gunji, A. Vasella, *Helv. Chim. Acta* **2000**, *83*, 1331.
[45] H. S. Gutowsky, A. Saika, *J. Chem. Phys.* **1953**, *21*, 1688.
[46] P. A. Levene, R. S. Tipson, *J. Biol. Chem.* **1934**, *106*, 113.
[47] A. Altomare, M. C. Burla, M. Camalli, G. L. Cascarano, C. Giacovazzo, A. Guagliardi, A. G. G. Moliterni, G. Polidori, R. Spagna, *J. Appl. Crystallogr.* **1999**, *32*, 115.
[48] G. M. Sheldrick, 'SHELXL97: Program for Refinement of Crystal Structures', University of Göttingen, Göttingen, 1997.

Received January 9, 2008